

# **The role of CD8<sup>+</sup> T cells in immune thrombocytopenia (ITP)**

**Anwar Abdulfattah A. Sayed**

**“A thesis submitted in partial fulfilment of the requirements for the degree of PhD of Imperial College London and the Diploma of Imperial College”**

**Imperial College London  
Department of Medicine  
October 2018**

**Supervisor: Dr Nichola Cooper**

## **1. Declaration of originality**

This is to certify that the copy of my thesis, which I have presented for consideration for my PhD degree, embodies the results of my own course of study and research, has been composed by myself and has been seen by my supervisor before presentation

## **2. Copyright Declaration**

The copyright of this thesis rests with the author and is made available under a Creative Commons Attribution Non-Commercial No Derivatives licence. Researchers are free to copy, distribute or transmit the thesis on the condition that they attribute it, that they do not use it for commercial purposes and that they do not alter, transform or build upon it. For any reuse or redistribution, researchers must make clear to others the licence terms of this work.

### 3. Abstract

Immune thrombocytopenia (ITP) is an autoimmune disorder characterised by isolated low platelet count and a skewed proinflammatory Th1/Th17 profile. However, little is known about the involvement of CD8<sup>+</sup> cytotoxic T-cells in ITP pathophysiology in peripheral blood and bone marrow(BM) and how this involvement is regulated. Thrombopoietin-receptor agonists (TPO-RA); eltrombopag(Elt) and romiplostim(Romi), which stimulate the BM to produce more platelets, are increasingly used. However, it is not clear how can these agents induce complete remission in patients.

Polychromatic flow cytometric panels were designed to characterize and functionally assess peripheral blood T-cells. Platelet reactivity has been addressed using an IFN $\gamma$  ELISpot assay. Sixty patients with ITP were included who were on Elt, Romi or on no treatment at the time of analysis. BM trephines were stained for CD4<sup>+</sup>, CD8<sup>+</sup> T cells and CD42b<sup>+</sup> megakaryocytes(MK), and slides were analysed automatically. MK were generated *in vitro* to assess their interaction with T-cells.

In peripheral blood, CD8<sup>+</sup>T-cells displayed an effector phenotype characterised by reduced CD4/CD8 T cell ratio and Treg/effector CD8<sup>+</sup> T-cell ratio and increased effector CD8<sup>+</sup> T-cell, which were associated with disease activity. This polyfunctional population expressed significantly higher intracellular TNF $\alpha$ , IFN $\gamma$  and Granzyme B compared to HC.

Elt seemed to significantly lower effector CD8<sup>+</sup>T cells and reduced their functionality *in vitro* in a dose dependent manner. In the BM, MK-T cell interaction and clustering was higher in patients, more prominently in chronic cases. MK demonstrated features of professional antigen-presenting-cells including the surface expression of functional MHC-I, MHC-II, PD-L1 and PD-L2, which controlled MK-T-cell interaction. CD8<sup>+</sup> T cells are involved in ITP pathology contributing the inflammatory milieu. These potentially autoreactive cells could target both platelets and MK. MK seems to govern the immune response in the BM; by its direct interaction with either CD4<sup>+</sup> or CD8<sup>+</sup>T-cells, and via its immunomodulation mainly by PD-L1 and PD-L2.

Word count:28,580 words

## 4. Table of Contents

1. Declaration of originality .....	2
2. Copyright Declaration.....	3
3. Abstract.....	4
4. Table of Contents.....	5
5. Table of Figures .....	8
6. Table of Tables .....	10
7. Acknowledgement .....	11
8. List of Abbreviations .....	13
9. Introduction.....	18
9.1. Adaptive immune system.....	18
9.1.1. Normal T cell response .....	19
9.2. Programmed death receptor-1 (PD-1) and its ligand-1 (PD-L1) and PD-L2 in normal response and disease. ....	22
9.3. Megakaryopoiesis and platelet production .....	23
9.4. Role of MK and platelets in immunity .....	26
9.4.1. Platelets and their immunological response.....	26
9.4.2. MK and their progenitors as antigen-presenting cells (APCs) .....	29
9.5. Immune thrombocytopenia (ITP).....	29
9.5.1. Definition and Classification .....	30
9.5.2. Pathophysiology of ITP .....	31
9.5.3. Clinical manifestations of ITP .....	37
9.5.4. Treatment .....	38
9.6. Research hypothesis and aims .....	42
9.6.1. Aims.....	42
10. Materials and methods .....	43
10.1. Patients and Controls .....	43
10.2. Plasma and Peripheral Blood Mononuclear Cells (PBMC) Isolation.....	43
10.3. PBMC Surface Staining.....	44
10.4. FoxP3 and PBMC Intracellular Cytokine Staining.....	45
10.5. Flow Cytometric Panel Design and Antibody Titration .....	45
10.6. Antibody Titration .....	49
10.7. Setting the Gating Strategy in Flow Cytometric Analysis.....	50

10.8. Flow Cytometric Analysis and Cell Sorting .....	52
10.9. IFN $\gamma$ Enzyme-Linked ImmunoSpot (ELISpot) Assay.....	53
10.10. <i>In Vitro</i> culture of PBMC with thrombopoietin receptor agonists (TPO-RAs).....	54
10.11. Bone Marrow Preparation for Histological Examination. ....	54
10.12. Bone marrow trephines Immunohistofluorescent (IHF) staining. ....	55
10.13. Imaging of the bone marrow trephines and image analysis.....	57
10.14. Bone marrow aspirate processing and CD34 <sup>+</sup> Haematopoietic stem cell selection..	60
10.15. <i>In vitro</i> megakaryopoietic assay. ....	60
10.16. Tracking the development of megakaryocytes. ....	61
10.17. MK-T cell Interaction Assay. ....	64
10.18. Statistical Analysis.....	66
11. CD8 <sup>+</sup> T cell pathophysiology of Immune thrombocytopenia (ITP) peripheral blood and their response to thrombopoietin receptor agonists (TPO-RAs).....	67
11.1. Introduction.....	67
11.2. Results.....	69
11.2.1. Patients characteristics. ....	69
11.2. Characterisation of T cell subsets. ....	72
11.2.3. ITP is associated with skewed T cell subsets towards an effector phenotype.....	74
11.2.4. Changes in the effector and central memory CD8 <sup>+</sup> T cell subsets corresponding to disease activity.....	76
11.2.5. Effector CD8 <sup>+</sup> T cell population lacks signs of exhaustion in patients with ITP.	78
11.2.6. Proinflammatory CD8 <sup>+</sup> T cells are significantly higher in patients with ITP.....	79
11.2.7. Polyfunctional CD8 <sup>+</sup> T cells are enriched within the effector population and have the highest Granzyme B and perforin expression. ....	83
11.2.8. Platelets-specific T cells are significantly higher in patients with ITP.....	86
11.2.9. Proinflammatory cytokines are significantly increased in the CD8 <sup>+</sup> T cell in patients receiving TPO-RAs. ....	88
11.2.10. Patients on Eltrombopag have a lower effector T cells and higher naïve T cells compared to Romiplostim.....	90
11.2.11. Eltrombopag significantly reduces CD8 <sup>+</sup> T cell functionality in a dose-dependent manner. ....	92
11.2.12. Functional regulatory T cells (Treg) and their Treg/effector CD8 <sup>+</sup> T cell ratio are reduced in patients with ITP, corresponding to disease activity.....	95
11.3. Discussion.....	97

12. Characterising the T cell involvement in the bone marrow pathophysiology of immune thrombocytopaenia (ITP).....	103
12.1. Introduction.....	103
12.2. Results.....	105
12.2.1 Patients characteristics .....	105
12.2.2. Automated Identification of the different cells in the BM trephines.....	107
12.2.3. Increased MK frequency in patients with ITP, more prominently in TPO-RA patients .....	110
12.2.4. T cell changes within the bone marrow in patients with ITP .....	113
12.2.5. Increased MK-T cell interaction in the BM of patients with ITP .....	115
12.2.6. Increased MK-T cell clustering in the BM of patients with ITP .....	117
12.3. Discussion.....	119
13. <i>In vitro</i> assessment of the megakaryocyte-CD8 <sup>+</sup> T cell interaction and its regulation....	124
13.1. Introduction.....	124
13.2. Results.....	126
13.2.1. Megakaryocyte development and maturation from bone marrow-derived CD34 <sup>+</sup> HSC.....	126
13.2.2. MHC-I and MHC-II surface expression on developing MK.....	129
13.2.3. PD-L1 and PD-L2 expression in developing MK.....	131
13.2.4. ITP plasma reduces PD-L1 expression on MK and increases MK death.....	134
13.2.5. Blocking PD-L1 and PD-L2 on MK promotes the development of the polyfunctional CD8 <sup>+</sup> T cells, when cultured with PBMC. ....	136
13.3. Discussion.....	139
14. Discussion.....	143
14.1. Limitations of this study .....	148
14.2. Future work.....	149
14.3. Conclusion .....	150
15. References.....	152

## 5. Table of Figures

Figure 7-1. Overview of stages of megakaryopoiesis.....	23
Figure 7-2. Differentiation markers of the megakaryocytic lineage.....	25
Figure 7-3. Overview of the proposed current understanding of the ITP pathophysiology.....	32
Figure 10-1. Example of Grnzyme B (GnB) antibody titration. ....	49
Figure 10-2. Setting the gating strategy in a multicolour panel based on fluorescence-minus-one controls.....	51
Figure 10-3. Using compensation beads for setting up voltages.....	52
Figure 10-4. Macro development to automatically Identify MK and T cells interactions and clustering. ....	59
Figure 10-5. Incucyte imaging system used to track MK development.....	62
Figure 10-6. Automated identification and quantification of developing MK using the Incucyte imaging system. ....	63
Figure 10-7. Interrogating MK - T interaction governed by Immune-related molecules. ....	65
Figure 11-2. CD4 <sup>+</sup> and CD8 <sup>+</sup> T cells populations, ratio and subsets in patients with ITP and HC. ....	75
Figure 11-3. Comparison between T cell subsets in patients with active and stable disease.....	77
Figure 11-4. The expression of exhaustion markers in naïve and effector CD8 <sup>+</sup> T cells. ....	78
Figure 11-5. Characterisation of the intracellular cytokines in CD8 <sup>+</sup> T cells. ....	80
Figure 11-6. Comparison of CD8 <sup>+</sup> T cell intracellular cytokines between HC and patients.....	81
Figure 11-7. Intracellular cytokines expression of the sorted CD8 <sup>+</sup> T cell subsets.....	84
Figure 11-8. The differential expression of intracellular cytokines in CD8 <sup>+</sup> T cells. ....	85
Figure 11-9. ELISpot assay of PBMC cultured with platelets of healthy donor. ....	87
Figure 11-10. Comparisons of the CD8 <sup>+</sup> T cell intracellular cytokines between patients on no treatment and on TPO-RAs.....	89
Figure 2011-11. Comparisons of the different T cell subsets between the patient treatment subgroups and HC.....	91
Figure 11-12. Reduction of CD8 <sup>+</sup> T cell functionality by Elt.....	93

Figure 11-13. Comparing the effect of Elt and Romi on the functionality of CD8+ T cells. ....	94
Figure 11-14. Functional Treg are reduced in patients with ITP and correspond to disease activity. ..	96
Figure 12-1. IHF staining of bone marrow trephine. ....	108
Figure 12-2. Identifying MK and T cells IPs and clustering.....	109
Figure 12-3. Examples of BM trephine staining in controls and patients with ITP.....	111
Figure 12-4. MK densities and diameters in patient cohorts and controls.....	112
Figure 12-5. T cell densities and diameters in the BM of controls and patients with ITP.....	114
Figure 12-6. MK - T cell IPs in controls and patients with ITP.....	116
Figure 12-7. MK - T cell clustering in controls and patients with ITP and its correlation to IP.....	118
Figure 13-1. Tracking the development of MK using the real-time imaging system (Incucyte).....	127
Figure 13-2. Tracking the development and maturation of MK using flow cytometry. ....	128
Figure 13-3. HLA-A/B/C and HLA-DR surface expression on developing MK. ....	130
Figure 13-4. Surface expression of PD-L1 on developing MK. ....	132
Figure 13-5. PD-L1 and PD-L2 expression on developing MK. ....	133
Figure 13-6. The impact of plasma from patients with ITP on developing MK.....	135
Figure 13-7. Interrogating MK - T interaction governed by Immune-related molecules. ....	137
Figure 13-8. Examination of the molecules governing the MK-T cell interaction. ....	138
Figure 14-1. Proposed mechanism of MK-CD8+ T cell interaction.....	147

## 6. Table of Tables

Table 7-1. List of the immune receptors and molecules used by the platelets .....	28
Table 10-1. Lists of the used T cell multi-colour flow cytometric panels. ....	48
Table 10-2. List of antibodies used for Immunohistofluorescent staining. ....	56
Table 10-3. List of fluorochromes detected by the lasers of the widefield microscope. ....	57
Table 10-4. List of antibodies used to track the development of MK. ....	61
Table 11-1. Clinical parameters of the patients with ITP enrolled in this study. ....	71
Table 11-2. Clinical parameters of patients receiving TPO-RAs. ....	71
Table 11-3. Comparison of the frequencies of the CD4 <sup>+</sup> and CD8 <sup>+</sup> T cells positive of the proinflammatory cytokines. ....	82
Table 12-1. Clinical parameters of the patients with ITP enrolled in this bone marrow study. .....	106

## 7. Acknowledgement

I am very grateful to my supervisor Dr Nichola Cooper for her great support, continuous encouragement and help throughout this project, setting an outstanding example of how PhD supervision should be. I would also like to thank my mentor and friend Dr Ahmad Khoder whom I have learnt a lot from and his generous help and support is greatly appreciated.

I would like to extend my thanks to Dr Amna Malik, Dr Luis Gonzales-Huerta, Thomas Mayo and Dr Elisa Luchinni for their help and assistance. Our engaging and thought-provoking discussions have definitely inspired me with great research questions and ideas.

The incredible support of our clinical team of Mrs. Deena Paul, Ms Camelia Vladescu and Ms Alice Glaser in arranging and obtaining patients' consent forms and samples even over the weekends is greatly appreciated. Thank you to all the patients and healthy donors for providing the samples needed for this project.

I would like to express my deepest gratitude to the Centre for Immunology and Vaccinology team especially Dr Nesrina Imami, Dr Peter Kelleher, Dr Alexander Cocker and Mrs Parisa Amjadi for welcoming me into their section. They have demonstrated an invaluable work ethics and set a perfect example of how a research facility should be run. One could not ask for a better place to work at, and without their generous support and insightful suggestions this project would not be where it is now.

Special thanks go to Mr Steven Rothery from Imperial's facility for imaging and light microscopy (FILM) for his tremendous help in developing the macro used to automatically analyse the bone marrow trephines which was the main bulk of the chapter 12.

I would also like to thank our collaborator Dr Beth Psaila from the University of Oxford for her kind help in complementing our findings by sharing with her unpublished findings on megakaryocyte single-cell RNA sequencing.

I would also like to thank Taibah University for providing me with such a generous scholarship to pursuit this PhD.

Last but not least, I am forever in debt to my heroes and role models, my parents; Dr Abdulfattah Sayed and Mrs Aeman Alsayed for believing in me, for their undivided and incessant support and encouragement. I cannot thank enough Bara'ah, my wife, for her patience with me and ongoing support during my crazy working schedule during the last two years.

Thank you to all my family and friends who have made this journey an enjoyable one.

## 8. List of Abbreviations

AA	Aplastic Anaemia
AD	Active Disease
AF	Alexa Fluor
APC	Allophycocyanin
BFA	Brefeldin A
BSA	Bovine Serum Albumin
BV	Brilliant Violet
CCL	CC-chemokine ligand
CD	Cluster of Differentiation
CM	Central Memory
CMV	Cytomegalovirus
CTL	Cytotoxic T lymphocyte
CTLA-4	Cytotoxic T-lymphocyte antigen-4
CXCL	CXC-chemokine ligand
Cy	Cyanine
DAPI	4',6-Diamidino-2-phenylindole dihydrochloride
DC	Dendritic cell
DMEM	Dublecco's Modified Eagle's Medium

DMSO	Dimethyl Sulfoxide
EBV	Epstein-Barr virus
EDTA	Ethylenediaminetetraacetic acid
ELISpot	Enzyme-Linked ImmunoSpot
Elt	Eltrombopag
FACS	Fluorescence-Activated Cell Sorting
FBS	Foetal Bovine Serum
FITC	Fluorescein isothiocyanate
FMO	Fluorescence-Minus-One
FoxP3	Forkhead box P3
GnB	Granzyme B
GP	Glycoprotein
GVHD	Graft versus Host Disease
HC	Healthy control
HIV	Human Immunodeficiency Virus
HLA	Human Leukocyte Antigen
HMGB1	High mobility group protein B1
HSC	Haematopoietic Stem Cell
ICF	Immunocytofluorescence

ICH	Intracranial Haemorrhage
ICOS	inducible T cell co-stimulator
IFN $\gamma$	Interferon- $\gamma$
IHC	Immunohistochemistry
IHF	Immunohistofluorescence
IL-2	Interleukin-2
IPEX	Immune dysregulation, Polyendocrinopathy, Enteropathy, X-linked
ITP	Immune Thrombocytopaenia
IVIG	Intravenous Immunoglobulin
KO	Knockout
LCMV	Lymphocytic Chriomeningitis Virus
L/D	Live/Dead discrimination dye
MEM	Eagle's Minimum Essential Medium
MEP	Megakaryocyte-Erythroid Progenitor
MFI	Median Fluorescent Intensity
MHC	Major Histocompatibility Complex
MK	Megakaryocyte
MMF	Mycophenolate mofetil
MPL	Myeloproliferative Leukaemia

mRNA	Messenger RiboNucleic Acid
NK	Natural killer cells
NOD	Non-Obese Diabetic
ON	Overnight
PAF	Platelet-activating factor
PBMC	Peripheral Blood Mononuclear Cell
PBS	Phosphate-Buffer Saline
PDGF	Platelet-derived growth factor
PD-1	Programmed-Cell Death Receptor -1
PD-L1	Programmed-Cell Death Ligand-1
PE	Phycoerythrin
PerCP	Peridinin Chlorophyll Protein
PLC	Platelet Count
PMA	Phorbol 12-myristate 13-acetate
PMN	Polymorphnuclear leukocyte
Romi	Romiplostim
RPMI	Rosewood-Park Memorial Institute
RT	Room temperature.
RT-PCR	Reverse-Transcription Ploymerase Chain Reaction

Runx1	Runt-related transcription factor 1
SD	Stable disease
SEB	<i>Staphylococcal Enterotoxin B</i>
SI	Staining Index
SLE	Systemic Lupus Erythematosus
TB	<i>Tuberculosis</i>
TCR	T-cell Receptor
Td	Terminally-differentiated
TGF- $\beta$	Transforming Growth Factor- $\beta$
T <sub>h</sub>	Helper T cells
Tim-3	T cell immunoglobulin-3
TLR	Toll-Like receptor
TNF $\alpha$	Tumour Necrosis Factor- $\alpha$
TPM	Transcripts Per Kilobase Million
TPO	Thrombopoietin
TPO-RA	Thrombopoietin Receptor Agonist
Treg	Regulatory T cells
TREM	Triggering Receptor Expressed on Myeloid cells
V450	Violet 450

## 9. Introduction

### 9.1. Adaptive immune system

The immune system has evolved to protect the host from disease-causing particles, known as pathogens. This function is delivered by preventing the entry of the pathogen, eliminating it upon recognition and ensuring little to no permanent damage caused to the host body.

The immune system is broadly classified into the innate immune system; which is considered as the first line of defence against invading pathogens and the adaptive immune system. The adaptive immune system has a highly discriminatory approach in which each cellular clone can detect a single sequence or part of the offending pathogen, known as an antigen. The enormous repertoire of the receptors of the generated cells allows the adaptive immune system to deliver a highly specific response sparing normal host tissue and other non-pathogenic organisms.

One of the prominent features of the adaptive immune response is the development of the immunological memory which the concept of vaccination is based on. This immunological memory enables the immune system to deliver an immediate and more powerful response upon subsequent exposure to the pathogen.

The delivered immune response is dependent on the nature of the causing pathogen and has been classified as either humoral or cell-mediated responses. These responses are broadly delivered by either B or T lymphocytes (or cell), respectively. T cells are heterogeneous subpopulations delivering distinct functions, and they are broadly classified as CD4<sup>+</sup> T helper (T<sub>h</sub>), CD8<sup>+</sup> T cytotoxic (CTL) and regulatory T (Treg) cells (1,2).

### 9.1.1. Normal T cell response

#### 9.1.1.1. CD4<sup>+</sup> T helper (T<sub>h</sub>) cell response.

CD4<sup>+</sup> T<sub>h</sub> cells are crucial elements in the immune system which coordinate other immune cells through a wide array of cytokines. They orchestrate the immune response by influencing the innate immune system, e.g. driving macrophages to ingest pathogens and to secrete further inflammatory cytokines to potentiate the response. T<sub>h</sub> cells also support the second arm of the adaptive immune system, B cells, to differentiate and become antibody-producing plasma cells. T<sub>h</sub> cells also have the capacity to activate the main killing machinery of the immune system, CTL and guide their response (3).

T<sub>h</sub> cells by using their T-cell receptors (TCR) can only recognise their targets if they are presented to them on a major histocompatibility complex class II (MHC-II) by an antigen-presenting cell (APC) such as Dendritic cells (DC). Depending on the nature of the presented peptide, T<sub>h</sub> cells can functionally differentiate into T<sub>h1</sub>, T<sub>h2</sub> or T<sub>h17</sub> characterised by their production of Interleukin-2 (IL-2), IL-4 or IL-17, respectively (4). The proinflammatory T<sub>h1</sub> and the more recently described T<sub>h17</sub> are considered as the hallmark in the pathophysiology of proinflammatory conditions such as systemic lupus erythematosus (SLE) and Hashimoto thyroiditis as they create an inflammatory milieu causing the immune system to be activated and attacking pathogens as well as self-tissue in autoimmune conditions (5,6). T<sub>h2</sub> through its distinct cytokines IL-4 and IL-10 is regarded as the anti-inflammatory subset and it is implicated as the main driver behind of the pathophysiology of allergic conditions such as asthma (4,7).

### 9.1.1.2. CD8<sup>+</sup> cytotoxic T cell response

CD8<sup>+</sup> T cells are the main killing machinery of the adaptive immune system. They were first described in 1974 when Zinkernagel and Doherty demonstrated their expansion in a mouse model infected with lymphocytic choriomeningitis virus (LCMV) (8). These mice had an expanded virus-specific CD8<sup>+</sup> population, which only responded to the viral antigen paired with MHC-I. This specificity has built the basis for the requirement of MHC-I in delivering CD8<sup>+</sup> T cell-mediated response. Callan and colleagues described similar expansion of CD8<sup>+</sup> T cell compartment in patients with infectious mononucleosis, mainly caused by Epstein-Barr virus (EBV) infection (9). Tetramers, which are complexes made of 4 MHC-I molecules bound together has become an essential tool in identifying peptide-specific CD8<sup>+</sup> T cells (10). The use of these tetramers has allowed researchers to characterise peptide-specific CD8<sup>+</sup> T cells in different conditions such EBV, Human Immunodeficiency virus (HIV) and LCMV infections (11–13).

Naïve CD8<sup>+</sup> T cells are primed by DCs i.e. have the antigenic-peptide presented to them on an MHC-I molecule. This priming process usually takes place in the secondary lymphoid organs such as the draining lymph node (14) or spleen (15) leading to phenotypic changes within the CD8<sup>+</sup> population giving rise to an effector population of cells. Once target cells are recognised by the primed cytotoxic CD8<sup>+</sup> T cells (CTL)'s TCR, they bind together via the well-organised tightly-bound immunological synapse. During this binding, CTL secrete preformed Perforin, a cytotoxic molecule that disrupts the membrane of the target cells by forming pores in it allowing CTL to release its cytotoxic granules into them. These cytotoxic granules contain an array of proapoptotic enzymes, including Granzyme A (GnA) and GnB, which upon their release inside the target cell's cytosol activate both the caspase-dependent and independent apoptosis pathways (16,17).

T cells are highly responsiveness cells that they could go through bystander phenotypic changes in response to the circulating cytokines, regardless of their specificity. However, these changes are temporary, and only the presence of the triggering antigen will lead to continuous rounds of expansion to the antigen-specific effector population of the CD8<sup>+</sup> T cells (18).

### **9.1.1.3. Regulatory T cell (Treg) response**

One of the major roles of the immune system is to regulate the immune response, either through preventing the immune cells from attacking host tissues or controlling the immune response after the clearance of the offending pathogen, known as central and peripheral tolerance, respectively (19). Regulatory T cells (Treg) are immunoregulatory CD4<sup>+</sup> T cells that are either generated from the thymus, known as natural Treg (nTreg) or produced peripherally, known as induced Treg (iTreg) (20). Treg cells are phenotypically characterised by their high expression of  $\alpha$ -chain of the IL-2 receptor (CD25) as they are highly responsive to IL-2 depending on it for their differentiation and survival (21). The transcription factor Forkhead box P3 (FoxP3) distinguishes Treg from the rest of CD4<sup>+</sup> T cells, and it is responsible for their development and function. Mouse studies have provided evidence demonstrating the role of FoxP3 in upregulating CD25 and the inhibitory cytotoxic T-lymphocyte antigen-4 (CTLA-4) surface expression and the production of the anti-inflammatory cytokine IL-10 (22,23). FoxP3 significance has been demonstrated either in its specific knockout (KO) or the scurfy mouse mutant that is characterised by massive lymphoproliferation. In human, FoxP3 mutations lead severe autoimmunity manifested as immune dysregulation, polyendocrinopathy, enteropathy, X-linked (IPEX) syndrome (24,25). Treg cells deliver their immunosuppressive function in a contact-dependent and independent manner via its CTLA-4 receptor and the secretion of the anti-inflammatory cytokines IL-10 and TGF- $\beta$ , respectively (26). Given the vital role of Treg in maintaining peripheral tolerance, it is not surprising that its functional, numerical or combined abnormalities have been implicated in a wide array of autoimmune disorders.

Mutations in IL-10 and its receptor has been indicated in early-onset inflammatory bowel disease (27). Studies on non-obese diabetic (NOD) mouse model have demonstrated a reduction in Treg along with its CD25 expression, with similar findings in patients with type 1 diabetes mellitus (28,29).

## **9.2. Programmed death receptor-1 (PD-1) and its ligand-1 (PD-L1) and PD-L2 in normal response and disease.**

Programmed-death 1 receptor (PD-1) and its ligands PD-L1 (CD274) and PD-L2 deliver inhibitory signals to T cells and thus contribute to their regulation, tolerance and prevention of immune-mediated tissue damage. PD-1 is expressed on activated T cells and Treg to contain the immune response and to prevent it from attacking the host tissue after eliminating the offending pathogen. PD-1 is also expressed on B cells and myeloid cells, and its absence has led to widespread autoimmune response characterised as lupus-like glomerulonephritis and arthritis demonstrated in a PD-1<sup>-/-</sup> mouse model (30). PD-L1 and PD-L2 have been described to have distinct expression patterns in lymphoid organs of mice. PD-L1 is expressed in the splenic marginal zone and both the thymic cortex and medulla, whereas PD-L2 is only expressed in the thymic medulla. The co-expression of PD-L1 and PD-L2 has only been found on DC, and hence could be attributed as a feature of a professional APC. Of note, only PD-L1 is expressed on non-haematopoietic organs such as heart, kidney and lungs (31). Disturbance in PD-L1 and PD-L2 has been noted during infectious diseases or autoimmune conditions such as graft-versus-host disease (32). PD-1/PD-L1 axis has been described as a hallmark mechanism of immune evasion in oncological conditions such as breast and ovarian cancers characterised by overexpression of PD-L1 in the tumour microenvironment (33,34). This overexpression of PD-L1 leads to early exhaustion of tumour-specific T cells preventing them from proliferating and delivering their cytotoxic function by interacting with the PD-1 receptor on T cells (35).

On the other hand, downregulation of PD-L1 expression has been implicated in autoimmune disorders. In paediatric patients with SLE, Mozaffarian and colleagues observed a significant reduction of PD-L1 expression on both immature myeloid DCs and monocytes from patients with active disease. Interestingly, this expression did not return to the values of the control cohort until the disease was in the remission state linking PD-L1 expression to disease status (36).

### 9.3. Megakaryopoiesis and platelet production

CD34<sup>+</sup> Haematopoietic stem cells (HSC) mainly in the bone marrow (BM), as well as liver and spleen, give rise through a series of developmental stages to the platelet-progenitors, megakaryocytes (MK). These MKs will eventually release platelets into circulation (37,38). In brief, these developmental stages can be described as four stages as demonstrated. (Figure 7-1).

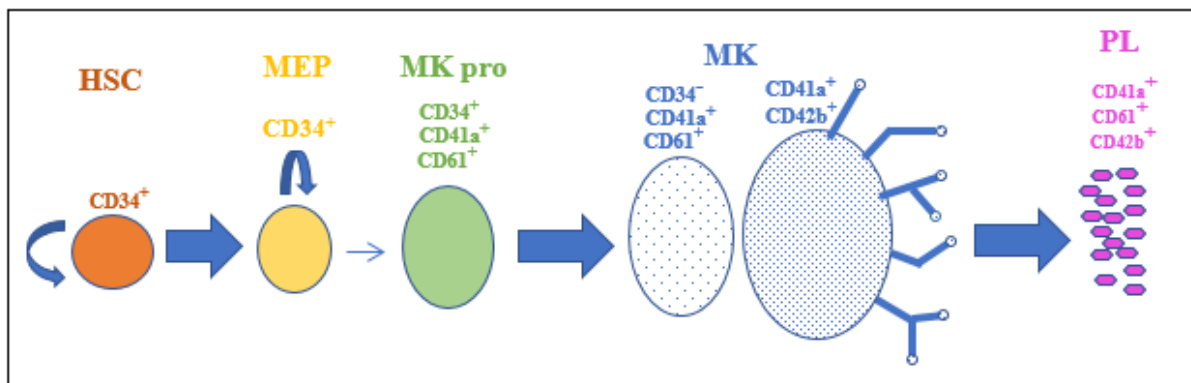


**Figure 7-1. Overview of stages of megakaryopoiesis**

Starting from a self-replicating HSC, they develop and commit to becoming megakaryocyte-erythroid progenitor followed by megakaryocyte progenitor, and eventually proplatelet-forming megakaryocytes. These proplatelets are released into the circulation as platelets.

HSC, haematopoietic stem cell; MEP, megakaryocyte-erythroid progenitor; MK pro, megakaryocyte progenitor (megakaryoblast); MK, megakaryocyte; PL, platelets.

HSCs have a proliferative capacity, allowing them to expand in numbers, and under the influence of specific environmental cues, they commit to becoming megakaryocyte-erythroid progenitor (MEP). This commitment is mediated by the influence of transcriptional factors, such as Runt-related transcription factor 1 (Runx1), and cytokines such as thrombopoietin (TPO). TPO is the main regulator for MK growth and development delivering its function through binding to its receptor myeloproliferative leukaemia protein (c-mpl), or TPO-R (39–41). TPO-related abnormalities could lead to severe thrombocytopenia and life-threatening bone marrow failure (42).

MEP cells continue to expand and are driven predominantly by TPO to become platelet-committed MK-progenitors (MKp), at which stage they lose their proliferative capacity and mature through multiple cycles of ploidy. MKs continue their maturation through endomitosis during which the nuclear content of a single MK of  $2n$ , as it is about to divide, duplicates further to  $4n$  and all the way to  $128n$  without dividing (37,43,44). It has been observed that MK from adult donors were bigger and demonstrated higher degree of ploidy compared to younger donors. However, whether such difference influences the overall platelet production remains controversial (45). These developmental stages of maturation are accompanied by phenotypic changes of the developing MK which can be used to track and compare the different stages of MK development. The surface expression of GP IIb/IIIa (CD41/CD61) has been identified as one of the earliest marker of the unipotent megakaryocytic lineage (46). Some of these phenotypic changes described in mice are demonstrated in figure 7-2.

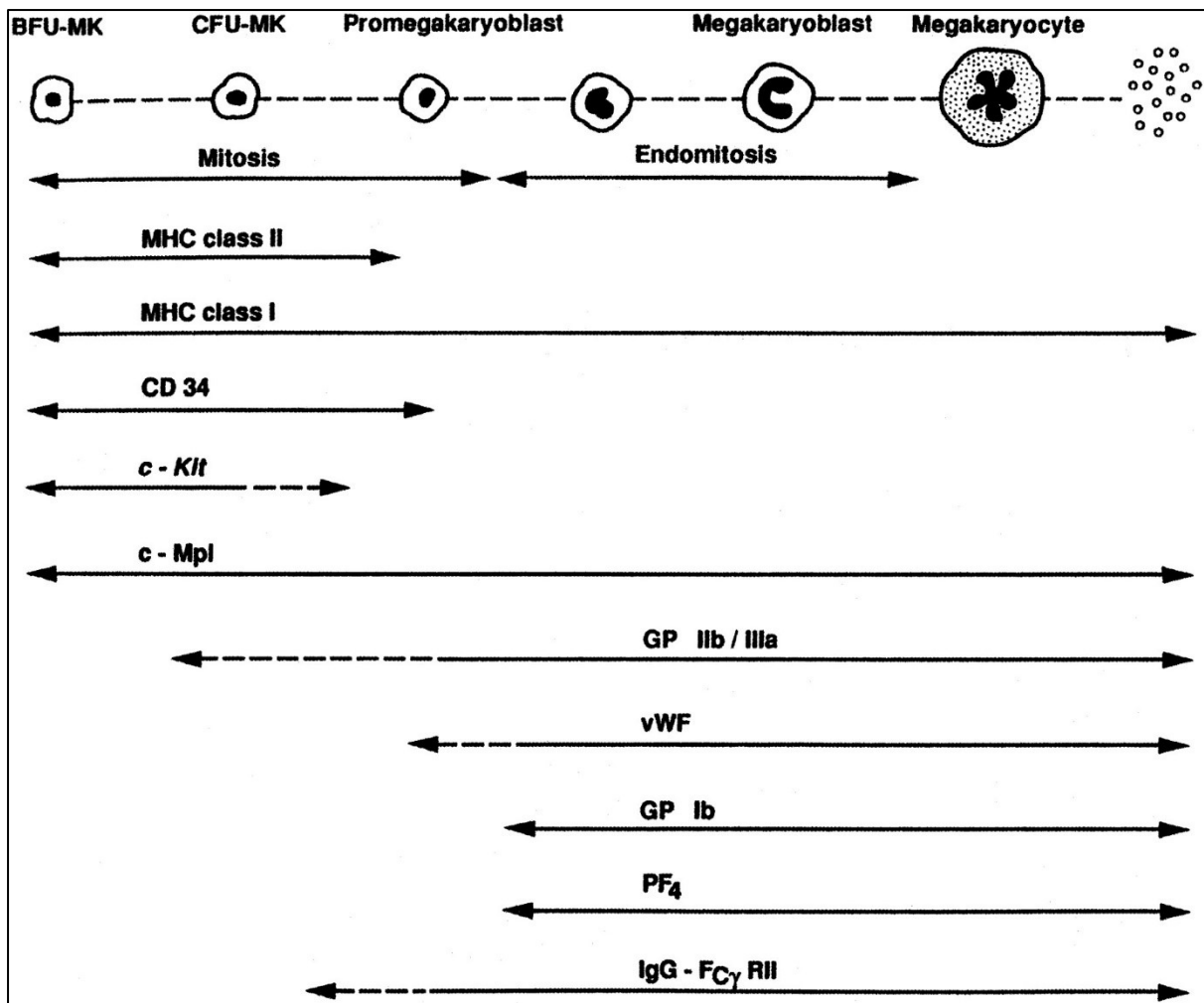


**Figure 7-2. Differentiation markers of the megakaryocytic lineage**

The figure demonstrates the phenotypic changes in differentiating MK from the early BFU-MK all the way through platelets. BFU-MK indicates megakaryocytic burst-forming unit; CFU-MK, megakaryocytic colony-forming unit; GP, Glycoprotein; MHC, major histocompatibility complex; *c-Kit*, cellular *Kit* gene that encodes for the receptor to stem cell factor. Adapted from (47).

MK subsequently develop long external protrusions carrying bulb-like structures at their ends, known as proplatelets, which extend into the vasculature to be eventually released as platelets into the circulation via the sheer force of the bloodstream. This observation was demonstrated by the elegant *in vivo* and live-cell imaging firstly presented by Junt and colleagues (48,49). Proplatelet production is governed primarily by  $\beta$ 1-Tubulin which enables the extension of proplatelets, along with F-actin.  $\beta$ 1-Tubulin abnormalities in human are linked to autosomally dominant thrombocytopaenia (50,51). Another factor enhancing production of proplatelet is fibrinogen which is an extracellular protein abundant around the bone marrow's sinusoids, which effect is also evident as MK cells producing proplatelets when plated on fibrinogen-covered plates (52).

#### **9.4. Role of MK and platelets in immunity**

The principal role of platelets and their progenitors MK has been considered for a long time to be a haemostatic-related function which is delivered via an array of receptors activated upon any detected insult to the endothelium. However, there has been an increasing body of evidence showing platelets and MK to be also involved in the immune response, including both the innate and adaptive immune responses, against different pathogens.

##### **9.4.1. Platelets and their immunological response**

Besides their well-established role in homeostasis, platelets also express a panel of immune receptors and molecules which are actively involved in the immune response against viral and bacterial infections (Table 7-1). Platelets have been demonstrated to have a direct antibacterial effect against bacterial pathogens identified through toll-like receptor-4 (TLR4) receptors, followed by their a direct cytotoxic response delivered by preformed thrombocidins (53). Platelets have also been shown to have an indirect immune response through activating either neutrophils or DC through cytokines, chemokines and TLRs (54). In a hepatitis B mouse

model, platelets were found to be essential in eliminating the virus as their reduction negatively impacted virus-specific CD8<sup>+</sup> T cells recruitment to the liver (55). Their CD154 expression plays an important role in activating neutrophils and supporting B cell differentiation and class-switching (56,57). Platelets also play an immune modulatory role delivered through their microparticles preventing the switch of Treg into T<sub>h17</sub> and the production of the proinflammatory IL-17 (58).

<b>Molecule</b>	<b>Location within platelet and mechanism of release</b>	<b>Functions</b>	<b>Cellular targets</b>
Histamine	Synthesized, location unknown; released during platelet activation	Promotes allergic-type hypersensitivities	Endothelial cells, monocytes, PMNs, NK cells, T cells, B cells, eosinophils
Serotonin (also known as 5-HT)	Dense granules; released during platelet activation	Actions on CNS; promotes coagulation and T cell activation	Monocytes, macrophages, platelets
Thromboxane A2	Plasma membrane	Promotes inflammation and coagulation	Platelets, macrophages, T cells
PAF	Plasma membrane	Promotes inflammation	Platelets, PMNs, monocytes, macrophages
PDGF	α-granules; released during platelet activation	Promotes wound healing	Monocytes, macrophages, T cells
TGFβ	α-granules; released during platelet activation	Growth inhibition; immunosuppression	Monocytes, macrophages, T cells, B cells
CXCL7 (also known as NAP2)	Not known	Chemokine	PMNs
CXCL4 (also known as PF4)	α-granules; released during platelet activation	Chemokine	PMNs, platelets
CXCL1 (also known as GROα)	α-granules; released during platelet activation	Chemokine	PMNs
CXCL5 (also known as ENA78)	α-granules; released during platelet activation	Chemokine	PMNs
CCL5 (also known as RANTES)	α-granules; released during platelet activation	Chemokine	Monocytes, eosinophils, basophils,

			NK cells, T cells, DCs, platelets
CCL3 (also known as MIP1 $\alpha$ )	$\alpha$ -granules; released during platelet activation	Chemokine	Monocytes, eosinophils, basophils, NK cells, DCs
CCL7 (also known as MCP3)	Not known	Chemokine	Monocytes, basophils, NK cells, DCs
IL-1 $\beta$ (and IL-1 precursor protein)	Not known	T cell activation; multiple effects	Monocytes, macrophages, DCs, T cells
HMGB1	Not known	Inflammatory gene regulation	Macrophages, PMNs, endothelial cells
Thrombocidins 1 and 2	$\alpha$ -granules; released during platelet activation	Antibacterial peptides	Bacterial cells
CD40	Plasma membrane	Co-stimulation; endothelial interactions	T cells
CD154 (also known as CD40L)	$\alpha$ -granules and plasma membrane; released and cleaved	Co-stimulation; endothelial interactions	B cells, DCs, macrophages, monocytes, endothelial cells
TLR1, TLR2, TLR3, TLR5, TLR6, TLR7	Plasma membrane	Pathogen detection	PMNs, DCs, macrophages, monocytes, platelets
TLR4	Plasma membrane	Pathogen detection	PMNs, DCs, macrophages, monocytes
TLR9	Unknown internal site; upregulated on plasma membrane during platelet activation	Pathogen detection	PMNs, DCs, macrophages, monocytes
TREM1 ligand	Plasma membrane; expression increased during platelet activation	Pathogen detection	PMNs, DCs, macrophages, monocytes

**Table 7-1. List of the immune receptors and molecules used by the platelets**

List of reported receptors and molecules found in platelets which deliver an immune function via its interaction with different immune cells. CCL, CC-chemokine ligand; CXCL, CXC-chemokine ligand; DC, dendritic cell; HMGB1, high mobility group protein B1; IL-1 $\beta$ , interleukin-1 $\beta$ ; NK, natural killer; PAF, platelet-activating factor; PDGF, platelet-derived growth factor; PMN, polymorphonuclear leukocyte; TGF $\beta$ , transforming growth factor- $\beta$ ; TLR, Toll-like receptor; TREM1, triggering receptor expressed on myeloid cells. Adapted from (54)

#### **9.4.2. MK and their progenitors as antigen-presenting cells (APCs)**

The role of MK and their progenitors in participating in the immune response has not been fully understood. Kang and colleagues were the first to address this using an SLE mouse model (59). In their study, MK progenitors (MKp) induced a proinflammatory  $T_{H17}$  response. A similar study by Finkielsztejn et al. showed that  $CD34^+$  human MKp were capable of inducing  $T_{H1}/T_{H17}$  response in  $CD4^+$  T cells, from both healthy donors and patients with SLE, through presenting autoantigens on their MHC-II molecules (60). Zufferey et al were the first to demonstrate that murine mature MK were capable of capturing foreign antigen, processing it and presenting the antigenic peptide on its MHC-I molecule to  $CD8^+$  T cells (61). In their experiment, they loaded MK with Ovalbumin leading to an active interaction between MK as an APC and OVA-specific T cells, which was assessed by  $CD8^+$  T cell proliferation and activation. Once an MK is loaded with a peptide, this MHC/peptide complex was transferred to the daughter platelets leading to a similar response on the peptide-specific  $CD8^+$  T cells. The expression of MHC-I molecules on mature human MK remain uncharacterized, and MK functionality and regulation as APCs remain to be explored.

#### **9.5. Immune thrombocytopaenia (ITP)**

Seminal studies by Harrington and colleagues (62) first determined the prominent role of serum-derived factors in the pathogenesis of immune thrombocytopaenia (ITP). Subsequent understanding of the importance of antibodies in removing platelets and the role of the extended immune system led to the change in terminology to immune, from idiopathic to immune thrombocytopenia (63). Since then, extensive studies into ITP attempting to understand its aetiology and exact mechanisms have proved to be more complicated than anticipated. This complexity could be attributed to the heterogeneity in the pathogenesis of

ITP. This heterogeneity may result in different progression of disease in individual patients and differential responses to treatment. Elucidation of the pathogenesis of ITP by attempting to understand; whether its due to increased platelet destruction or megakaryocytic abnormalities leading to reduced platelet production, whether it is antibody or T cell-mediated disease, will allow for a better understanding of the pathology of the disease. Correlation of these findings to biomarkers may allow us to improve our categorisation of ITP patients, which will subsequently enable us to choose more specific treatment options. This will spare patients unnecessary adverse effects and improve their quality of life.

### **9.5.1. Definition and Classification**

Primary immune thrombocytopaenia (ITP) is a type II autoimmune heterogeneous disorder defined by a reduction in the platelet count in peripheral blood below  $100 \times 10^6/\text{ml}$ , not associated with any other causes or diseases that can cause such reduction. There is no diagnostic test for ITP. Hence, it is a disease of exclusion.

The incidence rate of ITP is 1.72 – 4.4 per 100,000 people with a higher frequency among females of childbearing age. It occurs most commonly either at childhood (below 4 years) or at older age (above 60) during which it is higher in males (64–66). Paediatric ITP differs from that of adult ITP in that it is usually preceded by a viral infection or vaccination, lasting for few weeks and does not usually require treatment as most cases go into spontaneous remission (67).

ITP classification according to the international working group depends on the duration, rather than the extent of the disease. Patients are classified as; Newly diagnosed ITP, 0 to 3 months; persistent ITP, 3 to 12 months; and chronic ITP, a disease of more than a year duration. The term severe ITP is reserved for those who develop bleeding symptoms requiring medical attention or additional treatment with different medication or higher doses of the current ones.

Refractory ITP patients are those who are refractory to splenectomy and additional standard therapy (63).

### **9.5.2. Pathophysiology of ITP**

Despite the advancements in dissecting the different pathways involved in the pathophysiology of ITP, significant aspects of its pathophysiology remain unexplained. These aspects include the aetiology of the disease, the initiating event leading to this cascade of interactions and identifying key elements in the pathogenesis that could be intercepted leading to the disease resolution.

ITP is a complex disease characterised by a network of interactions between the different elements of the immune system. This could be taking place in the BM, where platelets are produced causing a reduction in platelet production, or in peripheral circulation and spleen where platelets are leading to increased platelet destruction (figure 7-3).

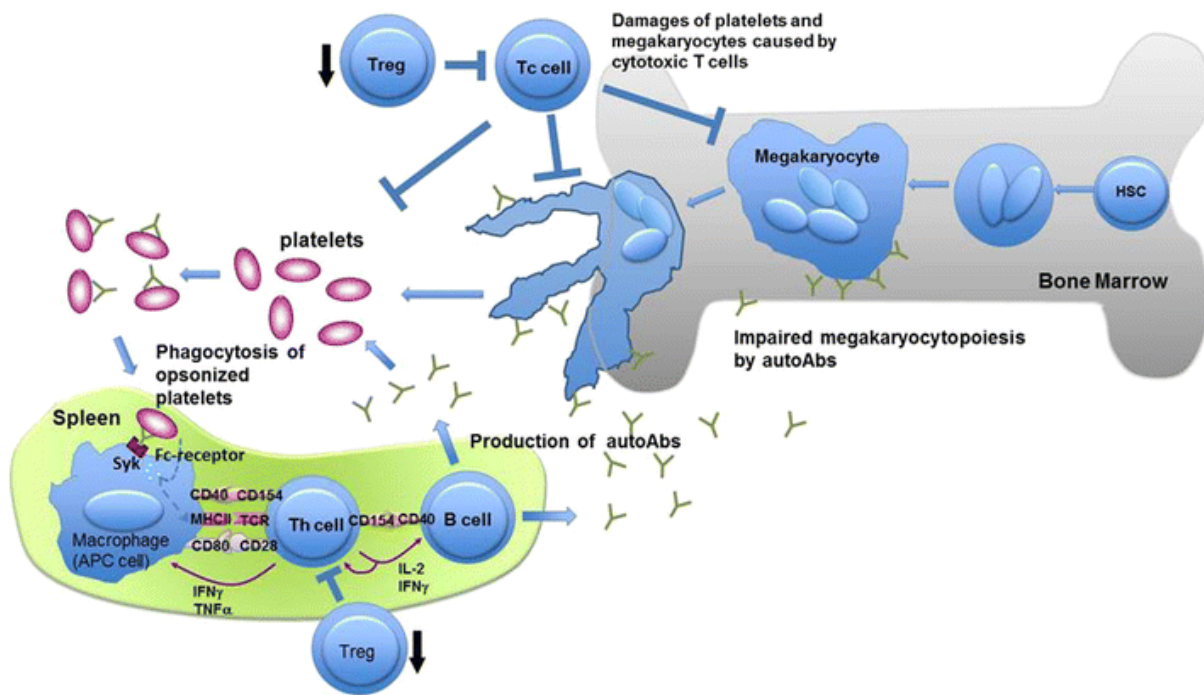


**Figure 7-3. Overview of the proposed current understanding of the ITP pathophysiology**

This schematic graph summarizes key concepts in the current understanding of ITP pathophysiology. The graph shows a network of interactions between platelets, MK and immune cells. The production of platelet and MK specific autoantibodies leads to coating of platelets by these autoantibodies causing them to be destroyed by the macrophages in the spleen. Macrophages in turn present platelet peptides to CD4<sup>+</sup> T<sub>h</sub> cells which in turn further stimulate B cells. Autoantibodies also target the MK in the bone marrow impairing overall platelet production. Cytotoxic T cells ((CTLs - Tc) may also cause direct platelet destruction in the circulation or influence the MK's capacity to produce the platelets, although this is less well established. There is also a reduction in Treg functionality and/or frequency resulting in a break of the peripheral tolerance leading to further damage caused by the immune system against the host platelets and MK. Adapted from (68). APC indicates antigen-presenting cell; autoAbs, autoantibodies; HSC, Haematopoietic stem cells; Tc, CD8<sup>+</sup> T cells.

## 9.5.1. Peripheral blood pathophysiology

### 9.5.1.1. B cell abnormalities

Harrington and his team first described a factor present in the plasma of patients with ITP capable of reducing the number of platelets when transfused to healthy volunteers (62). Subsequent studies showed that this thrombocytopenic effect of ITP plasma was dose-dependent, was accomplished through the immunoglobulin class G (IgG)-rich serum and most probably taking place in the spleen as much higher concentration was needed to mimic such an effect in splenectomised subjects (69). Additional studies managed to characterise these autoreactive antibodies finding them to be directed towards surface GPs present on platelets surface most frequently against GP-IIb/IIIa and could be accompanied by autoantibodies against GP-Ib/IX (70). Anti-GPIIb/IIIa and anti-GPIb/IX are present in the serum around 50% and 34% of chronic patients, respectively (71). Other less common targets may include GPIa/IIa (72).

The current understanding of how autoantibodies deliver their thrombocytopenic effect is based on two major pathways; increasing platelet clearance and reducing platelet production.

The principal site of platelet clearance is the spleen which is the biggest secondary lymphoid organ where most of the antibodies are produced. Hence platelets are highly exposed to autoantibodies when passing through the spleen allowing for faster platelet antibody-mediated elimination. This has been concluded from studies showing rapid uptake of labelled platelets by the spleen and liver, and from the reduction in platelet clearance in patients who have gone through splenectomy (69). These autoantibodies opsonise the platelets to be phagocytosed by splenic and hepatic macrophages which seem to demonstrate an increase in their phagocytic activity through their Fc $\gamma$  receptors (Fc $\gamma$ R). Treatments for ITP such as IVIg and anti-D have been proposed to reduce reticuloendothelial phagocytosis either via a competitive block of

Fc $\gamma$ R or by causing structural changes to these receptors leading to defective clearance of opsonised platelets (73–77).

Understanding the inhibitory mechanism of autoantibodies on megakaryopoiesis has developed over the last decade. Megakaryocytes share some surface markers with platelets such as GPIIb/IIIa and GPIb/IX, which appear at different maturation points making them target for these autoantibodies (78). Morphological studies of megakaryocytes in ITP patients showed abnormal features including extensive apoptotic and para-apoptotic changes with mitochondrial enlargement and nuclear fragmentation (79). Such changes can also be induced when co-culturing megakaryocytes, derived from CD34<sup>+</sup> haematopoietic stem cells (HSC) from healthy donors, with ITP plasma (79,80). *In vitro* studies of autoantibodies demonstrated an inhibitory effect on megakaryopoiesis through interfering with apoptosis and maturation (81,82). More recent studies showed conflicting results showing that ITP plasma instead decreased proplatelet formation (83), while sparing the total number of megakaryocytes, ploidy, cell size and caspase activation status (84)

### **9.5.1.2. T cell abnormalities**

#### **9.5.1.2.1. Proinflammatory T<sub>h</sub> cells**

A number of features of ITP suggest that the autoantibody pathway does not represent the full picture of ITP; transfusing plasma of some ITP patients did not cause the expected thrombocytopenic effect (62); The non-responsiveness of some patients with ITP to the B-cell-depletion therapy, Rituximab, suggests that T cells could deliver the platelet-destroying effect independently of B cells (85). Therefore, it became apparent that it was essential to examine the role of the T cells in ITP.

As with most autoimmune diseases, ITP was first described to be proinflammatory exhibited as Th<sub>1</sub> response in which there is an increase in Interleukin-2 (IL-2), Interferon-gamma (IFN- $\gamma$ ) and IL-10 (86). Later evidence showed a significant increase in Th<sub>17</sub> and other proinflammatory cytokines such as IL-17, IL-18, IL-22 and IL-23(87–90). However, establishing a correlation between these cytokines and disease severity and/or potential treatment outcomes is lacking.

Additionally, these autoreactive T cells appear to be more resistant to apoptosis in active disease than healthy T cells as their DNA microarray analysis shows changes in the apoptotic balance favoring the antiapoptotic state (91). This will prevent the immune system from eliminating these autoreactive T cells leading to an increase in their count which will lead to further autoimmune platelet destruction (92,93).

#### **9.5.1.2.2. CD8<sup>+</sup> T cells**

Olsson and colleagues first noticed direct cytotoxicity of T cells towards platelets, evident as an increase in the destruction of autologous platelets when incubated with T cells from patients with active disease compared to healthy subjects or patients who were in remission (94). This destruction was suggested to be mediated through CD8<sup>+</sup> T cells and was accompanied by increased expression of cytotoxicity-related genes such as Apo-1/Fas, Granzyme and Perforin (94,95).

The effect of CD8<sup>+</sup> T cell on MK and megakaryopoiesis remains undetermined. Reports have shown conflicting results with some reports suggesting that CD8<sup>+</sup> T cells are protecting MK (96), while others have shown that CTLs inhibit MK apoptosis leading to an increase in their numbers but limits MK ploidy and overall platelet production (68,97).

#### **9.5.1.2.3. Regulatory T cells**

It has been reported that patients with ITP have a decline in Treg numbers and/or function that correlated with the disease activity in (98,99). The success of treatment has been mainly recorded as a recovery of platelet count, but it has also been associated with a return of Treg function and number to their normal levels, even when its B-cell-depleting therapy showing a link between a potential link between Treg and B cells in ITP pathophysiology (100,101).

#### **9.5.2. Bone marrow pathology in ITP.**

Houwerzijl and colleagues were the first to reported that ITP negatively impacts the structure of MK *in vivo*. Using electron microscopy, they examined showed that MK in patients with ITP exhibit structural changes of apoptotic nature which were not found in healthy subjects. Moreover, to examine whether these changes were specific to ITP, they have grown MK from HSC from healthy donors and co-cultured them plasma from patients with ITP and HC. Co-culturing with patients' plasma led to similar apoptotic changes found in the patients' bone marrow trephines (79).

#### **9.5.3. PD-1, PD-L1 and PD-L2 in ITP.**

The role of PD-1 pathway in the ITP pathophysiology has not been fully explored. Atesoglu and colleagues described serum level of PD-1 to be significantly lower in patients with ITP compared to HC (102). Zhong *et al.* showed similar results of lower mRNA expression of PD-1 and PD-L1 in PBMC from patients with ITP using real-time polymerase chain reaction (RT-PCR) (103). Conflicting results of increased serum levels of PD-1 in patients with ITP has been

demonstrated in a recent study, which was associated with a significantly elevated PD-L1<sup>+</sup> DC (104). These studies described how PD-1 and PD-L1 are dysregulated in the blood suggesting a potential mechanism of imbalanced immune regulation in the periphery. The role of PD-1/PD-L1 and PD-L2 axis dysregulation on megakaryopoiesis remains unexplored.

### **9.5.3. Clinical manifestations of ITP**

The change in the nomenclature ITP from Idiopathic Thrombocytopaenic Purpura to Immune Thrombocytopaenia shifts the emphasis on the thrombocytopaenia in patients rather than the presence of bleeding (purpura) indicating that a huge proportion of patients with ITP are asymptomatic (63). The symptoms in patients with ITP are primarily due to the thrombocytopaenic nature of the disease, which involves bleeding in different forms. Skin petechiae and purpura could appear in dependent areas of the body resulting in micro-bleeding accumulating under the skin (105). Epistaxis is another symptom of ITP, which may serve as an indicator of more serious bleeding if it required intervention to be stopped. More rare symptoms could occur in the form of severe haemorrhage such as intracranial haemorrhage (ICH), heavy menstrual bleeding, haematuria and evident gastrointestinal bleeding. These severe haemorrhages were demonstrated in a systematic review of clinical studies to occur in 1.4% for the ICH and 9.4% for the other forms of haemorrhages (106). Although patients with very low platelet count ( $<10 \times 10^9/L$ ) are more likely to have bleeding symptoms, potentially severe ones, such correlation between platelet count and bleeding has not been firmly established (107).

Although it is still not clearly understood, fatigue was also found to be a common problem among different cohorts of patients with ITP which became more debilitating with lower platelet counts (108). The impact of ITP on patients was self-reported in a study including

1491 patients from 12 countries, demonstrating how ITP affected several aspects of patients' daily lives. Patients with ITP reported a decrease in energy levels, capacity to exercise and ability to perform daily tasks. Furthermore, patients also reported that ITP had a great toll on their work productivity, social life and emotional well-being. Taken together, these findings suggest that ITP significantly impair patients' quality of life (109).

#### **9.5.4. Treatment**

Immunosuppression is the cornerstone of ITP treatment. First line of treatment for ITP includes steroid and IVIG, which are considered as rescue therapy for rapid correction of the thrombocytopenia. Anti-D is an effective treatment that is used when IVIG cannot be used. For those who do not go into an immediate remission and develop persistent ITP, other steroid-sparing agents are considered. The international working group and the American Society of Hematology ITP treatment guidelines included an array of different treatments as second-line treatment options including splenectomy, agents which target T cells such as immunosuppression (Mycophenolate mofetil; MMF), B cells (rituximab) and more recently agents which stimulate the bone marrow to produce more platelets (thrombopoietin receptor agonists; TPO-RAs) (63,110,111).

Splenectomy has been considered an effective treatment for ITP on the based on the evidence that it is the main site of platelet destruction, leading to remission in up to two-thirds of the patients (112). Given, its irreversible nature and the associated life-long risk of infection and increased risk of thrombo-embolic events, it is currently avoided and a trial of other second-line treatments is given before proceeding to splenectomy (113).

Rituximab, B-cell depleting agent, is a useful therapy in patients who do not respond to first-line treatment or needs higher doses to increase their platelet count. Given its nature of

targeting B cells, it is characterised by its long effect and could lead to longer periods of remission compared to other treatment modalities (114). Although Rituximab is not effective in all patients, Rituximab could achieve remission of up to 70% depending on the treated cohort and the timing of the treatment (115).

The variety of responses to these diverse agents and the failure to identify antiplatelet antibodies in all patients with ITP leads us to believe there may be different pathologies in individual patients. To dissect these causes, we need a better understanding of the interaction between platelets and their precursors the megakaryocyte and the immune system.

#### **9.5.4.1. Thrombopoietin receptor agonists.**

As the mainstay of ITP treatment is immunosuppressive therapy, and due to its chronic nature with a successful response to therapy varying between 20-70%, it is inevitable that most patients with ITP suffer from long-standing side-effects from these agents (85,116). Therefore, there was a need to develop new agents that correct the thrombocytopaenia without these unwanted immune-related side effects. Recombinant TPO agents have been developed to correct thrombocytopaenic disorders, including ITP, and was successful initially until the development of autoantibodies to TPO leading to further worsening of the cases. So, there was a need to develop thrombopoietic agents that stimulate platelet production without eliciting an autoreactive response leading to the development of two currently used TPO-RAs Romiplostim (Romi) and Eltrombopag (Elt) (117).

#### 9.5.4.1.1. Eltrombopag (Elt)

Elt is a small-molecule considered as second-generation TPO-RA due to its capacity to stimulate TPO-R downstream signalling pathway. Elt differs from Romi in that it binds to the transmembrane and juxtamembrane region of the TPO-R, in contrast to endogenous TPO and Romi which only binds to the extracellular domain binding site of TPO-R (117–119). This binding capacity of Elt prevents it from competing with TPO on the receptor allowing for a potential additive or even synergistic effects. Elt is highly specific, it does not activate cell lines that are responsive to other growth factors, and it is species-specific activating TPO-R only in human and chimpanzees (120). Elt delivers its function through TPO-R via activating both JAK2 and STAT5 from early HSC all the way through mature MK. It drives early HSC into committed MK-P in a dose-dependent manner, and it supports MK-P proliferation and differentiation into mature MK (121). The use of Elt has also been reported to have immunomodulatory effects which might explain how some patients with ITP achieve sustained response after discontinuing therapy (122). Treg function and frequency has been reported to improve post-treatment with Elt. It also has an impact on B cell function via reducing plasma levels of APRIL in patients with ITP (100,123). Bart-Smith and colleagues were also the first to report a CD4-mediated effect in a case report of severe aplastic anaemia with HIV infection being successfully treated with Elt, resulting in an increased Treg/T<sub>h</sub> ratio (124). One of the mechanisms by which Elt could deliver its off-target effects has been attributed to its superior iron-chelating property compared to other clinically-used iron chelators (125). However, these clinical observations do not take into consideration that the recovery of platelets could potentially influence the immune system, either by direct suppression or exhausting the immune cells leading to a sustained remission after discontinuing the treatment.

#### **9.5.4.1.2 Romiplostim (Romi)**

Romiplostim is a recombinant fusion protein which is made of two identical subunits. Each unit is made of a human IgG1 Fc domain linked at the C terminus to a peptide which contains multiple TPO-R binding domains. The 60Da Romi is characterised by its prolonged half-life, due to the presence of the Fc domain, and there is no homology to endogenous TPO and thus preventing the development of autoantibodies against endogenous TPO described previously (1–3).

Romi delivers its function via binding to the extracellular domain of the TPO-R in a competitive manner with endogenous TPO. This binding results in potent downstream activation of the TPO-R pathway including tyrosine phosphorylation of Mpl, JAK2 and STAT5. This activation supports megakaryocytic colony formation and maturation (2). The first study of Romi in human showed efficacy and well tolerability in healthy volunteers with promising results of its use in patients with ITP (4). This was followed by two studies in the US and Europe assessing the efficacy of Romi in patients with ITP which showed very good response and tolerance to the treatment (5,6).

Treatment with Romi showed significantly better outcomes in adult patients with ITP in the form of platelet response, lower treatment failure, less bleeding events and fewer blood transfusions needed compared to those receiving the medical standard of care (7). Currently, it is considered as second-line treatment for adult patients with ITP (8,9). Recent evidence also suggested that Romi is also effective in treating paediatric ITP (10,11), however, further work is still needed to determine its long-term efficacy and remission in children.

Romi was also reported to correct thrombocytopaenia in conditions other than ITP, such as in myelodysplastic syndromes, in which it led to reduced bleeding events and platelet transfusion without any immunomodulatory influence on the progression of disease (12).

## 9.6. Research hypothesis and aims

CD8<sup>+</sup> T cells play an important role in the pathophysiology of ITP, both in peripheral circulation as well as in the bone marrow. This pathogenic role is possibly due to break in the immune regulation of MK-T cell interaction leading to an autoreactive response. The use of TPO-RA may have an off-target immunoregulatory effect on CD8<sup>+</sup> T cells.

### 9.6.1. Aims

- a) Phenotype patients with ITP based on their T-cell profiles which will be further associated with their disease severity and treatment options.
- b) Investigate *in vivo* bone marrow pathology by staining bone marrow trephines looking for potential T-cell and MK abnormalities.
- c) Establish *in vitro* megakaryopoiesis assay to interrogate the immune regulatory mechanism governing the possible interaction between MK and autoreactive T cells.
- d) Examining the effect of TPO-RAs, Elt and Romi, on the functionality of CD8<sup>+</sup> T cells *in vitro*.

## **10. Materials and methods**

### **10.1. Patients and Controls**

Sixty ITP patients attending the Imperial Haematology department have been enrolled into the UK ITP registry. Patients are diagnosed based on previously established criteria (63). For the purpose of this study, subjects with concurrent infections such as Hepatitis B, Hepatitis C or HIV and secondary thrombocytopaenia were excluded. Of these patients, 20 patients have had bone marrow aspiration and trephines and 40 patients have had their PBMC and plasma samples stored in the Imperial Tissue Bank at different stages of disease.

Thirty healthy age and gender matched controls with normal platelet count ( $150 - 450 \times 10^9/L$ ), who worked at the Centre for Haematology or relatives of the patients, who were not receiving any steroid or immunosuppressive therapy were included in the study.

Both Patients and control samples were obtained after written informed consents were given and samples were stored at Imperial College Healthcare Tissue Bank. This study was done in accordance to The Multi Centre Research Ethics Committee in Wales guidelines MREC Wales reference 07/MRE09/54: R12039, R12033.

### **10.2. Plasma and Peripheral Blood Mononuclear Cells (PBMC) Isolation.**

Venous Blood was collected in Vacutainers coated with either Heparin or Ethylenediaminetetraacetic acid (EDTA; BD Bioscience, Oxford, UK) and processed on the same day of collection under a sterile condition. Blood vacutainer was spun at 800g for 10 minutes at room temperature (RT) and 1 ml of the separated plasma was collected in a cryovial and kept in the  $-80^\circ\text{C}$  freezer. PBMC were separated and isolated using a standard density gradient centrifugation protocol. Briefly, blood was diluted with phosphate buffered saline

(PBS; Sigma-Aldrich, Dorset, UK) at 1:1 ratio. The blood-PBS was layered gently on top of Histopaque (Sigma-Aldrich) at 2:1 ratio and tubes were centrifuged at 500g for 20 minutes at RT without brakes. Then, the separated PBMC layer was isolated and washed once by centrifuging PBMC in PBS at 300g for 5 minutes at 4°C. Cells were then resuspended in a freezing buffer made of 10% dimethyl sulfoxide (DMSO; Sigma-Aldrich) in foetal bovine serum (FBS; Life Technologies, Paisley, UK) stored in -80°C freezer.

### **10.3. PBMC Surface Staining**

Frozen vials of PBMCs were thawed in 37°C water bath for 2 minutes and then washed with prewarmed complete medium (CM) made of Rosewood-Park Memorial Institute (RPMI) 1640 medium supplemented with L-Glutamate (Sigma-Aldrich), 10% FBS (Life Technologies), 100U/ml of Penicillin/Streptomycin (Fisher Scientific, Loughborough, UK) and Eagle's minimum essential medium (MEM) non-essential amino acid solution (Sigma-Aldrich). Cells are cultured in CM and rested overnight (ON) in a 37°C humid incubator with 5% CO<sub>2</sub> at a seeding density of 400,000 cells/ml. Cells are harvested and washed in cold PBS at 300g for 5 minutes and counted using trypan blue exclusion method.

500,000 cells in a total volume of 100 µl are stained in 5-ml polypropylene FACS tubes and stained with Live/Dead exclusion dye (Thermo Fisher Scientific, Waltham MA, United States) for 15 minutes at RT in the dark. Cells are washed once with 1 ml of cold PBS and after removing supernatant cells were stained with a panel of titrated primary conjugated antibodies against surface markers at 4°C for 20 minutes in the dark. Cells are washed again and resuspended in 300 µl for analysis.

#### **10.4. FoxP3 and PBMC Intracellular Cytokine Staining**

To stain the Treg transcription factor, FoxP3, 1 million cells are stained with L/D exclusion dye and the Treg surface staining panel (Table 2-1). Cells then fixed and permeabilised using the FoxP3/Transcription factor staining buffer set (ThermoFisher Scientific) according to manufacturer's instruction. Briefly, cells are fixed with 500 µl of Fix/Perm buffer for 30 minutes at RT in the dark and then 500 µl of the permeabilization buffer is added to the FACS tubes and washed at 500g for 4 minutes at RT. After removing the supernatant carefully, cells are washed once with the permeabilization buffer. Cells are then stained with a conjugated anti-human FoxP3 antibody (eBioscience, Hatfield, UK) and incubated for 30 minutes in the dark at RT. Cells are washed twice with permeabilization buffer after FoxP3 staining and then resuspended in 300 µl of PBS for flow cytometric analysis. All the antibodies used in this study were purchased from Abcam (Cambridge, UK), Biolegend (London, UK), BD Bioscience, eBioscience, Life Technologies Ltd. and AbD Serotec (Kidlington, UK).

#### **10.5. Flow Cytometric Panel Design and Antibody Titration**

Designing a multi-colour flow cytometric panel requires choosing antibodies conjugated to different fluorochromes that target certain markers in order to identify desired populations and describe certain functional aspects of the cells. The choice of the fluorochromes conjugated to the used primary antibodies was based on a converse relation between the brightness of the fluorochromes and the abundance of the target antigen on the cells. For example, the fluorochromes for the abundant CD3 were selected to be mostly dim such as Peridinin Chlorophyll Protein (PerCP) or Violet 450 (V450) whereas fluorochromes for the less frequent targets such as CD25 or CD45RA were chosen to be very bright such as Phycoerythrin (PE) or PE-Cyanine (Cy)7. Care was taken to avoid fluorochromes with a complete spectral overlap such as Fluorescein isothiocyanate (FITC) and Alex Fluor (AF) 488 or Allophycocyanin (APC)

and AF647. The list of antibodies used in the different panels in this study are summarised (Tables 10-1).

<b>Panel</b>	<b>General T cell subsets</b>							
<b>Fluorochrome</b>	V450	FITC	APC	PE	PE-Cy7	V500	Brilliant Violet (BV) 605	V711
<b>Laser (Excitation wave length in nm)</b>	Violet (V;405)	Blue (B;488)	Red (R;633)	Yellow/Green (YG; 561)	YG561	V405	V405	V405
<b>Detector Band Pass</b>	450/50	525/50	660/20	575/26	780/60	525/50	610/20	720/40
<b>Antigen</b>	CD3	CD4	CD8	CD45RA	CD62L	L/D Dye	PD-1	Tim-3
<b>Strain</b>	Mouse	Mouse	Mouse	Mouse	Mouse	N/A	Mouse	Mouse
<b>Isotype</b>	IgG2a, κ	IgG2b, κ	IgG1, κ	IgG2b, κ	IgG1, κ	N/A	IgG1, κ	IgG1, κ
<b>Amount of used antibody (µl)</b>	1	2	1	1	1	0.5	2	2

Panel	Regulatory T cells					
Fluorochrome	V450	PE-Cy7	PE	FITC	APC	V500
Laser (Excitation wave length)	V405	YG561	YG561	B488	R633	V405
Detector Band Pass	450/50	780/60	575/26	525/50	660/20	525/50
Antigen	CD3	CD4	CD25	CD127	FoxP3	L/D Dye
Strain	Mouse	Mouse	Mouse	Mouse	Rat	N/A
Isotype	IgG2a, $\kappa$	IgG2b, $\kappa$	IgG1, $\kappa$	IgG1, $\kappa$	IgG2b, $\kappa$	N/A
Amount of used antibody ( $\mu$ l)	1	2	2	2	2	0.5

Panel	General T cell Proinflammatory Intracellular Cytokines							
Fluorochrome	PerCP	FITC	PE	PE-CF594	APC	V500	V450	AF700
Laser (Excitation wave length)	B488	B488	YG561	YG561	R633	V405	V405	R633
Detector Band Pass	675/20	525/50	575/26	610/20	660/20	525/50	450/50	695/40
Antigen	CD3	CD4	IFN $\gamma$	IL-2	CD8	L/D Dye	IL-17A	TNF $\alpha$
Strain	Mouse	Mouse	Mouse	Mouse	Mouse	N/A	Mouse	Mouse
Isotype	IgG2a, $\kappa$	IgG2b, $\kappa$	IgG1, $\kappa$	IgG1, $\kappa$	IgG1, $\kappa$	N/A	IgG1, $\kappa$	IgG1, $\kappa$
Amount of used antibody ( $\mu$ l)	1	2	2	2	2	0.5	2	2

<b>Panel</b>	<b>CD8<sup>+</sup> T cell Proinflammatory Intracellular Cytokines</b>							
<b>Fluorochrome</b>	PerCP	APC	PE	PE- CF594	FITC	V500	BV421	AF700
<b>Laser (Excitation wave length)</b>	B488	R633	YG561	YG561	B488	V405	V405	R633
<b>Detector Band Pass</b>	675/20	660/20	575/26	610/20	525/50	525/50	450/50	695/40
<b>Antigen</b>	CD3	CD8	IFN $\gamma$	IL-2	Granzyme B	L/D Dye	Perforin	TNF $\alpha$
<b>Strain</b>	Mouse	Rat	Mouse	Mouse	Mouse	N/A	Mouse	Mouse
<b>Isotype</b>	IgG2a, $\kappa$	IgG1, $\kappa$	IgG1, $\kappa$	IgG1, $\kappa$	IgG2b, $\kappa$	N/A	IgG2b, $\kappa$	IgG1, $\kappa$
<b>Amount of used antibody (<math>\mu</math>l)</b>	1	2	2	2	2	0.5	2	2

**Table 10-1. Lists of the used T cell multi-colour flow cytometric panels.**

Tables demonstrating the different flow cytometric panels used in staining T cells to detect describe their subsets as well as assessing their functionality. The tables highlight antibodies' fluorochromes, target antigen, strain, isotype and amount used in staining.

## 10.6. Antibody Titration

Antibody titration is essential to determine the optimal concentrations of various primary conjugated antibodies used in a single panel that would best separate the cell populations of interest. The optimum titre or dilution is the concentration which produces the highest resolution of the desired populations, measured by high staining index with minimum background / nonspecific binding and with minimal loss of population positivity. Titration requires staining the same number of cells in a similar total volume with serial concentrations of the same antibody to determine which concentration gives the best signal of positive population (Figure 10-1). This is determined by calculating the staining index (SI) which is the difference between the positive and the negative mean fluorescent intensity (MFI) divided by the standard deviation (SD) of the negative population doubled.

$$\text{Staining index (SI)} = \frac{\text{MFI (+ve population)} - \text{MFI (-ve population)}}{2 \times \text{SD}(-\text{ve population})}$$

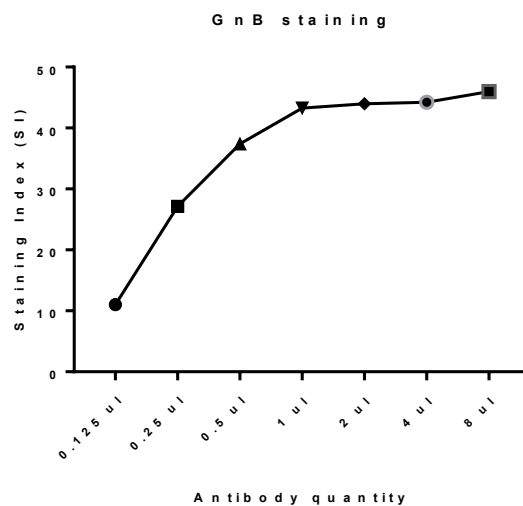


**Figure 10-1. Example of Grnazyme B (GnB) antibody titration.**

The graph demonstrates the difference in SI of GnB when using different quantities of the antibody. For this antibody, 2 ul was determined to be the optimal concentration after which the curve plateaus indicating no extra benefit is gained by increasing the antibody quantity.

## **10.7. Setting the Gating Strategy in Flow Cytometric Analysis.**

The identification of cell populations in flow cytometry depends on the separation of the positive events from the negative ones with respect to each of the study markers. However, in a multicolour panel this could be challenging as the spectral overlap between the fluorochromes could influence the signal resolution. Therefore, the use of appropriate controls is essential to distinguish between a true positive signal and a spill of a different fluorochrome into the channel of the fluorochrome of interest. In this study, we have adopted the fluorescence-minus-one (FMO) (126,127), defined as staining the sample with all the fluorochromes except the one of interest e.g. FITC FMO control would be stained with all fluorochromes except FITC. The use of such controls allows for consistent unbiased gating strategy in the panels used in this study (Figure 10-2). Although certain markers can be easily distinguishable from each other such as CD4<sup>+</sup> and CD8<sup>+</sup> in T cells, it could be more challenging distinguish other parameters such as CD45RA and CD62L (Figure 2-2).

## FMO Control

## Stained sample

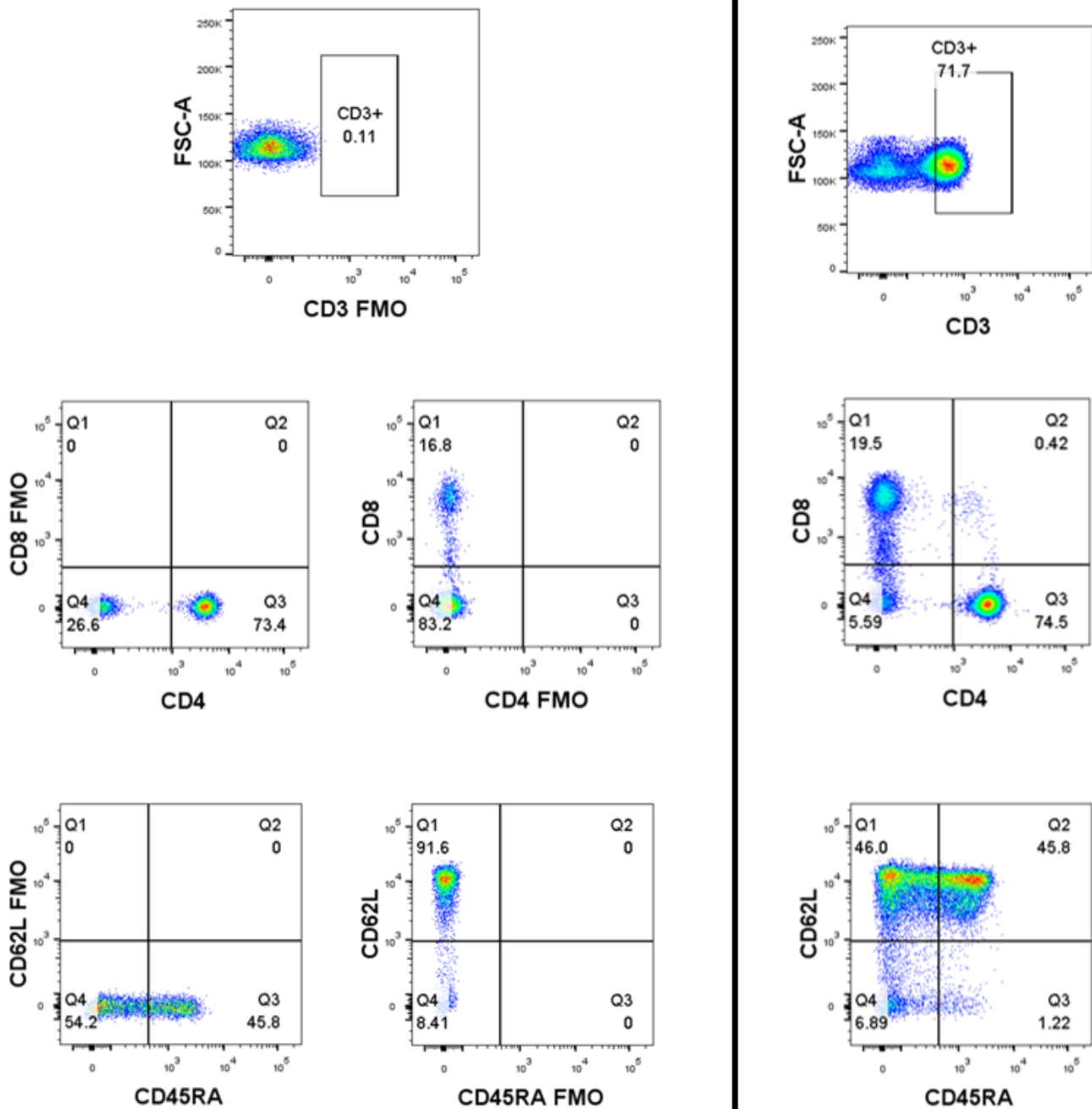


**Figure 10-2. Setting the gating strategy in a multicolour panel based on fluorescence-minus-one controls.**

Dot plots demonstrate an example of using FMO controls to determine gates' positions in a multicolour panel made of CD3, CD4, CD8, CD45RA and CD62L conjugated with different fluorochromes with partial spectral overlap.

## 10.8. Flow Cytometric Analysis and Cell Sorting

To set up the BD LSR II cytometer (BD Bioscience) used in our study, unstained cells were used to setup the limit for negative staining and count for any possible cellular autofluorescence. BD Compensation beads (BD Bioscience), both positive (capable of binding to antibodies) and negative (unable of binding to antibodies) were used to setup the proper voltages for each fluorescent channel and to ensure minimum spill over between fluorochromes' detectors (Figure 10-3). Once voltages are set properly and the gates are set using FMO controls (Figure 10-2), a minimum number of 50,000 events (cells) are acquired and recorded per sample using BD FACSDIVA software (BD Bioscience) and analysed using FlowJo software (Tree Star, Oregon, United States).

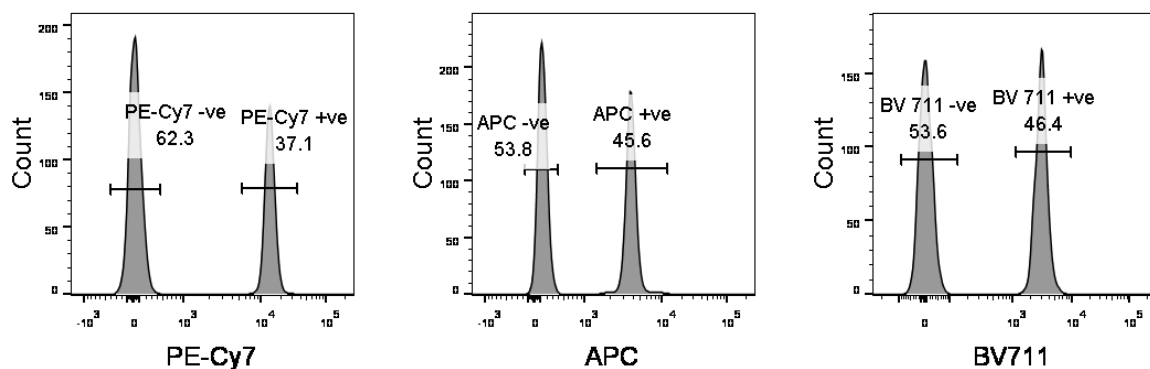


**Figure 10-3. Using compensation beads for setting up voltages.**

Histograms demonstrating the separation between the positive and negative staining of the beads. (A) Examples of staining positive and negative beads by fluorochromes on excited by the cytometer yellow-green laser e.g. PE-Cy7, (B) by the red laser such as APC or (C) by the violet laser like BV711.

For flow cytometric cell sorting, similar setup was used to set gates (Figure 10-2) and voltages (Figure 10-3) to sort the specific CD8<sup>+</sup> T cell subsets used in this study. CD8<sup>+</sup> T cell subsets were 4-way sorted using the BD Aria III sorter (BD Bioscience) on purity mode allowing for a purer population at a slower sorting speed. Purity checks were performed at the end of each sorting sessions to ensure high purity population; typically 95%.

### **10.9. IFN $\gamma$ Enzyme-Linked ImmunoSpot (ELISpot) Assay**

IFN $\gamma$  ELISpot assay was performed in a sterile condition according to the Chelsea and Westminster Hospital Immunotherapy Group standard operating procedure for 'IFN $\gamma$  ELISpot Assay for Quantifying Release of Cytokines from PBMC when Stimulated with Recombinant Ag or Overlapping Peptides' established by Dr Imami and colleagues. Briefly, the assay was performed on Millipore 96-well PVDF plates (Fisher Scientific) which was coated with the anti-human IFN $\gamma$  capture antibody (Mabtech, Nacka, Sweden) diluted in sterile PBS and incubated ON at 4°C. Plates were washed and blocked with 10% heat inactivated, screened human male AB serum (Sigma-Aldrich) in sterile PBS for 1 hour at RT. After removing the blocking buffer, PBMCs were then incubated in CM (with 20% heat inactivated human male AB serum instead of the 10% FBS) and were cultured either alone, with platelets or with a *Staphylococcal Enterotoxin B* (SEB) as a positive control for 40 hours in 37°C humid chamber with 5% CO<sub>2</sub>. Plates were washed and incubated with biotinylated anti- IFN $\gamma$  detection antibody (Mabtech) and incubated ON at 4°C. Plates were washed and incubated with Streptavidine-alkaline phosphatase conjugate for 1 hour at RT. After washing the plates, they were incubated with a freshly-made chromagen (Bio-Rad, Hertfordshire, UK) and incubated for 10 minutes at RT and then washed off. All the washing steps were consisted of 6-times wash by sterile PBS. The plates were finally left to dry at RT away from light and were analysed using Zeiss Compact ELISpot Reader (Zeiss, Oberkochen, Germany).

### **10.10. *In Vitro* culture of PBMC with thrombopoietin receptor agonists (TPO-RAs).**

The two clinical-grade TPO-RAs; Elt, known as Revolade (GlaxoSmithKline, Brentford, UK) and Romi, known as Nplate (Amgen, California, United States) were used in an *in vitro* culture in this study. A single 50 mg Elt tablet was dissolved in 50 ml of prewarmed CM to prepare a 1mg/ml solution and was filtered twice in 40 µm mesh (Sigma-Aldrich) to remove any solid additives that might impact the culture. Isolated PBMC were stimulated with functional azide-free anti CD3/CD28 antibodies (Biolegend) and cultured with serial concentrations of Elt (7.5µg/ml, 18.75µg/ml, 31.25µg/ml, 62.5µg/ml and 125µg/ml) ON in a 37°C incubator with 5% CO<sub>2</sub>. Two Hundred and fifty micrograms of Romi was dissolved in 250 µl of CM to prepare 1µg/µl solution of Romi and was filtered once through 40µm mesh. Stimulated PBMCs were cultured with 31.55µg/ml of Romi ON in 37°C incubator. Cells were washed and stained with the 'CD8<sup>+</sup> T cell Proinflammatory Intracellular Cytokines' panel described previously (Table 8-1).

### **10.11. Bone Marrow Preparation for Histological Examination.**

Bone marrow trephines were prepared in the histopathology department at Hammersmith Hospital where sections were cut at a thickness of 5µm and mounted on slides, fixed and Paraffin-embedded to be stored. To stain these trephines, slides were first deparaffinised in a step-wise protocol starting with Xylene followed by serially diluted Ethanol (Xylene with Ethanol, 100% Ethanol, 95% Ethanol, 70% Ethanol, 50% Ethanol) (Sigma-Aldrich). Each step consisted of keeping the slides in a Coplin jar for 3 minutes and slides were finally washed with water for 5 minutes. Antigens were retrieved using heat-induced epitope retrieval method. Slides were kept in an antigen-retrieval buffer made of 0.01 M trisodium citrate or Tris-EDTA

(Sigma-Aldrich), and heated in a microwave for 20 minutes. Slides were left to cool down at RT for 5 minutes in the buffer and then washed once with the washing buffer (1% TWEEN (Sigma-Aldrich) in PBS) for 5 minutes. Care was taken not allow the slides to dry as this would impact the integrity of the tissue and subsequently the staining.

### **10.12. Bone marrow trephines Immunohistofluorescent (IHF) staining.**

After deparaffinising and hydrating the trephines, sections were blocked with 1% Goat serum (Sigma-Aldrich)-PBS for 30 minutes at RT.

A total volume of 100 µl of PBS-diluted primary antibodies were added to each slide and incubated ON at RT in the dark in a humid staining chamber to ensure the slides not to dry out. Slides were washed three times with the washing buffer, each wash consistent of keeping the slides in PBS for 5 minutes and then the washing buffer is replaced with fresh washing buffer. PBS-diluted secondary antibodies were added individually, each incubated for an hour at RT in the dark, followed by washing three times before adding the next secondary antibody for the multi-colour staining. Excess washing buffer was wiped off and slides were mounted using Fluoroshield mount (Sigma-Aldrich) and a coverslip (Raymond A Lamb Ltd, Eastbourne, UK) left to settle ON at 4°C in the dark.

A List of antibodies used for Immunohistofluorescence (IHF) is provided (Table 10-2). All antibodies were diluted in PBS at an optimum concentration prior to staining and they were purchased from Abcam, Biolegend, BD Bioscience, eBioscience, Life Technologies Ltd. and AbD Serotec.

Antibody	Strain	Isotype	Fluorophore	Dilution	Vendor
Anti-human IgG2a Isotype control	Rat	IgG2a	Unconjugated	1:50	AbD Serotec
Anti-human IgG1 Isotype control	Mouse	IgG1	Unconjugated	1:50	Biolegend
Anti-human CD4	Mouse	IgG1	Unconjugated	1:50	Biolegend
Anti-human CD8	Mouse	IgG1	Unconjugated	1:50	Biolegend
Anti-human CD4	Rat	IgG2a	Unconjugated	1:50	AbD Serotec
Anti-human CD8	Rat	IgG2a	Unconjugated	1:50	AbD Serotec
Anti-human CD42b	Rabbit	IgG	Unconjugated	1:100	Abcam
Anti-Rabbit secondary antibody	Goat	IgG	Alexa Fluor 488 (AF488)	1:200	Life Technologies Ltd.
Anti-Rabbit secondary antibody	Goat	IgG	AF 555	1:200	Life Technologies Ltd.
Anti-Rabbit secondary antibody	Goat	IgG	AF 647	1:200	Life Technologies Ltd.
Anti-Rat secondary antibody	Rabbit	IgG	AF 488	1:200	Life Technologies Ltd.
Anti-Rat secondary antibody	Rabbit	IgG	AF 647	1:200	Life Technologies Ltd.

**Table 10-2. List of antibodies used for Immunohistofluorescent staining.**

### 10.13. Imaging of the bone marrow trephines and image analysis.

Slides were visualised using the multi-channel Zeiss Axio Observer inverted widefield microscope and Zeiss LSM-780 confocal microscope (Zeiss) using Zen Lite software (Zeiss) to capture the images. Using the tiling function of the widefield microscope, a series of images capturing all regions of the trephine at 20x magnification and then stitched together to produce a combined single large image of the whole trephine. Each region was captured using a set of lasers to detect the different fluorochromes attached to primary antibodies using the appropriate filters as described (Table 10-3).

<b>Fluorochrome of the 2ry antibody</b>	<b>Primary Antibody Marker</b>	<b>LED illumination source</b>	<b>Filter used</b>
<b>AF488</b>	CD42b	LED 470 nm	472/30 (Semrock)
<b>AF555</b>	CD4	LED 540 - 580 nm	534/20 (Semrock)
<b>AF647</b>	CD8	LED 625 nm	631/22 (Zeiss)

**Table 10-3. List of fluorochromes detected by the lasers of the widefield microscope.**

With the help of Mr Stephen Rothery from the Facility for Imaging and Light Microscopy (FILM) at Imperial College London, we developed a macro to analyse captured images. A macro is a list of commands used to perform certain analytical functions (Figure 10-4A), in the open-source software Fiji (University of Wisconsin, Madison, United States) (128). This macro was provided with minimum threshold values of each fluorescent signal to differentiate each stained cell from non-specific background staining (Figure 10-4B). The macro was also provided with a minimum diameter of 20  $\mu\text{m}$  for MK and 5  $\mu\text{m}$  for T cells which eliminated any debris that was stained non-specifically. Provided with these parameters, the macro could

automatically quantify each cell type that were stained in the trephines. To ensure consistency in comparison between the slides, cellular quantification of the stained cells was reported as frequencies which were determined by dividing the number of the detected cells by the area of the imaged tissue.

$$\text{Cellular frequency (cell}/\mu\text{m}^2) = \frac{\text{Number of cells in a trephine}}{\text{Surface area of the tissue}}$$

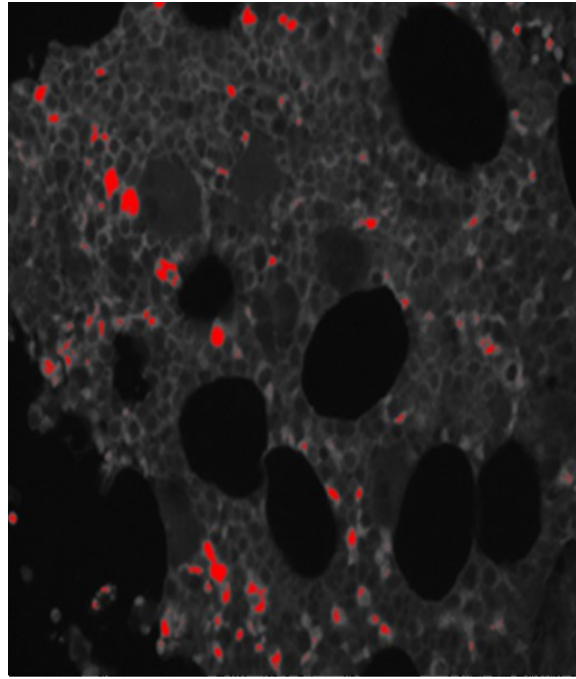
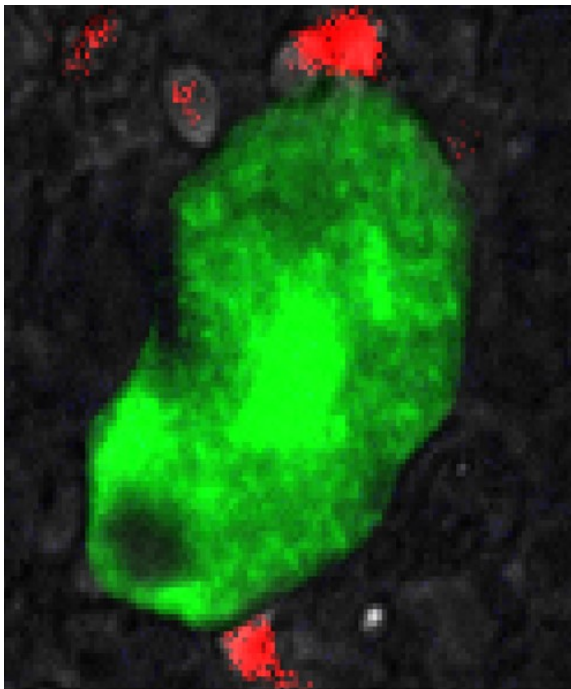
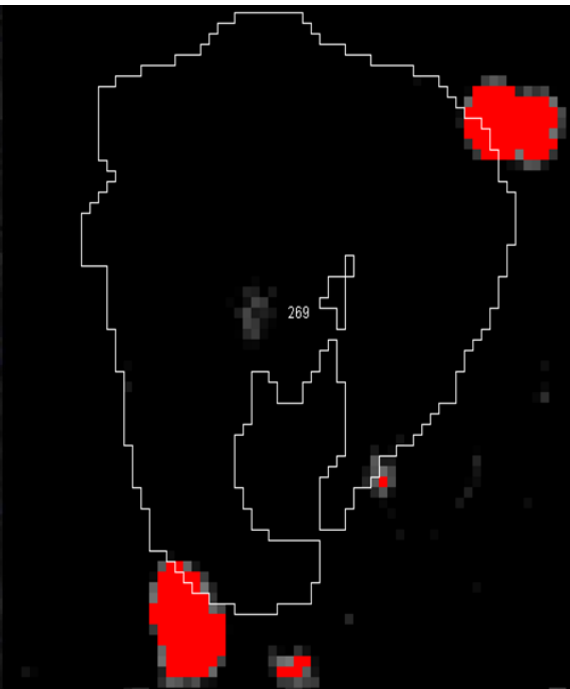
The next important function of the macro was to determine the interaction between MK and T cells in the trephine. Given the fixed nature of the trephines, MK-T cell interaction was determined based on their close distance to each other and reported as immediate proximity (IP). IP was set at the lowest measurable distance at 1 pixel, which equals to 400 nm at 20x magnification, and if a T cell falls within a pixel from a MK it was considered to be in IP (Figure 10-4C). The presence of multiple T cells in IP to a single MK was reported as MK-T cell clustering (Figure 10-4D).

**A.**

```

1 //Initialise
2 run("Clear Results");
3
4 fn=getTitle();
5 rename("temp");
6 run("Split Channels");
7
8 roiManager("Reset");
9
10 //Megakaryocyte measurement and creating ROIs
11 selectWindow("C1-temp");
12 rename("MGK-CD42b "+fn);
13 setAutoThreshold("Default dark");
14 run("Threshold...");
15
16 title = "Threshold";
17 msg = "Set the appropriate CD42b+ threshold \n Press OK to continue";
18 waitForUser(title, msg);
19
20
21 run("Analyze Particles...", "size=50.00-infinity include summarize add");
22
23 n=roiManager("Count");
24 fn = fn + "_" + n + ".roi";

```

**B.****C.****D.**

**Figure 10-4. Macro development to automatically Identify MK and T cells interactions and clustering.**

(A) A macro was developed with a list of a pre-set criteria to (B) identify the cells of interest in a trephine and highlight them in red. (C) A focused field of a single MK (Green) in IP with multiple T cells, which the macro can identify, (D) outline the MK and count the number of clustered T cells.

#### **10.14. Bone marrow aspirate processing and CD34<sup>+</sup> Haematopoietic stem cell selection.**

CD34<sup>+</sup> HSC were either obtained by the Stem Cell Laboratory at the Hammersmith Hospital or isolated from bone marrow aspirate of healthy donors. As previously described (129), CD34<sup>+</sup> HSC were isolated from BM aspirate by positively selecting CD34<sup>+</sup> using anti-human CD34 magnetic separation beads, separation columns and AutoMACS machine (Miltenyi Biotec, Germany) according to the manufacturer instructions. Briefly, mononuclear cells (MNC) were separated from the BM aspirate using density gradient centrifugation similar to isolating PBMC. MNC were washed once with PBS and resuspended in 90 µl separation buffer (PBS, 0.5% BSA and 2 mM EDTA) per 1x10<sup>7</sup> cells and incubated with anti-human CD34 microbeads for 15 minutes at 4°C. Separation columns were washed once with cold separation buffer prior to passing the cells through them. Cells were passed through the columns gently to ensure proper separation of the CD34<sup>+</sup> cells from the MNC. After passing the cells, the columns were plunged with cold PBS to collect CD34<sup>+</sup> cells and a minimum purity of 80% was obtained. Cells were either used for downstream application or resuspended in a freezing buffer to be stored in the -80°C freezer.

#### **10.15. *In vitro* megakaryopoietic assay.**

Frozen CD34<sup>+</sup> HSC cells were thawed for 2 minutes in a 37°C water bath and washed once with prewarmed RPMI 1640 supplemented with 10% FBS. Cells were resuspended in filtered serum-free media StemSpan II (STEMCELL Technologies, Cambridge, UK) supplemented with StemSpan Megakaryocyte Expansion Supplement (STEMCELL Technologies), 50 ηM of human recombinant thrombopoietin (TPO) (Peprotech, London, UK), 10 ηM of human interleukin-1β (IL-1β; Life Technologies) and 500U/mL of Penicillin/Streptomycin (Fisher

Scientific). Cells were plated in a 6-well plate at seeding density of 30,000 cell/ml and incubated in 37°C humid incubator with 5% CO<sub>2</sub> and media was replenished on Day (D5).

### 10.16. Tracking the development of megakaryocytes.

MK development was tracked on D3, D7 and D10 by flow cytometry using a panel of primary conjugated antibodies summarised in Table 10-4.

Panel	MK staining panel							
<b>Fluorochrome</b>	PerCP-Cy5.5	APC	PE	PE-Cy7	FITC	V500	Pacific Blue	AF700
<b>Laser (Excitation wave length)</b>	B488	R633	YG561	YG561	B488	V405	V405	R633
<b>Detector Band Pass</b>	675/20	660/20	575/26	780/60	525/50	525/50	450/50	695/40
<b>Antigen</b>	HLA-DR	CD41	CD42b	CD34	PD-L1 or PD-L2	L/D Dye	HLA-A/B/C	CD38
<b>Strain</b>	Mouse	Mouse	Mouse	Mouse	Mouse	N/A	Mouse	Mouse
<b>Isotype</b>	IgG2a, κ	IgG1, κ	IgG1, κ	IgG2, κ	IgG2b, κ	N/A	IgG2a, κ	IgG1, κ
<b>Amount of used antibody (µl)</b>	2	2	2	1	2	0.5	2	1

**Table 10-4. List of antibodies used to track the development of MK.**

Cultured CD34<sup>+</sup> HSC were monitored using the imaging system Incucyte (Essen Bioscience, Hertfordshire, UK). The imaging system is kept inside an incubator allowing for imaging the cells without the need to remove it from the incubator (Figure 10-5A). Using 10x lenses, 16 images were captured from each well every 2 hours for a duration of 6 days (Figure 10-5B).

Cellular proliferation is monitored by determining cellular confluence i.e. the percentage of the area occupied by the growing cells. The confluence continues to increase until the cells are densely packed covering the whole imaged area. The Incucyte creates a mask over cells (Figure 10-6A) allowing for cell identification and provides cell confluence metrics in real time for automated quantification and plotting of the growing cells (Figure 10-6B) without the need for them to be stained.

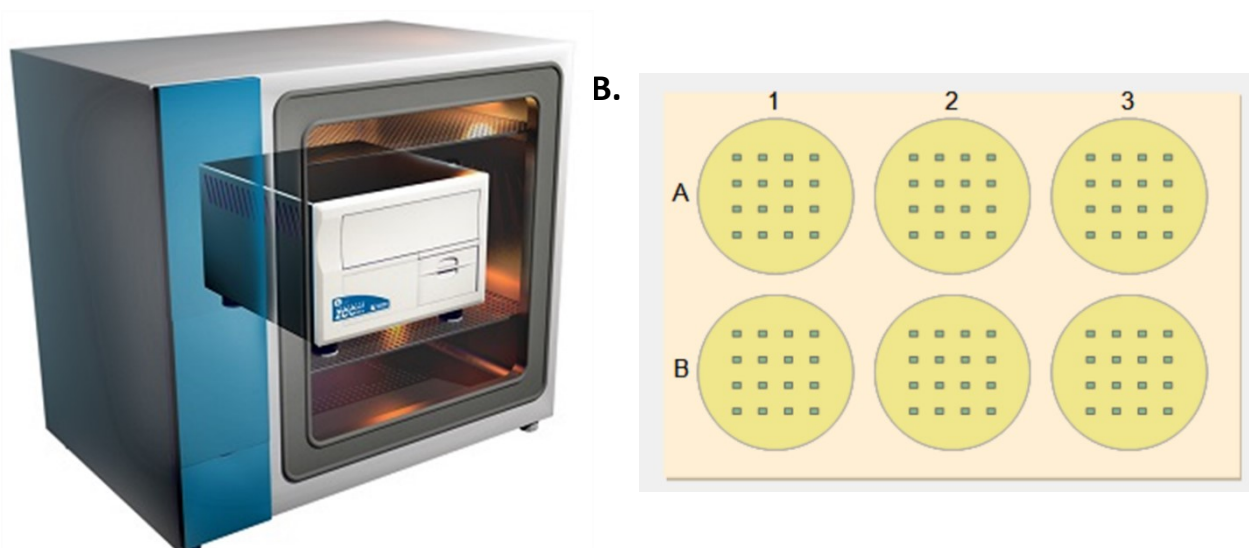
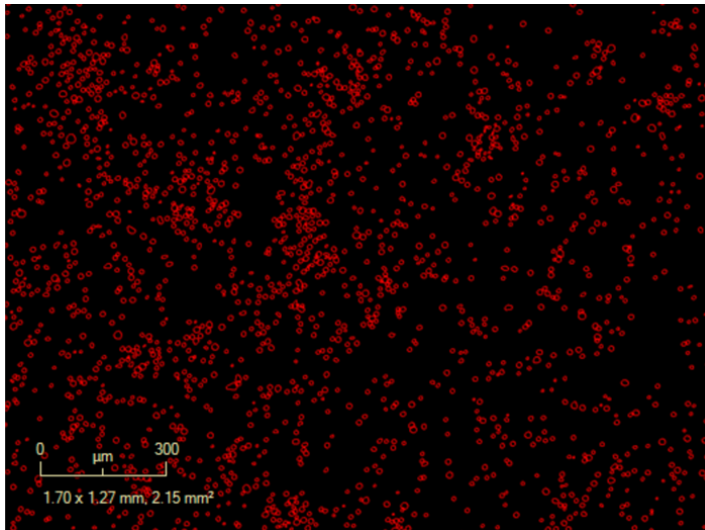


**Figure 10-5. Incucyte imaging system used to track MK development.**

(A) A representative image of the Incucyte imaging system placed inside a 37°C incubator having a moving microscope lenses taking images (B) at different locations of each well in a 6-well plate.

**A.**



**B.**

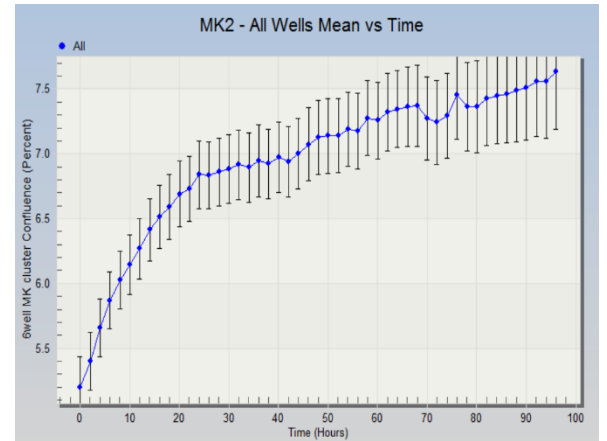


**Figure 10-6. Automated identification and quantification of developing MK using the Incucyte imaging system.**

(A) The system creates a virtual mask around the cells enabling the system to identify developing MK without staining. (B) The graph demonstrates the automated quantification of the growing cells plotted as confluency of the imaged field.

### **10.17. MK-T cell Interaction Assay.**

Mature MK at D7, as they express all of the maturation markers at that point of development, were cultured with PBMC from patients with ITP. To underline the involved pathways governing MK-T cell interacts, MKs were blocked with functional azide-free antibodies (Biolegend) targeting either MHC-I (HLA-A/B/C), PD-L1 or PD-L2 (Figure 10-7A). MK were incubated with these functional antibodies for 30 minutes at 4°C and then washed twice with PBS. To confirm the blocking of these receptors, an aliquot of the blocked MKs were stained with a conjugated antibody against the same blocked receptors. As these receptors were occupied by blocking antibodies, this prevented the staining of these markers as demonstrated (Figure 10-7 B-C).

MK cells were then cultured with PBMC in a 37°C incubator ON and all the cells were harvested afterwards. The outcome of this interaction was determined by quantifying the percentage of the polyfunctional CD8<sup>+</sup>IFN $\gamma$ <sup>+</sup>TNF $\alpha$ <sup>+</sup> T cells as described earlier (Section 10.4).

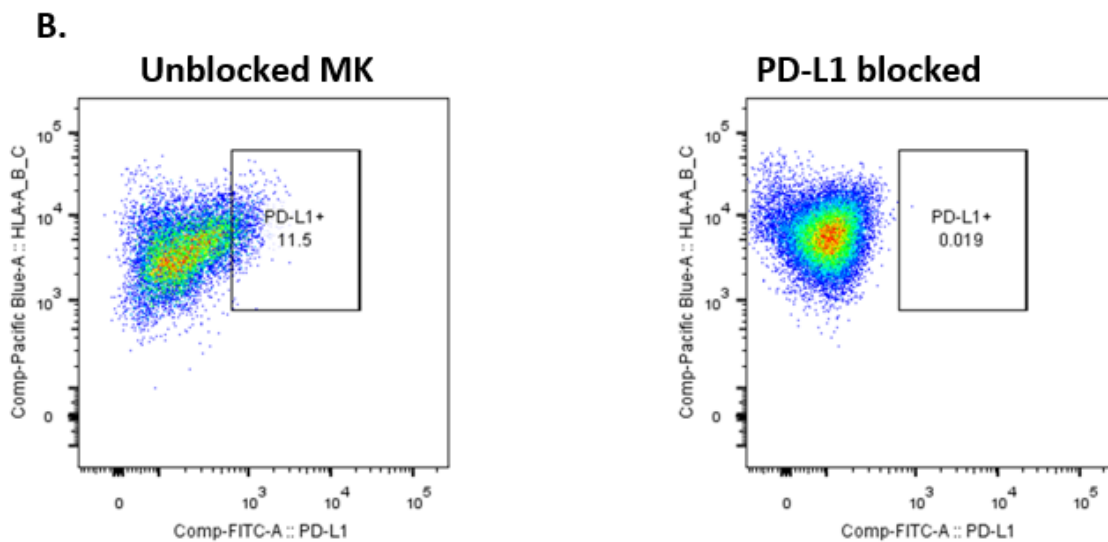
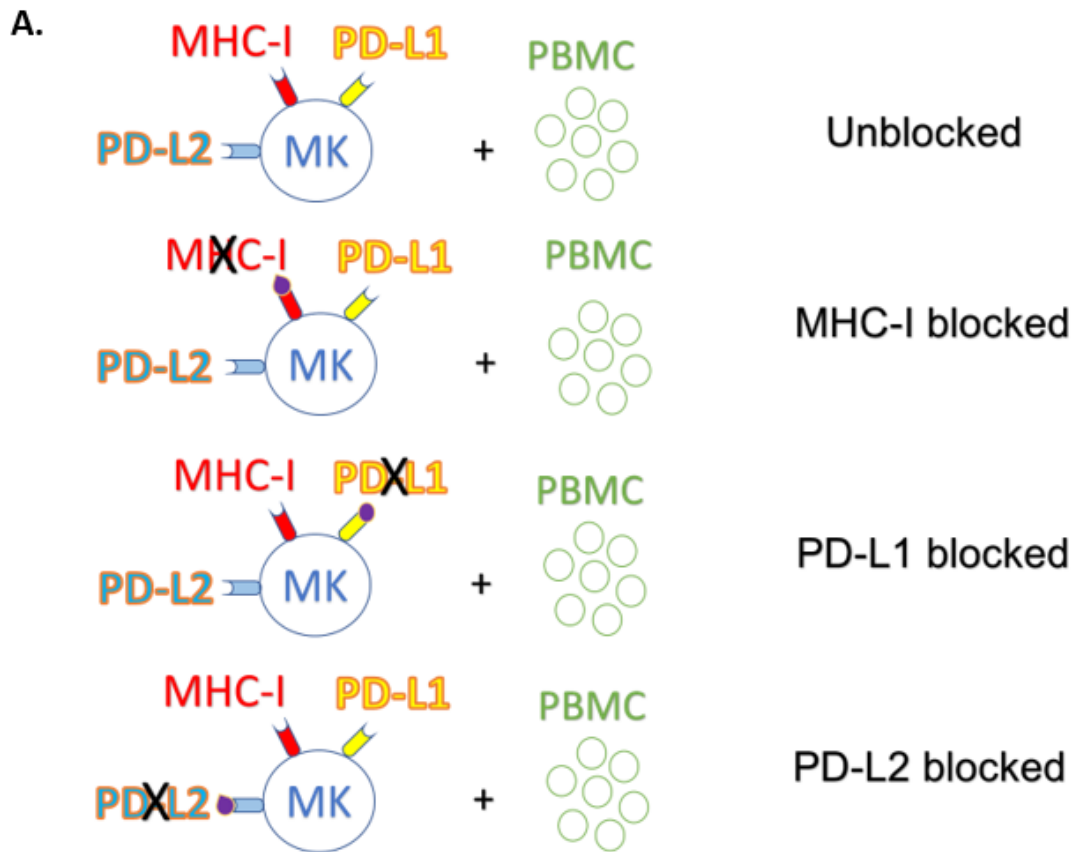


**Figure 10-7. Interrogating MK - T interaction governed by Immune-related molecules.** using blocking antibodies against HLA-A/B/C, PD-L1 and PD-L2 which govern MK-T cell interaction. Drawings demonstrate the blocked surface receptors on MK prior to their culture with PBMC. (B) Dot plots demonstrate an example of confirming the blocking of PD-L1 on MK demonstrated by lack of staining in PD-L1 blocked MKs (right), compared to the positive staining in unblocked MKs (left).

### **10.18. Statistical Analysis.**

Unpaired data sets were compared using two-tailed T test and Mann-Whitney U tests based on their parametric and nonparametric distribution, respectively. Paired data sets were compared using paired T tests or Wilcoxon matched-pairs tests for parametric and nonparametric data sets, respectively.

For comparisons between more than 2 groups, one-way ANOVA and Kruskal-Wallis tests for parametric and nonparametric data sets, respectively. Bonferroni correction was applied to counteract the effect of multiple comparison between the compared data sets.

Two-tailed spearman correlation test was applied to determine correlation between different data sets. P value was considered significant when it is lower than 0.05. All statistical analyses were performed using GraphPad Prism 7 (GraphPad, California, United States).

# **11. CD8<sup>+</sup> T cell pathophysiology of Immune thrombocytopaenia (ITP) peripheral blood and their response to thrombopoietin receptor agonists (TPO-RAs)**

## **11.1. Introduction**

Immune thrombocytopaenia (ITP) has long been thought to be autoantibody-mediated causing premature platelet destruction in the spleen (83,130). More recently, an increasing bulk of evidence suggests involvement of other immune elements in ITP pathophysiology, more specifically T cells (86,93,131). The seminal work of Olsson and colleagues has laid the foundation for the concept of CD8<sup>+</sup> T cell involvement in the pathophysiology of ITP. However, how CD8<sup>+</sup> T cells are influenced in ITP and how they contribute to the ongoing pathology has not been fully addressed.

Similar to other autoimmune conditions, immunosuppressive therapy has been the cornerstone of ITP treatment, being part of both first and second lines of treatments (110). However, some patients do not respond to standard treatments, and some get adverse effects from long-term immunosuppression (85,116). This has led to the development of two currently used thrombopoietin receptor agonists (TPO-RAs); Eltrombopag (Elt) and Romiplostim (Romi) that correct the thrombocytopaenia without immune-related side effects (117). The monotherapy of either TPO-RAs has been reported to lead to sustained remission i.e. recovery of platelet count beyond pathological levels after stopping the treatment in a proportion of patients suggesting immune-modulation (132,133). However, it is unclear how this remission is achieved without any reported immunomodulatory effect of TPO-RAs.

In this chapter, I examine the changes within the T cell populations in 40 patients with ITP and compared them to 26 healthy controls (HC). These patients were either on no treatment or on one of the 2 TPO-RAs; Elt or Romi. Using the described methods (Chapter 10) to phenotype both general T cell subsets; CD4<sup>+</sup> T<sub>h</sub> and CD8<sup>+</sup> CTL, and more specific subsets; naïve, central memory (CM), effector memory and terminally-differentiated (td) effector cells.

The changes within T cell subsets in patients are described, how these changes correlate with disease activity, and how CD8<sup>+</sup> T cells are dysregulated immunologically expressing low levels of exhaustion markers which are needed to control their activity. The functionality of T cells was assessed by their intracellular cytokines and their reactivity to platelets was demonstrated.

The treatment impact of Elt on T cells was demonstrated using T cell phenotyping of patients and *in vitro* culture with stimulated T cells.

Treg were described in patients, assessed functionally, and Treg/effector CD8<sup>+</sup> T cell ratio was calculated and linked to disease activity.

## 11.2. Results

### 11.2.1. Patients characteristics.

Forty patients with ITP were recruited between November 2014 and September 2017 at the immune-haematology clinic at the Hammersmith Hospital for this study (Table 11-1). The median age of the patients was 47.5 years old, ranging between 22 and 86 years old. They were equally distributed for gender (20 males and 20 females). The median platelet count (PLC) at the time of the analysis was  $56.5 \times 10^9/L$  [ $6 - 281 \times 10^9/L$ ], and their disease activity was either classified as active disease (AD;  $PLC < 30 \times 10^9/L$ ) or stable disease (SD;  $PLC > 30 \times 10^9/L$ ) depending on their platelet count at time of sample collection. In the absence of any comorbidity, it is not necessary to initiate or modify treatment if  $PLC > 30 \times 10^9/L$  (134). In the cohort analysed here, there were 15 AD patients and 25 SD patients. There were no significant differences in the age of male and female patients [48 vs 46.5;  $P$  value  $> 0.05$ ] and their PLC [45.5 vs  $70 \times 10^9/L$ ;  $P$  value  $> 0.05$ ]. Eleven patients were on ELT (19.44%), 13 on Romi (27.78%) and the rest ( $n=16$ , 52.78%) did not receive any treatments for at least 2 months prior to the time of sample collection.

Patients who were receiving either one of the TPO-RAs; Elt or Romi; are described (Table 11-2). Both Elt and Romi-treated patients group had a male predominance at M:F ratio of 1.2:1 and 1.16:1, respectively. The median age of patients receiving Elt was significantly higher than the Romi cohort. However, there was no significant difference in PLC between these two cohorts.

Patient ID	Age	Gender	Treatment*	Platelet count (x 10 <sup>9</sup> /L)*	Disease duration (Months)	Previous treatments
1	22	F	Romi	9	36	Steroids - MMF- Rituximab
2	28	M	Romi	7	4	Steroids - IVIG
3	58	M	Romi	131	6	Steroids – IVIG - Rituximab
4	23	M	Romi	123	18	Steroids - Rituximab
5	78	M	Romi	16	156	Steroids – IVIG - Rituximab
6	41	F	Romi	77	76	None
7	41	F	Romi	95	106	Steroids – IVIG – MMF - Rituximab
8	59	M	Romi	11	4	IVIG - Rituximab
9	46	F	No treatment	22	5	Steroids - IVIG
10	50	F	No treatment	64	37	None
11	32	F	No treatment	49	36	Steroids – IVIG
12	86	F	ELT	98	44	Steroids – IVIG - MMF
13	72	F	No treatment	76	2	None
14	51	M	No treatment	167	68	Steroids - IVIG
15	31	F	No treatment	25	120	None
16	70	F	Romi	66	240	IVIG
17	47	F	No treatment	7	46	Steroids - IVIG
18	38	F	No treatment	32	69	None
19	45	F	No treatment	86	8	Steroids - IVIG
20	53	F	Romi	6	4	Steroids - MMF
21	22	M	No treatment	105	10	None
22	49	F	ELT	6	3	Steroids - IVIG
23	38	F	No treatment	281	51	Steroids - IVIG
24	78	F	ELT	36	180	Steroids - IVIG
25	48	M	No treatment	44	100	Rituximab
26	71	M	No treatment	116	15	Steroids - IVIG
27	38	M	No treatment	19	324	Steroids - IVIG
28	58	M	ELT	167	18	Steroids - IVIG
29	46	M	ELT	164	404	MMF
30	48	M	ELT	47	144	Steroids
31	79	M	ELT	9	44	IVIG - Rituximab
32	59	M	No treatment	30	36	Steroids
33	42	F	Romi	21	89	Steroids – IVIG – MMF - Rituximab
34	47	M	Romi	249	21	Steroids - IVIG
35	30	M	Romi	13	5	Steroids - IVIG
36	34	M	No treatment	9	11	Steroids
37	71	M	ELT	45	120	Rituximab - MMF

38	43	F	ELT	50	103	None
39	60	M	ELT	105	75	Steroids – IVIG – Rituximab - MMF
40	66	F	ELT	110	54	Steroids - IVIG

**Table 11-1. Clinical parameters of the patients with ITP enrolled in this study.**  
Received treatment, platelet count and disease duration at the time of sample collection.

Treatment	Eltrombopag	Romiplostim
<b>Number of patients</b>	11	13
<b>Age</b>	60 (52.17 – 72.19)	42 (34.91 – 56.17)*
<b>Gender (M:F ratio)</b>	1.2:1	1.16:1
<b>Platelet count (x 10<sup>9</sup>/L)</b>	76.09 (56.54)	63.38 (72.18)

**Table 11-2. Clinical parameters of patients receiving TPO-RAs.**

Patients ages are displayed as median (lower – upper 95% confidence interval). Platelet count at the time of collection are displayed as mean ( $\pm$  standard deviation). \* denotes P value < 0.05.

## 11.2. Characterisation of T cell subsets.

To identify the different T cell subsets, isolated PBMC were first characterised based on their size and granularity, and dead cells were excluded using L/D viability staining. Single cells were gated based on forward and height scatters, followed by T cell identification based on their positive surface expression of CD3 (Figure 11-1A). Either CD4 or CD8 single positive cells were gated on (Figure 11-1B) to differentiate between T helper (Th) and cytotoxic T cells (CTL), respectively. Further dissection of the subsets based on the dual surface expression of CD45RA and CD62L (Figure 11-1 B-C) divide cells into four subsets; naïve ( $CD45RA^+CD62L^+$ ), terminally-differentiated (td) effector ( $CD45RA^+CD62L^-$ ), central memory (CM;  $CD45RA^-CD62L^+$ ) and effector memory ( $CD45RA^-CD62L^-$ ). The td effector population will be referred to as effector from now onwards. The surface expression of CD27 and CD57 were used to confirm this CD45RA/CD62L phenotypic discrimination. Naïve and effector subpopulations expressed high levels of CD27 and CD57, respectively (Figure 11-1D-E).

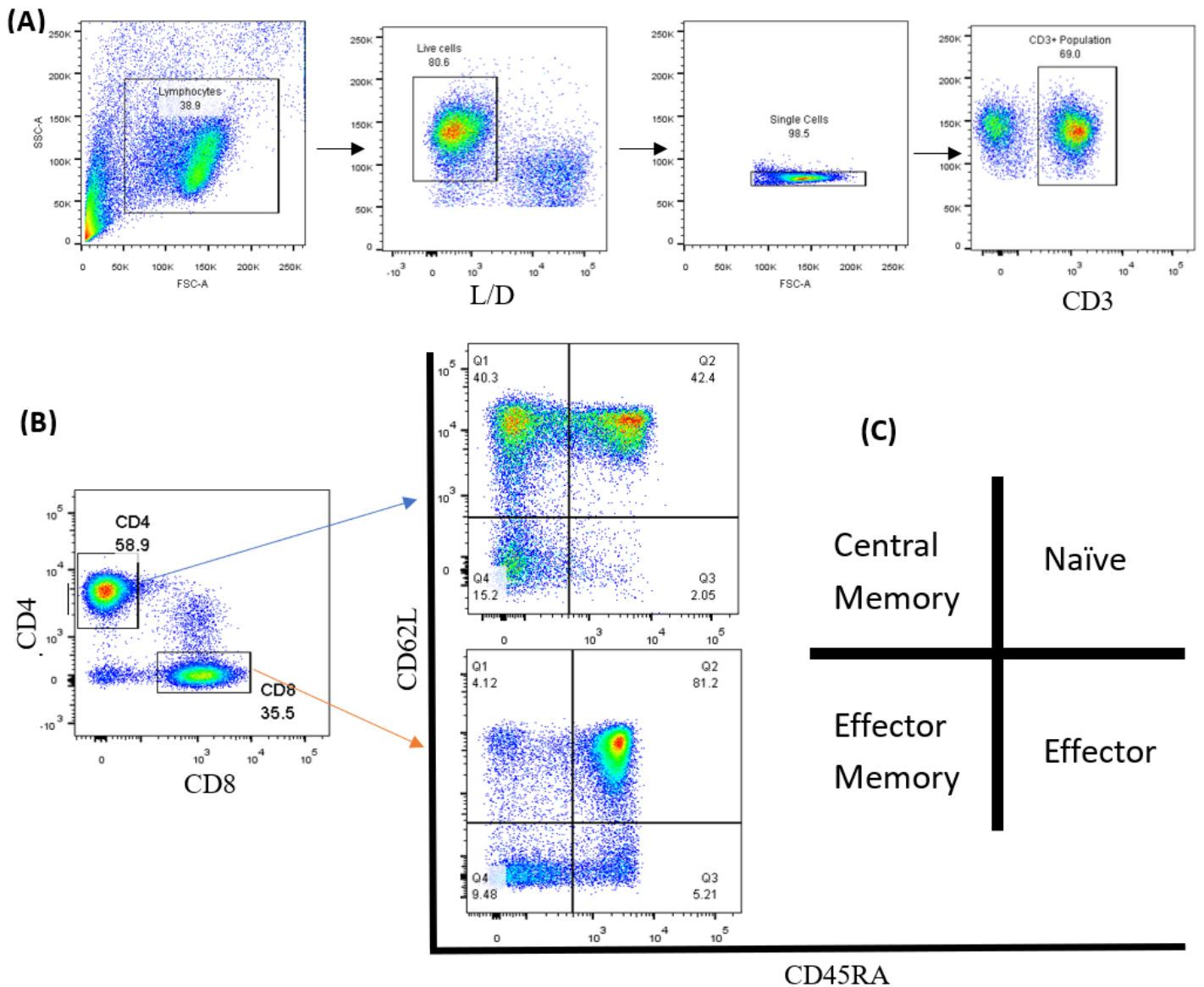


**Figure 11-1. Flow Cytometric characterisation of T cell subsets in a HC.** (A) Gating strategy for T cells starts by gating the PBMC population based on their forward and side scatter, dead cell exclusion based on Live/Dead (L/D) viability staining and doublets were excluded based on forward and height scatter. T cells were identified first using CD3 expression cells, then either (B) CD4 or CD8 single-positive cells were gated and followed by subset characterisation based on the expression of CD45RA and CD62L. (C) Diagram demonstrates subsets distribution based on their single, double-positive or double-negative of CD45RA and CD62L. Surface expression of CD27 and CD57 were used to confirm the subset phenotype, (D) as naïve CD8<sup>+</sup> T cells expressed high levels of CD27 and very low levels of CD57 while (E) the effector subset conversely expressed low levels of CD27 and very high levels of CD57.

### 11.2.3. ITP is associated with skewed T cell subsets towards an effector phenotype

T cell subsets showed significant changes in patients with ITP compared to HC. The percentage of CD4<sup>+</sup> T cells were significantly lower in patients [60.35% vs. 72.2%; P value < 0.05] (Figure 11-2A), while CD8<sup>+</sup> T cells were higher in patients [31.15% vs. 18.6; P value < 0.01] (Figure 11-2B). These changes influenced the CD4/CD8 T cell ratio leading to a significant reduction in patients [1.77 vs. 3.97; P value < 0.001] (Figure 11-2C).

Patients had a significant increase, compared to HC, in the effector CD4<sup>+</sup> [46.2% vs. 6.8%; P value < 0.001] (Figure 11-2D) and CD8<sup>+</sup> T cell populations [66.3% vs. 8.56%; P value < 0.001] (Figure 3-2E). On the other hand, there was a major reduction in the naïve CD4<sup>+</sup> [18.4% vs. 64.5%; P value < 0.001] (Figure 11-2G) and CD8<sup>+</sup> T cell populations [16% vs. 57%; P value < 0.001] (Figure 3-2H) in patients compared HC.

T cell subsets are reported to be influenced with age (135) affecting the distribution of naïve, CM and effector subsets. Similarly in this patients cohort, effector CD4<sup>+</sup> T cells had an indirect significant correlation with age [ $r = -0.4$ ; P value < 0.05] (Figure 11-2F), which was not observed in the CD8<sup>+</sup> population. Although CM CD4<sup>+</sup> T cells did not differ significantly between patients and HC, it displayed direct correlation with age [ $r = 0.38$ ; P value < 0.05].

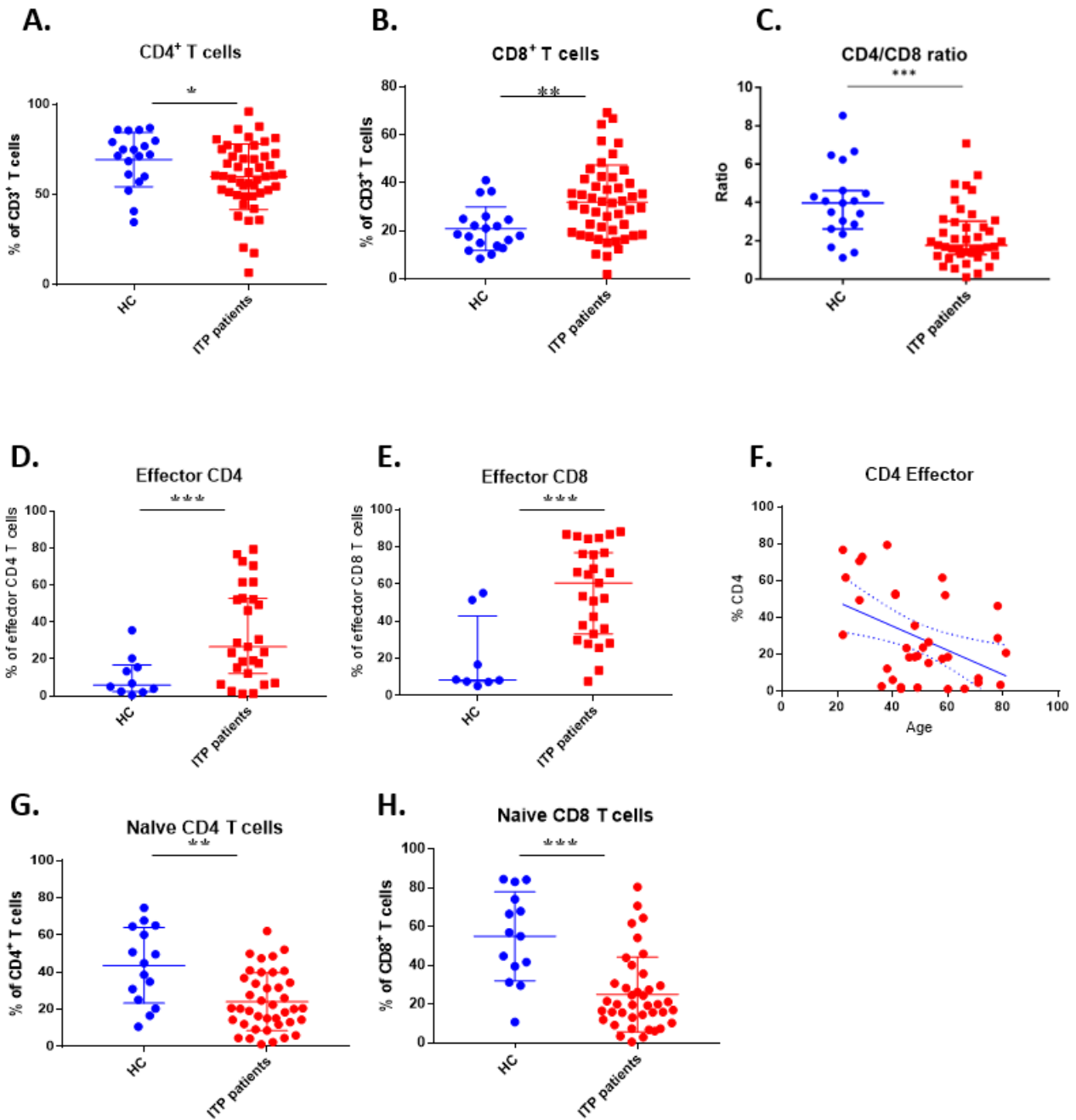


**Figure 11-2. CD4<sup>+</sup> and CD8<sup>+</sup> T cells populations, ratio and subsets in patients with ITP and HC.**

The graphs show (A) significantly lower CD4<sup>+</sup> T cells, (B) higher CD8<sup>+</sup> T cell frequency, (C) lower CD4/CD8 ratio in patients (n=26) compared to HC (n=19). Both (D) effector CD4<sup>+</sup> and (E) CD8<sup>+</sup> T cells were significantly higher in patients, with (F) an inverse correlation between the effector CD4<sup>+</sup> and patients age. Both (G) naïve CD4<sup>+</sup> (H) and CD8<sup>+</sup> T cells were significantly lower in patients compared to HC. Blue points represent HC and red denotes patients.

#### **11.2.4. Changes in the effector and central memory CD8<sup>+</sup> T cell subsets**

##### **corresponding to disease activity.**

To further understand the association between these T cell changes and disease activity, T cell subsets were compared between patients who exhibited active disease (AD; PLC < 30 x 10<sup>9</sup>/L) to those with stable disease (SD; PLC > 30 x 10<sup>9</sup>/L).

Effector CD4<sup>+</sup> population was significantly higher in AD patients compared to SD patients [50.7% vs. 18%; P value < 0.001] (Figure 11-3A). Similar finding was found in the effector CD8<sup>+</sup> population [66% vs. 44.4%; P value < 0.05] (Figure 11-3B). Although CM CD4<sup>+</sup> population did not show significant differences between HC and patients, a significant increase was observed in SD patients compared to AD patients [21.22% vs. 8.2%; P value < 0.05] (Figure 11-3C). Although not statistically significant, similar increase was found in the CM CD8<sup>+</sup> population. Both naïve CD4<sup>+</sup> and CD8<sup>+</sup> T cells were slightly raised in SD patients compared to AD patients [P value > 0.05] (Figure 11-3D).

There were no significant differences in the overall CD4, CD8 or CD4/CD8 ratio between AD and SD patients [P value > 0.05].

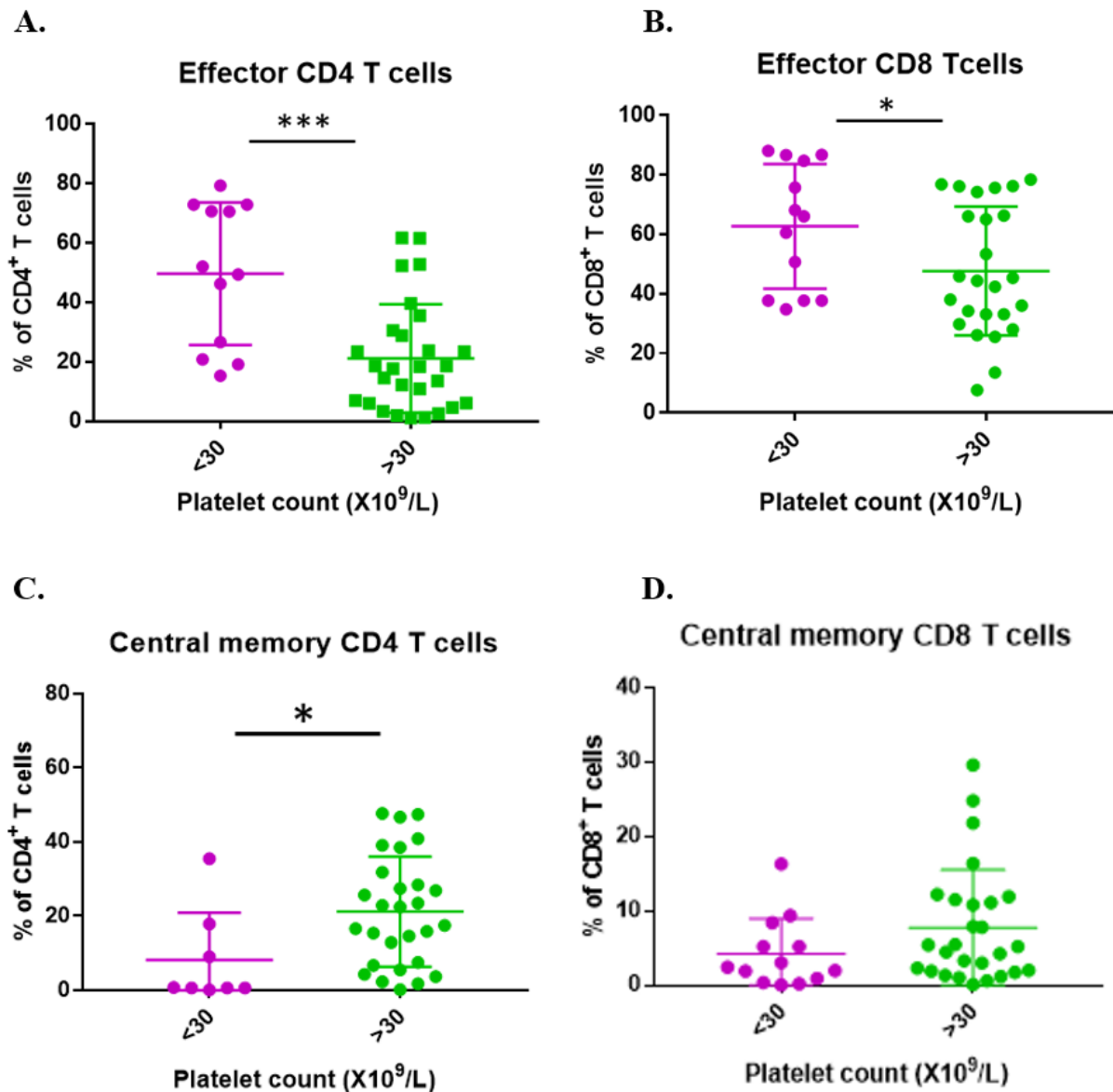


**Figure 11-3. Comparison between T cell subsets in patients with active and stable disease.**

Graphs show patients with active disease (AD; purple dots, n=13) have significantly higher (A) effector CD4<sup>+</sup> and (B) CD8<sup>+</sup> T cells compared to those with stable disease (SD; green dots, n=25). On the other hand, (C) CM CD4<sup>+</sup> T cells were significantly lower in active disease, and (D) so were the CM CD8<sup>+</sup> T cells (p value > 0.05).

### 11.2.5. Effector CD8<sup>+</sup> T cell population lacks signs of exhaustion in patients with ITP.

To determine the exhaustion status of the increased effector CD8<sup>+</sup> T cell population in patients with ITP who are on no treatment, exhaustion markers; namely PD-1 and Tim-3 were assessed. These markers are overexpressed in activated T cells and they serve as immunomodulatory receptors controlling T cell activity (136).

PD-1 expression was reduced in effector CD8<sup>+</sup> T cells compared to naïve ones [1.63% vs. 2.18%; P value > 0.05] (Figure 11-4A) and Tim-3 was significantly decreased [0.26% vs. 0.48%; P value <0.05] (Figure 11-4B).

Other inhibitory receptors such as CTLA-4 and LAG-3 were not tested in this study.

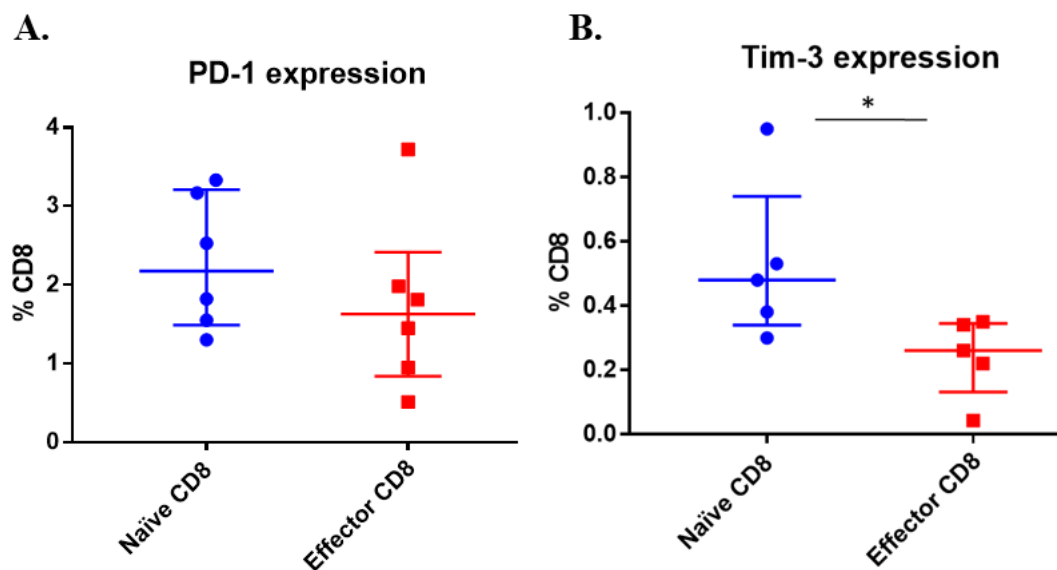


**Figure 11-4. The expression of exhaustion markers in naïve and effector CD8<sup>+</sup> T cells.**

(A) PD-1 expression on effector CD8<sup>+</sup> T cells (n=6) was reduced compared to its naïve counterpart (n=5), this reduction was not as significant as the reduction in (B) Tim-3 expression in the effector population when compared to the naïve ones.

### 11.2.6. Proinflammatory CD8<sup>+</sup> T cells are significantly higher in patients with ITP.

To assess the functionality of these abnormally distributed CD4<sup>+</sup> and CD8<sup>+</sup> T cells, intracellular cytokines were analysed in both CD4<sup>+</sup> and CD8<sup>+</sup> T cells. The analysed cytokines were the proinflammatory TNF $\alpha$ , IFN $\gamma$ , IL-2 and IL-17, as well as Granzyme B (GnB) and perforin, the latter two are key elements in the CD8<sup>+</sup>-mediated killing process (Figure 11-5 A-G).

The proinflammatory cytokines TNF $\alpha$  and IFN $\gamma$  were heterogeneously expressed in the CD4<sup>+</sup> and CD8<sup>+</sup> T cells (Figure 11-5D), dividing these populations into 4 subsets based on their expression; TNF $\alpha$ IFN $\gamma$ <sup>-</sup>, TNF $\alpha$ <sup>+</sup>IFN $\gamma$ <sup>-</sup>, TNF $\alpha$ IFN $\gamma$ <sup>+</sup> and TNF $\alpha$ <sup>+</sup>IFN $\gamma$ <sup>+</sup>. IL-2 and GnB had distinctive expression (Figure 11-5E) reflective of their functional nature as IL-2 is essential for cell proliferation and survival, while GnB is part of the killing machinery of CD8<sup>+</sup> T cells. Expectedly, perforin, like GnB, had a distinct expression from IL-2 (Figure 11-5G) and showed almost a linear expression pattern with GnB (Figure 11-5F) reflecting the direct concurrent nature of these two cytokines.

CD8<sup>+</sup> T cells, in patients with ITP compared to HC, had a more prominent proinflammatory signature in the form of increased CD8<sup>+</sup> T cells that were expressing proinflammatory cytokines. Compared to HC, patients had significantly higher CD8<sup>+</sup> T cells expressing IFN $\gamma$  [28.85% vs. 6.57%; P value < 0.01] (Figure 11-6A), IL-2 [26.35% vs. 5.49%; P value < 0.01] (Figure 11-6B), TNF $\alpha$  [15.77% vs. 7.94%; P value <0.01] (Figure 11-6C), GnB [28.55% vs. 9.42%; P value < 0.05] (Figure 11-6D), and Perforin [16.5% vs. 4.8%; P value <0.05] (Figure 11-6E). CD8<sup>+</sup>IL17<sup>+</sup> was also higher in patients compared to HC, although not statistically significant. Of note, the frequency of the CD4<sup>+</sup> T cells expressing TNF $\alpha$  was significantly lower in patients with ITP compared to HC [24.1% vs 46.9%; p value <0.05]. However, unlike the CD8<sup>+</sup> T cell compartment, no statistically significant differences were observed in the expression of IFN $\gamma$ , IL-2 or IL-17 in the CD4<sup>+</sup> T cell compartment (Table 11-3).

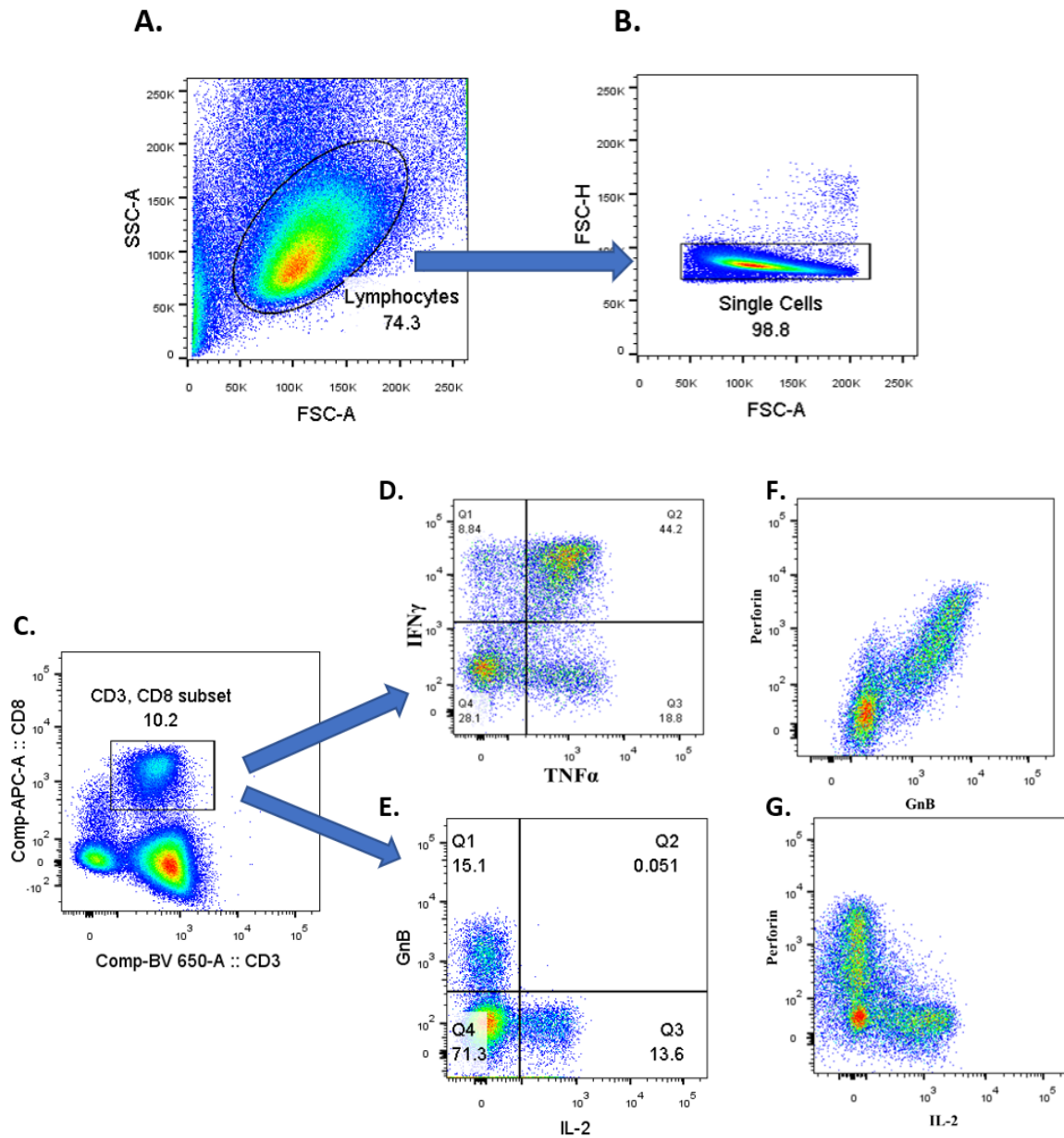


**Figure 11-5. Characterisation of the intracellular cytokines in CD8+ T cells.**

Dot plots are showing the gating strategy to characterise the intracellular cytokines in CD8<sup>+</sup> T cells. (A) Starting from gating on the forward and side scatters, followed by doublet exclusion and (B) the gate was set on (C) CD3<sup>+</sup>CD8<sup>+</sup> population. The expression of intracellular cytokines of the CD3<sup>+</sup>CD8<sup>+</sup> T cell population is represented (D-G). The dual expression of (D) TNF $\alpha$  with IFN $\gamma$  and (E) IL-2 with GnB were demonstrated. Perforin showed very similar expression to GnB (F-G).

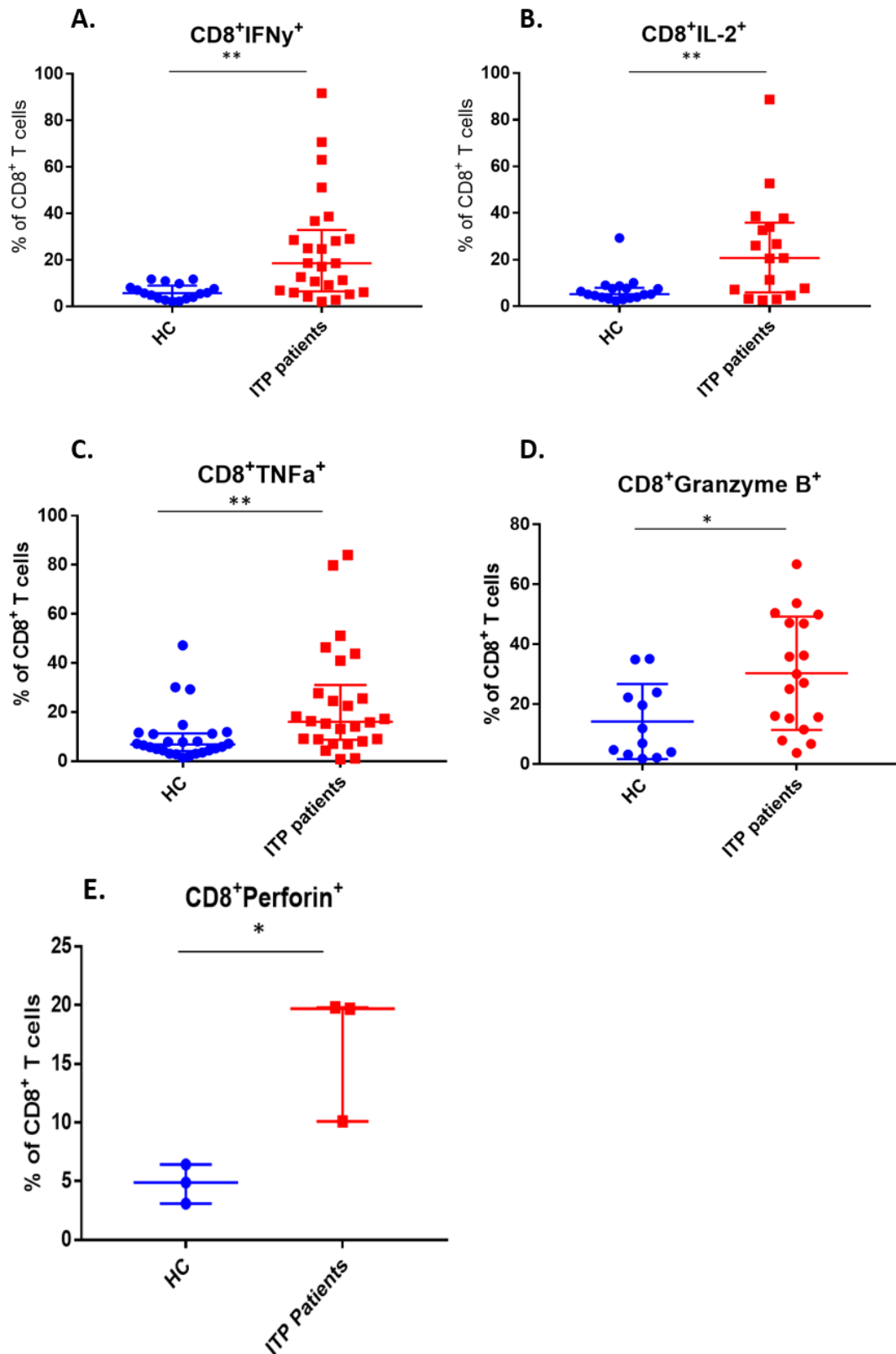


**Figure 11-6. Comparison of CD8<sup>+</sup> T cell intracellular cytokines between HC and patients.** Graphs demonstrate significant differences in the frequencies of CD8<sup>+</sup> T cells expressing (A) IFN $\gamma$ , (B) IL-2, (C) TNF $\alpha$ , (D) GnB and (E) perforin in patients compared to HC.

Markers/Cohort	Control (n=26)	Patients (n=26)
<b>CD4<sup>+</sup>IFN<math>\gamma</math><sup>+</sup></b>	16 [8.55 – 21.12]	17.76 [10.4-22.2]
<b>CD4<sup>+</sup>IL-17<sup>+</sup></b>	1.02 [0.03 – 1.6]	1.53 [0.33 – 5.4]
<b>CD4<sup>+</sup>IL-2<sup>+</sup></b>	41.5 [28.65 – 45.92]	38.45 [20.97 – 41.02]
<b>CD4<sup>+</sup>TNF<math>\alpha</math><sup>+</sup></b>	<b>46.9 [24.78 – 50.55] *</b>	<b>24.1 [9.69 – 43.45]</b>
<b>CD8<sup>+</sup>IFN<math>\gamma</math><sup>+</sup></b>	<b>6.57 [2.55 – 10.14]</b>	<b>28.85 [24.85 – 48.07] **</b>
<b>CD8<sup>+</sup>IL-17<sup>+</sup></b>	0.02 [0 – 0.11]	0.3 [0.06 – 7.84]
<b>CD8<sup>+</sup>IL-2<sup>+</sup></b>	<b>5.49 [2.13 – 7.95]</b>	<b>26.35 [10.9 – 33.65] **</b>
<b>CD8<sup>+</sup>TNF<math>\alpha</math><sup>+</sup></b>	<b>7.94 [5.37 – 12.62]</b>	<b>15.77 [21.35 – 44.7] **</b>
<b>CD8<sup>+</sup>GnB<sup>+</sup></b>	<b>9.42 [ 2.09 – 35.1]</b>	<b>28.55 [6.67 – 66.7] *</b>
<b>CD8<sup>+</sup>Perforin<sup>+</sup></b>	<b>4.8 [ 3.1 – 6.8]</b>	<b>16.5 [10.1 – 19.8] *†</b>

**Table 11-3. Comparison of the frequencies of the CD4<sup>+</sup> and CD8<sup>+</sup> T cells positive of the proinflammatory cytokines.**

Summary of the CD4<sup>+</sup> and CD8<sup>+</sup> T cell populations that are positive for the various proinflammatory cytokines in patients and HC. The values represent the median value with the range included in the brackets. Populations that are highlighted in bold show statistical significance between HC and patients. \*P value < 0.05 \*\*P value < 0.01. † n=3

### **11.2.7. Polyfunctional CD8<sup>+</sup> T cells are enriched within the effector population and have the highest Granzyme B and perforin expression.**

In order to link the functionality of CD8<sup>+</sup> T cells to the T cell subsets, CD8<sup>+</sup> cells were sorted based on their CD45RA and CD62L phenotypes, allowing for intracellular cytokine analysis in each CD8 subset (Figure 11-7A).

Naïve CD8<sup>+</sup> T cells expressed the lowest levels of inflammatory cytokines. On the contrary, effector CD8<sup>+</sup> T cells were highly polyfunctional, i.e. expressing multiple cytokines (137), with the highest expression of IFN $\gamma$ , TNF $\alpha$  and GrB (Figure 11-7 A-B). CM CD8<sup>+</sup> T cell expressed the highest levels of IL-2, in keeping with its nature of being long-lived population (Figure 11-7C).

The polyfunctional IFN $\gamma$ <sup>+</sup>TNF $\alpha$ <sup>+</sup> CD8<sup>+</sup> T cell population is representative of the effector CD8<sup>+</sup> population as it has the highest expression of both GrB and perforin (Figure 11-8), while the IFN $\gamma$ <sup>-</sup>TNF $\alpha$ <sup>+</sup> population was reflective of a CM phenotype; expressing high levels of IL-2 and low levels of GrB and perforin (Figure 11-8).

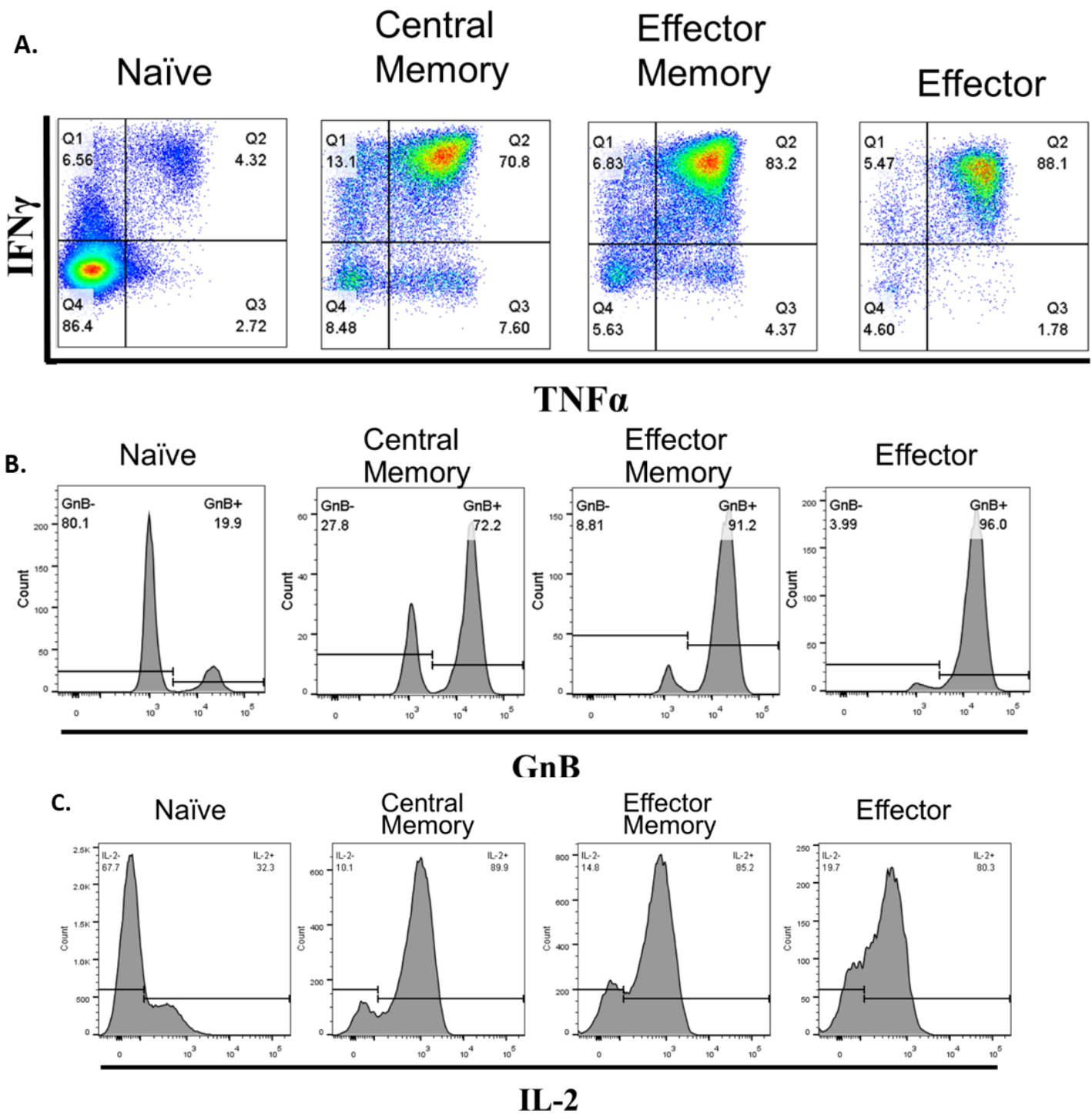


**Figure 11-7. Intracellular cytokines expression of the sorted CD8<sup>+</sup> T cell subsets.**

(A) the first set of dot plots is showing the dual expression of IFN $\gamma$  and TNF $\alpha$  in the FACS sorted CD8<sup>+</sup> T cell subsets. Sets of histograms showing the intracellular expression of (B) GnB and (C) IL-2 in the sorted CD8<sup>+</sup> T cell subsets.

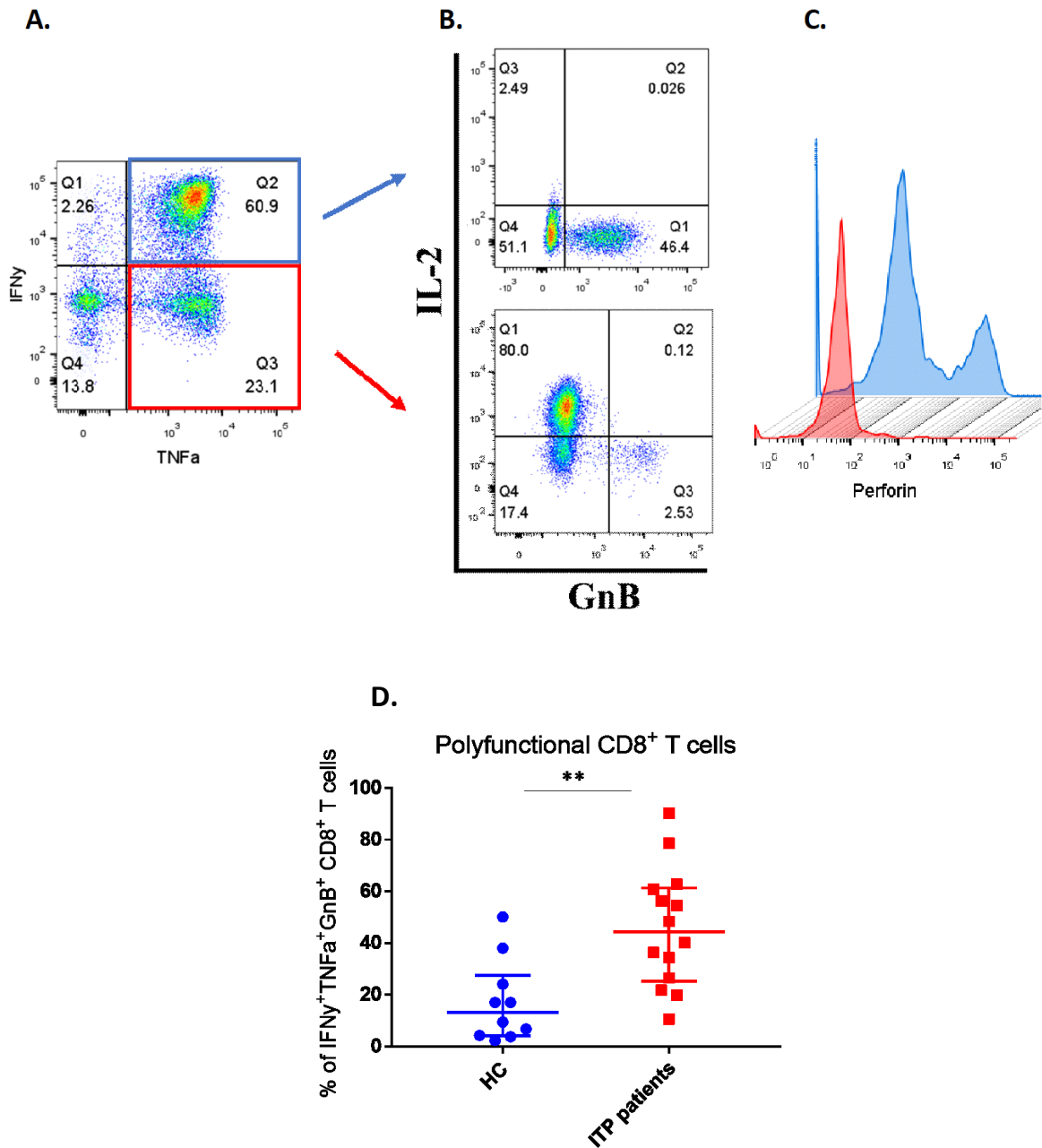


**Figure 11-8. The differential expression of intracellular cytokines in CD8<sup>+</sup> T cells.**

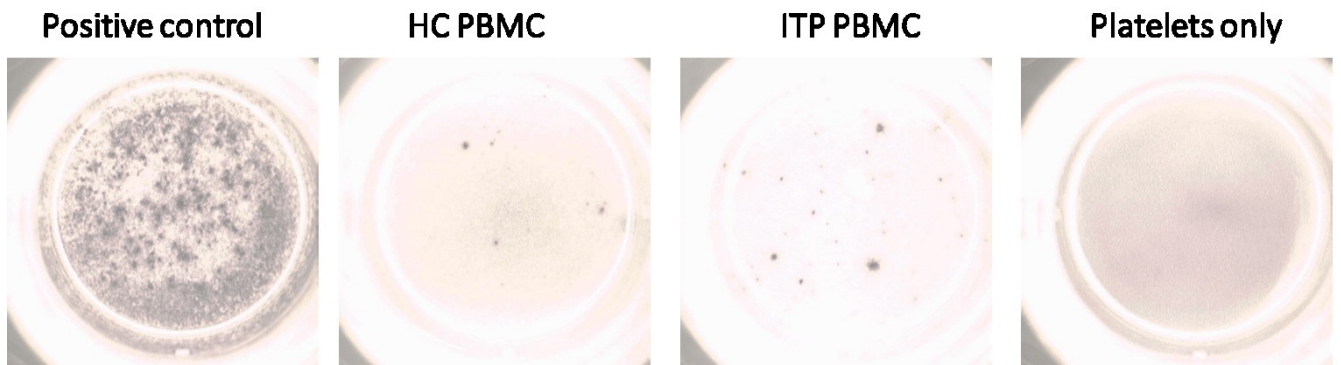
Based on (A) the intracellular cytokine expression of IFN $\gamma$  and TNF $\alpha$ , the polyfunctional IFN $\gamma$ <sup>+</sup>TNF $\alpha$ <sup>+</sup> population (highlighted in blue) seems to reflect an effector subset which is characterised by (B) high GnB and (C) perforin expression (blue histogram) and low IL-2 expression. While IFN $\gamma$ <sup>+</sup>TNF $\alpha$ <sup>+</sup> population (highlighted in red) seems to reflect memory subset characterised by high IL-2 expression and low GnB and perforin (red histogram). (D) The graph shows significantly higher polyfunctional CD8<sup>+</sup> T cells in patients (n=14) compared to HC (n=10).

### **11.2.8. Platelets-specific T cells are significantly higher in patients with ITP.**

To determine whether the observed changes in T cell subsets were driven by platelets, the production of IFN $\gamma$  by PBMC from HC and patients with ITP was assessed after co-culturing with platelets from healthy donors using an ELISpot assay, where every dot represents an IFN $\gamma$ -secreting cell (Figure 11-9A). PBMC stimulated with a *Staphylococcal Enterotoxin B* (SEB); a potent stimulator of IFN $\gamma$  production, or cultured alone in culture media were used as positive and negative controls respectively. Platelet-only condition was also used as negative control.

PBMC from patients were more activated in culture medium alone without platelets when compared to HC displaying significantly higher dot count [2 vs. 0; P value < 0.05] (Figure 11-9B). The addition of healthy donor platelets to the culture media resulted in a higher counted number of IFN $\gamma$ -secreting cells in both HC and ITP patient's plates, compared to cultures without added platelets. Interestingly, co-cultured with platelets, PBMC from patients had significantly higher IFN $\gamma$ -secreting cells compared to PBMC from HC [12.50 vs 4; P value < 0.05].

**A.**



**B.**

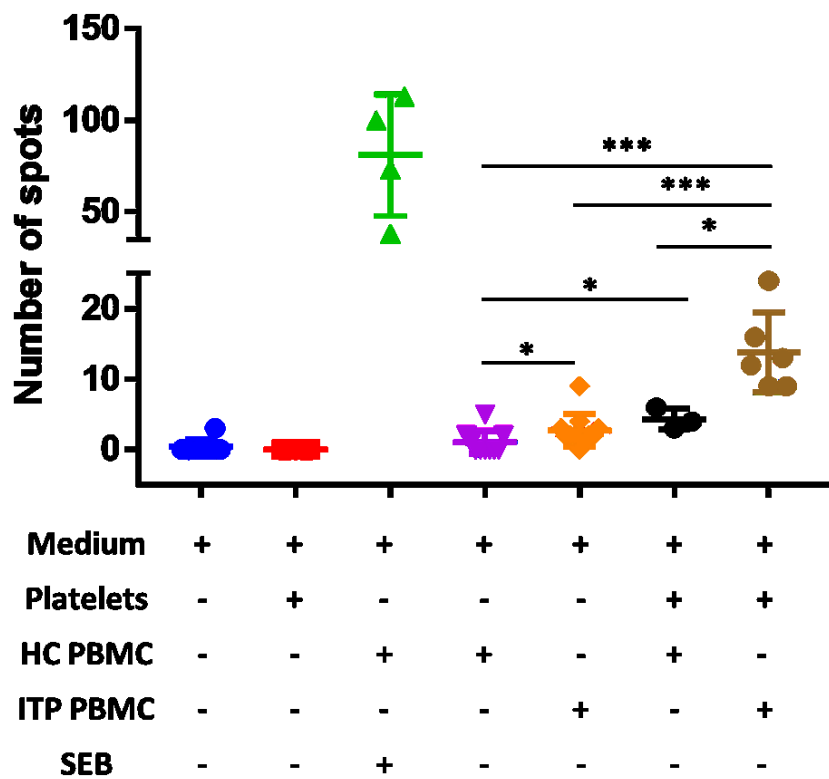


**Figure 11-9. ELISpot assay of PBMC cultured with platelets of healthy donor.**

(A) an example of ELISpot wells of (Left to right) a positive control, HC PBMC with platelets, patients PBMC with platelets and platelet-only condition. (B) The graph is demonstrating the significant differences in the dot count between HC and patients that were not cultured with platelets, purple and orange, respectively. Culturing platelets with PBMC from HC (black) or patients (brown) resulted in more IFN $\gamma$ -secreting cells. Negative experimental controls included medium only (blue), platelets without PBMC (red) and PBMC cultured with a super-antigen SEB (green).

### **11.2.9. Proinflammatory cytokines are significantly increased in the CD8<sup>+</sup> T cell in patients receiving TPO-RAs.**

As described previously (Section 11.6), patients with ITP had significantly higher proportion of CD8<sup>+</sup> T cells expressing proinflammatory cytokines, as well as the CD8<sup>+</sup> T cell killing machinery namely, G $\eta$ B and perforin (Figure 11-6). A comparison was made between patients who are not on treatments and those who are receiving TPO-RAs in order to assess the impact of these treatments on proinflammatory cells.

Patients on TPO-RA had significantly higher CD8<sup>+</sup>IFN $\gamma$ <sup>+</sup> T cells [25% vs. 6.56%; P value < 0.05] (Figure 11-10A) and CD8<sup>+</sup>IL-2<sup>+</sup> T cells [20.5% vs. 0.87%; P value < 0.01] compared to those who are no treatment (Figure 11-10B).

In addition, patients on TPO-RA had increased CD8<sup>+</sup>G $\eta$ B<sup>+</sup> (Figure 11-10C) and CD8<sup>+</sup> TNF $\alpha$ <sup>+</sup> T cells compared to those on no treatment, however, this increase did not reach statistical significance (Figure 11-10D). Although G $\eta$ B and TNF $\alpha$ -associated changes in the TPO-RA-treated cohort were not significantly different compared with untreated patients, there were still significantly higher than the HC [40.6% vs 9.42%; P value < 0.05] and [18.2% vs 7.94%; P value < 0.01] respectively.

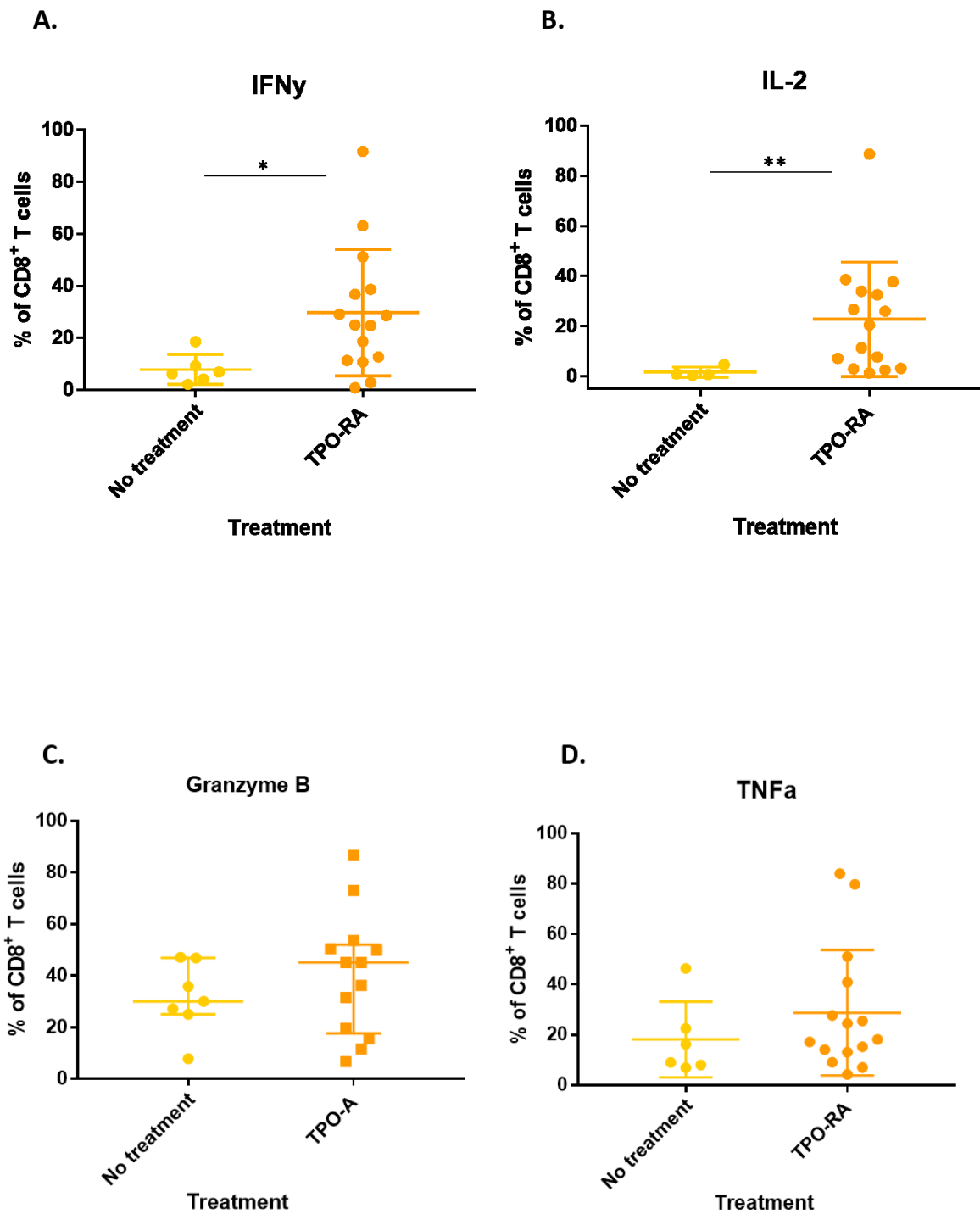


**Figure 11-10. Comparisons of the CD8<sup>+</sup> T cell intracellular cytokines between patients on no treatment and on TPO-RAs**

Graphs demonstrating the significant differences in the (A) IFN $\gamma$ <sup>+</sup> and (B) IL-2<sup>+</sup> CD8<sup>+</sup> T cells between the patient receiving no treatment (yellow dots, n=7) and patients receiving TPO-RA (orange dots, n=15). (C) GnB<sup>+</sup> and (D) TNF $\alpha$ <sup>+</sup> CD8<sup>+</sup> T cell did not demonstrate any significant differences between these two patients' cohorts.

### **11.2.10. Patients on Eltrombopag have a lower effector T cells and higher naïve T cells compared to Romiplostim.**

A further analysis of the patients receiving either of the two TPO-RAs, Elt or Romi, was done to identify any impact from the received treatment on T cell subsets. Although both effector CD4<sup>+</sup> and CD8<sup>+</sup> T cell subsets were significantly higher in patients compared to HC (Section 11-3), patients on Elt, compared to the other TPO-RA Romi, had significantly lower percentages of effector CD8<sup>+</sup> T cells [42.4% vs 76.8%; P value <0.01]. However, Elt-treated patients still had higher effector CD8<sup>+</sup> than HC [42.4% vs 14.65%; P value < 0.05] (Figure 11-11A). Patients on Elt also had significantly lower effector CD4<sup>+</sup> subsets compared to those on Romi [19.1% vs 52.8%; P value <0.001] to a comparable level to HC [P value > 0.05] (Figure 11-11B).

On the other hand, as described above (Section 11-3), ITP patients had significantly lower naïve CD4<sup>+</sup> and CD8<sup>+</sup> T cell subsets compared to HC. Patients on Elt exhibited a similar normalising effect with increased frequency of naïve CD8<sup>+</sup> T cells compared to those on Romi [26.3% vs 15.7%; P value < 0.05]. However, Elt-treated patients still had significantly lower naïve CD8<sup>+</sup> T cells compared to HC [26.3% vs 56.05%; P value < 0.05] (Figure 11-11C). Moreover, naïve CD4<sup>+</sup> T cells were significantly higher in Elt-treated patients compared to Romi [31.8% vs 14.15%; P value < 0.5] (Figure 11-11D).

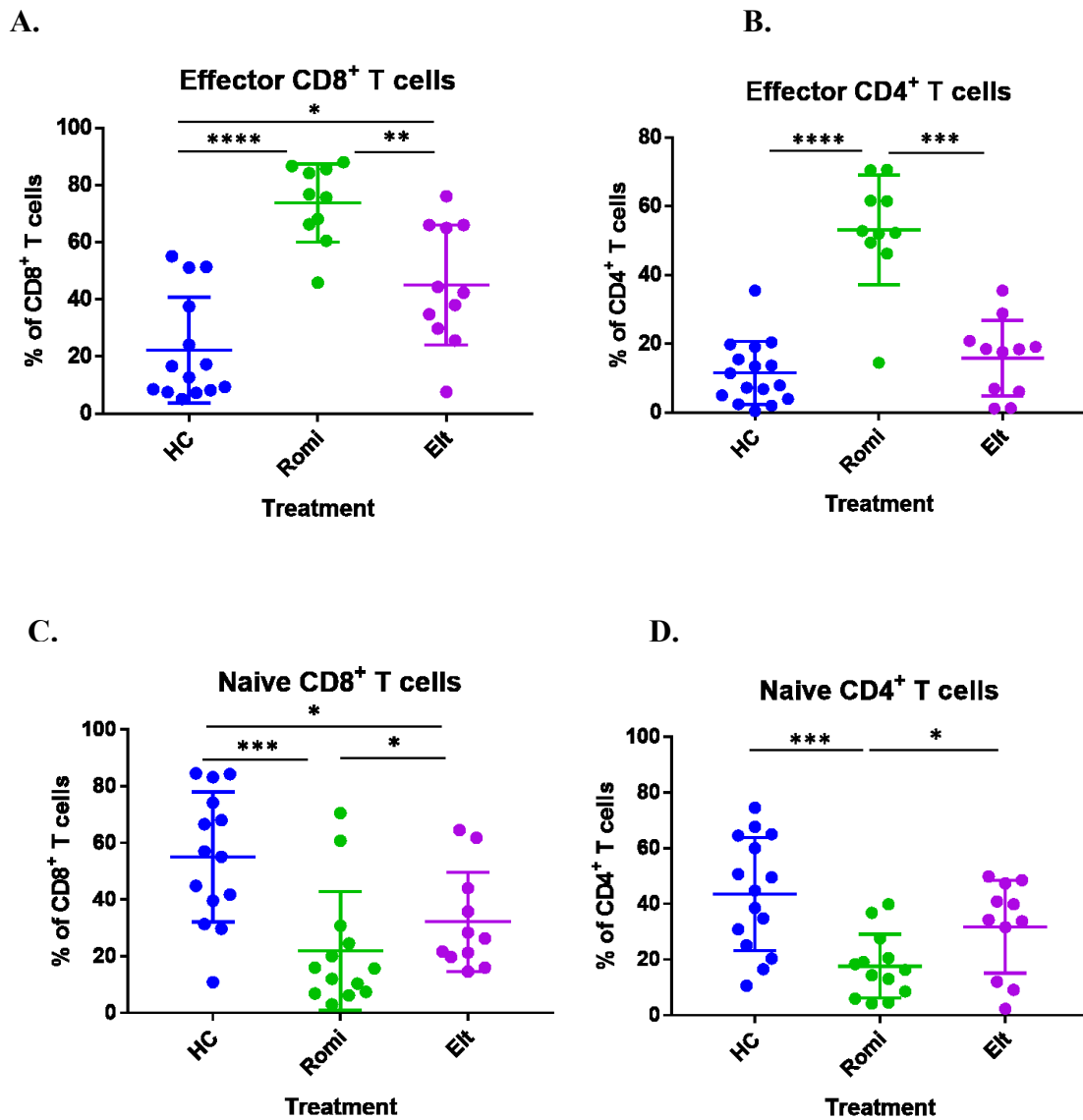


**Figure 11-11. Comparisons of the different T cell subsets between the patient treatment subgroups and HC**

Graphs demonstrating the significant differences between the patients' subgroups and HC as well as differences among the patients on Romi or Eit. Romi-treated patients (green dots, n=10) had the highest levels of effector CD8<sup>+</sup> (A) and CD4<sup>+</sup> T cells (B) compared to the other subgroups. All treatment subgroups had significantly lower naïve CD8<sup>+</sup> (C), and CD4<sup>+</sup> T cells (D) compared to HC (blue dots, n=14). The Eit-treated group (purple dots, n=11) had significantly higher naïve CD8<sup>+</sup> T cells compared to the Romi-treated group.

### **11.2.11. Eltrombopag significantly reduces CD8<sup>+</sup> T cell functionality in a dose-dependent manner.**

To study the impact of Elt on CD8<sup>+</sup> T cells, PBMC isolated from HC were stimulated *in vitro* overnight with anti-CD3/CD28 antibodies, to replicate the stimulatory nature of the disease, and were co-cultured with serial concentrations of Elt ranging from 7.5 to 125 µg/ml. This dosing range includes the therapeutic dose of Elt used in ITP. A single concentration of Romi (31.25µg/ml) was used to compare its impact to Elt. The proinflammatory intracellular cytokines in CD8<sup>+</sup> T cells were analysed to demonstrate the effect of Elt on CD8<sup>+</sup> T cell functionality.

Elt significantly reduced the functionality of CD8<sup>+</sup> T cells in a dose-dependent manner. More specifically, the percentage of CD8<sup>+</sup> GnB<sup>+</sup> T cells were significantly reduced when cultured with 7.5µg/ml of Elt compared to untreated cells [69.14% vs. 80.70%; P value < 0.01] (Figure 11-12A). This impact was further demonstrated with a higher dose, 125µg/ml, of Elt [33.90% vs 80.70%; P value < 0.0001]. Similarly, CD8<sup>+</sup> TNFα<sup>+</sup> T cells were significantly lowered with the treatment of Elt and more prominently at a higher dose of 125µg/ml [46.79% vs. 75.45%; P value < 0.0001] compared to untreated cells (Figure 11-12B). Furthermore, the polyfunctional CD8<sup>+</sup> IFNγ<sup>+</sup> TNFα<sup>+</sup> T cells were also significantly reduced by Elt, most prominently at the high dose of 125µg/ml when compared to untreated cells [32.12% vs. 70.07%; P value < 0.0001] (Figure 11-12C).

Stimulated cells were then cultured with 31.25µg/ml of Romi and compared to 2 concentrations of Elt, 31.25 and 125µg/ml, as well as untreated cells. Romi did not show any remarkable impact on the median fluorescent intensity (MFI) of GnB of CD8<sup>+</sup> T cells compared to untreated cells [P value > 0.05]. However, GnB MFI was significantly reduced by 31.75µg/ml of Elt [1247 vs. 1678; P value < 0.05] and 125µg/ml [867 vs. 1678; P value < 0.01] when compared to Romi (Figure 11-13A).

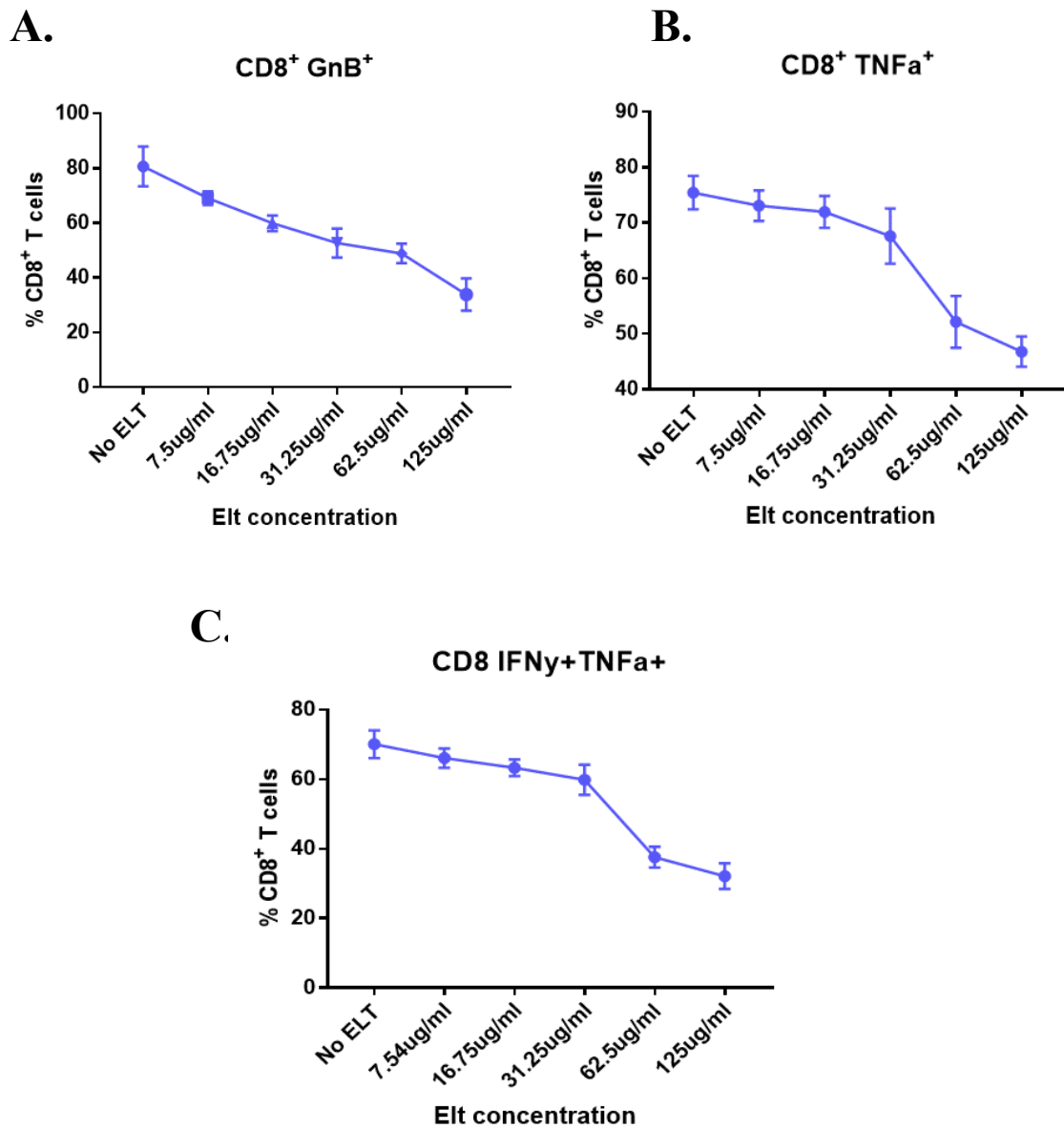


**Figure 11-12. Reduction of CD8<sup>+</sup> T cell functionality by Elt**

Plots demonstrating the impact of the increasing dose of cultured Elt with stimulated T cells.

(A) The percentage of CD8<sup>+</sup>GnB<sup>+</sup> T cells were decreasing significantly with the increase in Elt concentration. Similarly, (B) CD8<sup>+</sup> TNF $\alpha$ <sup>+</sup> and (C) the polyfunctional CD8<sup>+</sup> IFN $\gamma$ <sup>+</sup> TNF $\alpha$ <sup>+</sup> T cells decreased significantly with the increasing dose of Elt (n=3).

Similarly, Romi did not affect the percentage of CD8<sup>+</sup> IFN $\gamma$ <sup>+</sup> TNF $\alpha$ <sup>+</sup> T cells compared to untreated cells [P value > 0.05]. However, CD8<sup>+</sup> IFN $\gamma$ <sup>+</sup> TNF $\alpha$ <sup>+</sup> T cells were decreased with 31.25 $\mu$ g/ml of Elt [19.25% vs. 32.10%; P value < 0.05] and 125 $\mu$ g/ml [17.90% vs. 32.10%; P value < 0.01] when compared to Romi (Figure 11-12B).

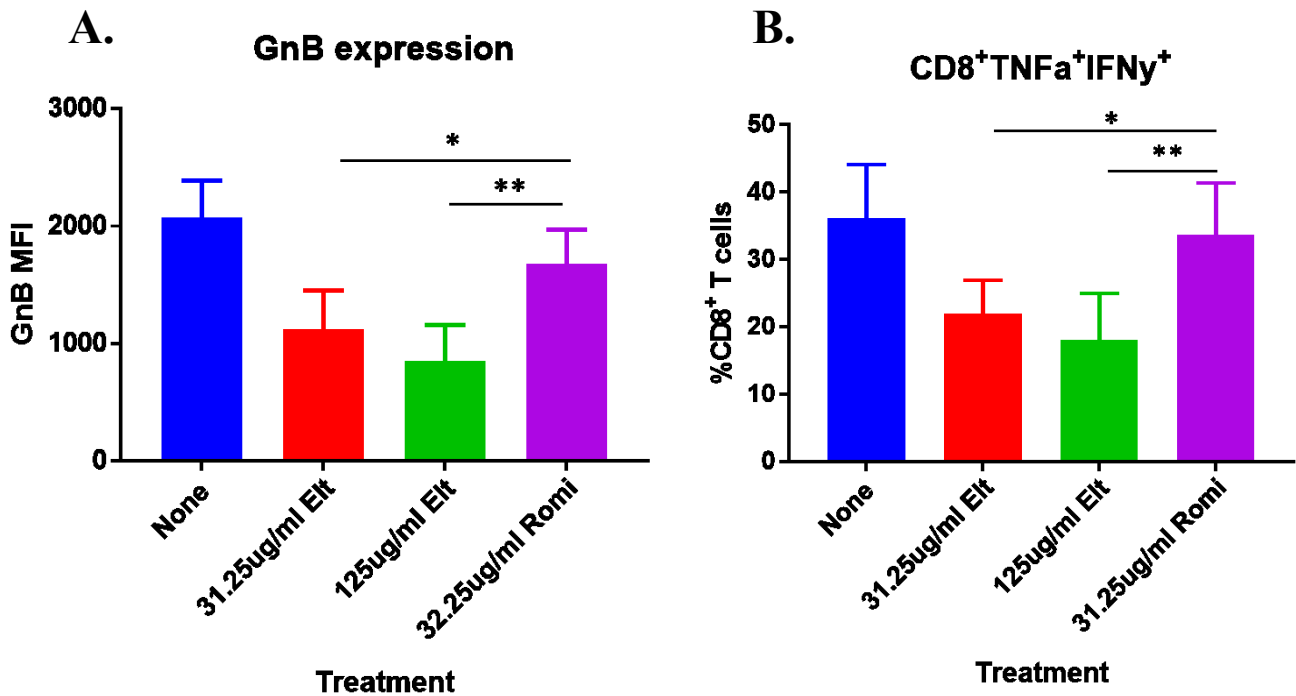


**Figure 11-13. Comparing the effect of Elt and Romi on the functionality of CD8+ T cells.**

Bar charts demonstrating the impact of the 2 TPO-RAs, Elt and Romi, on the functionality of T cells. Figure (A) shows the significant reduction of GnB MFI with both doses of Elt, 31.25 $\mu$ g/ml (Red) and 125 $\mu$ g/ml (Green), compared to Romi (Purple). Romi-treated cells did not differ significantly from the untreated (blue) group. Similar effect of Elt was observed (B) on the percentage of CD8<sup>+</sup> IFN $\gamma$ <sup>+</sup> TNF $\alpha$ <sup>+</sup> T cells, whereas Romi did not differ significantly from the untreated cells.

### **11.2.12. Functional regulatory T cells (Treg) and their Treg/effector CD8<sup>+</sup> T cell ratio are reduced in patients with ITP, corresponding to disease activity.**

Treg were characterised by their surface expression of CD3<sup>+</sup>CD4<sup>+</sup>CD25<sup>hi</sup>CD127<sup>lo</sup>, which was confirmed by the high expression of the Treg-specific transcription factor FoxP3 (Figure 11-14A-C).

The frequency of Treg, determined as a percentage of the total CD4<sup>+</sup> T cell population, did not differ significantly in patients compared to HC [P value > 0.05] (Figure 11-14D). But given the above described reduction in the percentages of CD4<sup>+</sup> population in our cohort of patients (Section 11-3), it could be deduced that the Treg population was also lower in patients. The functionality of Treg, as determined by their intracellular expression of IL-2, did not differ significantly compared to HC [P value > 0.05]. However, Treg were significantly lower in patients with active disease compared to patients with higher platelet count [2.32% vs. 4.46%; P value < 0.05] (Figure 11-14E).

As the function of Treg is dependent on its interaction with other T cell subsets, Treg/effector CD8<sup>+</sup> T cell ratio was calculated. Interestingly, this was significantly lower in patients compared to HC [0.06 vs. 0.16; P value < 0.01] (Figure 11-14F). This ratio was also influenced by disease activity as it was significantly lower in active disease (AD) compared to stable disease (SD) [0.038 vs. 0.098; P value < 0.05] (Figure 11-14G).

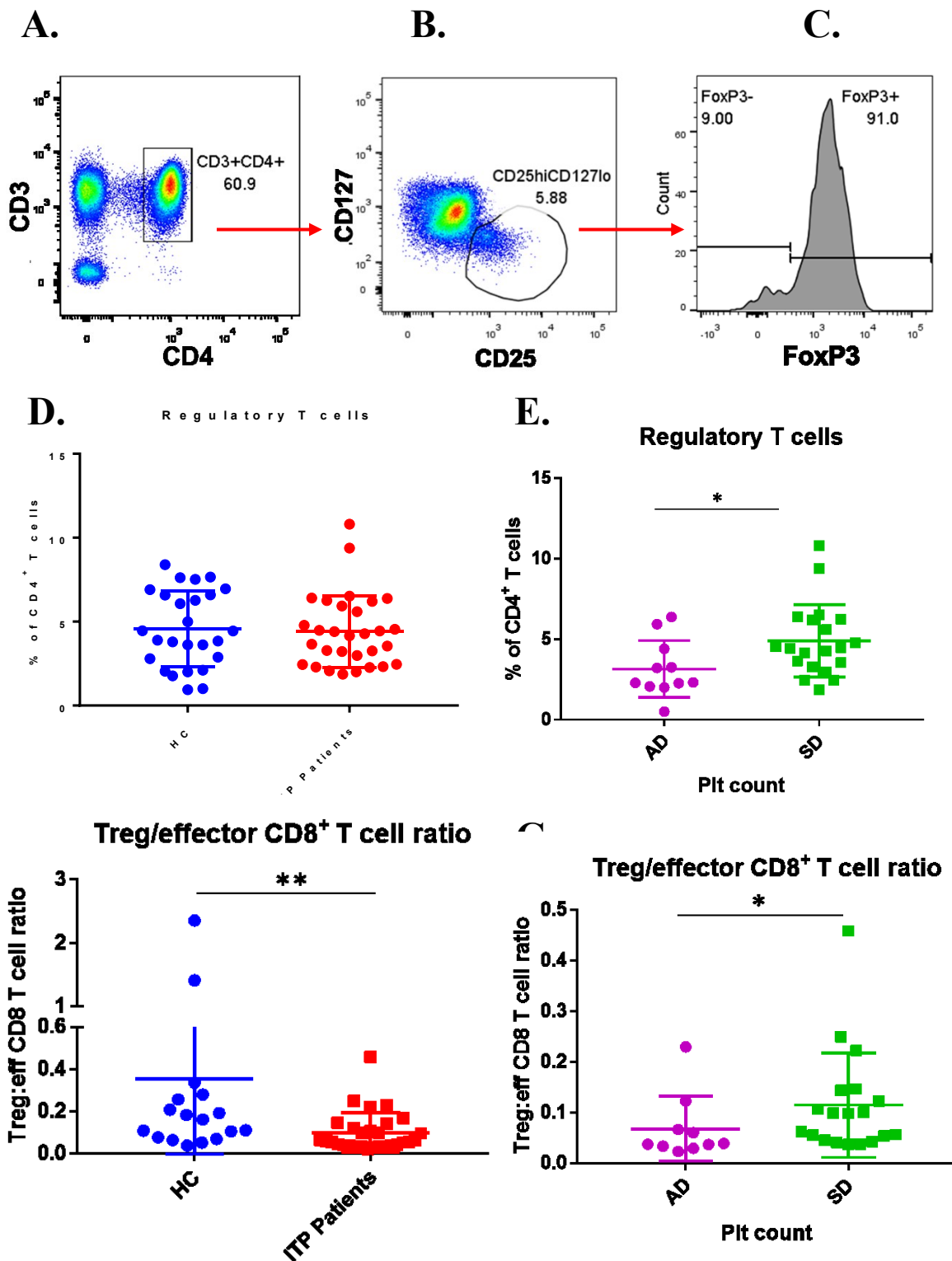


**Figure 11-14. Functional Treg are reduced in patients with ITP and correspond to disease activity.** The gating strategy for Treg is set on (A) CD3<sup>+</sup>CD4<sup>+</sup> population, followed by (B) gating on the CD25<sup>hi</sup>CD127<sup>lo</sup> population which has (C) the highest intracellular expression of FoxP3. (D) Comparison of Treg between patients (n=30) and HC (n=26), which was (E) lower in patients with AD (n=11). (F) Treg/effector CD8<sup>+</sup> T cell ratio was significantly lower in patients, (G) more prominently in AD.

### 11.3. Discussion

Forty patients who have met the diagnostic criteria of ITP (138) have been enrolled for this project. PLC in ITP does not always correlate with bleeding risk as not all patients bleed at low PLC (107). Therefore, a PLC of  $> 30 \times 10^9/L$  in the absence of any co-morbidities that could increase the risk of bleeding is considered stable disease (SD) not requiring any medical intervention (134), while a PLC of  $< 30 \times 10^9/L$  represents active disease (AD). Although the median age of patients receiving Elt was significantly higher than that of Romi-treated patients, no significant difference was observed in the PLC between these two cohorts.

The use of surface markers to phenotype T cells has been a debatable issue that still needs standardisation to be reached by international consensus (139,140). An important consideration in designing these panels is the inclusion of a Live/Dead (L/D) discrimination dye to exclude dead cells. Dead cells, besides their autofluorescence, may bind non-specifically to antibodies giving false positivity (141). In this study, T cells in peripheral blood were described by their positivity of the pan T cell marker CD3, and either CD4 or CD8. CD45RA and CD62L have been used to characterise CD4<sup>+</sup> and CD8<sup>+</sup> T cell subsets; naïve, effector memory, central memory (CM) and terminally-differentiated (td) effector referred to as effector population. These subsets have been further validated by the differential distribution of CD27 and CD57 in them (142).

ITP is an autoimmune disease that has long been thought to be antibody-mediated, targeting platelets in the circulation, leading to their increased destruction in the spleen (62,130). However, an increasing bulk of evidence is suggesting an alternative pathway of platelet destruction which is thought to be due to T cells (86,93,143). Olsson and colleagues were the first to report a CD8<sup>+</sup> T cell-mediated platelet destruction *in vitro* suggesting it as an alternative pathway of platelet destruction to the autoantibody-mediated destruction *in vivo* (94).

However, this work did not show whether this is reflective of disease activity or whether CD8<sup>+</sup> T cells in patients with ITP are functionally different from HC. This work demonstrates CD8<sup>+</sup> T cell activity from various aspects suggesting their involvement in disease pathophysiology. Numerically, the percentages of CD8<sup>+</sup> T cells are increased in patients with ITP and contribute to the significant reduction in CD4/CD8 T cell ratio in line with what has been reported earlier (144–146). Although the median CD4/CD8 T cell ratio in our HC cohort was slightly higher than some of the reported literature, potentially due to differences in measuring methods, the range of ratios was in line with previously reported studies (147–149). Patients with ITP have significantly higher effector CD8<sup>+</sup> T cells, which corresponded to disease activity. Similar findings of increased effector CD8<sup>+</sup> T cells have been described in other autoimmune conditions such as AA and myelodysplasia. However, the increase in the effector CD8<sup>+</sup> T cells did not reflect disease severity in these conditions (150).

Exhausted T cells have a sustained overexpression of exhaustion markers like PD-1 and Tim-3 which serve as immunomodulatory receptors controlling T cell activity (151,152). Exhausted T cells have reduced proliferative capacity and decreased functional cytokines such as IFN $\gamma$  and IL-2 (136). Tim-3 was previously reported to be significantly lower in CD4<sup>+</sup> T cells in patients with ITP, but not in CD8<sup>+</sup> T cells (153). The surface expression of the exhaustion markers PD-1 and Tim-3 in CD8<sup>+</sup> T cells have been assessed. Tim-3 was significantly lower in effector CD8<sup>+</sup> T cells compared to its naïve counterpart highlighting the differential expression of Tim-3 in CD8<sup>+</sup> T cell subsets. PD-1 was also lower in effector CD8<sup>+</sup> T cells, similar to the work of Zhong and colleagues demonstrating lower PD-1 in PBMC of patients with ITP (154). These findings suggest a dysregulation in peripheral tolerance where these effector CD8<sup>+</sup> T cells are continuously activated without proceeding to physiological exhaustion. This complements the genetic findings of upregulated anti-apoptotic genes such as BCL2 in patients with ITP (91).

Several studies have addressed the proinflammatory nature of ITP with conflicting results. ITP has been described as an autoimmune condition characterised by  $T_{H1}/T_{H17}$  proinflammatory milieu with elevated plasma levels of proinflammatory cytokines such IL-2,  $IFN\gamma$  and IL-17 (86,155,156). On the other hand, other studies have reported that the levels of these proinflammatory cytokines are not statistically different or even lower in patients compared to HC (157,158). However, these studies addressed the proinflammatory nature of the disease, without demonstrating the  $CD8^+$  T cell contribution to this inflammatory milieu. In this study, the proinflammatory nature of the disease has been determined by characterising the intracellular cytokines in  $CD8^+$  T cells.  $CD8^+$  T cells expressing proinflammatory cytokines (IL-2,  $IFN\gamma$  and  $TNF\alpha$ ) were significantly higher in patients compared to HC. Similarly, the essential killing machinery of  $CD8^+$  T cells, Granzyme B (GnB) and Perforin, were significantly higher in patients. These findings link the previous findings of increased gene expression of IL-2,  $IFN\gamma$  and GnB-related genes in  $CD3^+$  T cells in patients with ITP (94), and the increased levels of GnB,  $TNF\alpha$  and Perforin mRNA in  $CD8^+$  T cells from patients with ITP (159). These findings suggest that  $CD8^+$  T cells carry a proinflammatory signature in patients with ITP, similar to other conditions such as AA (160), and they contribute to the overall proinflammatory milieu observed in these patients.

The advancement of polychromatic flow cytometry has enabled scientists to assess  $CD8^+$  T cell polyfunctionality i.e. their capacity to produce multiple cytokines together in response to different pathogens such as vaccinia and HIV-1 viruses as well as Tuberculosis (TB) (161–163). As far as this study is concerned, this is the first study to address the polyfunctionality of  $CD8^+$  T cells in ITP. Polyfunctional  $CD8^+IFN\gamma^+TNF\alpha^+$  T cell population was significantly higher in patients compared to HC and was enriched within the effector  $CD8^+$  T cells. This polyfunctional population also has the highest GnB and Perforin co-expression compared to the other subsets reflecting an effector function of producing apoptosis-inducing cytokines and

the killing machinery of CD8<sup>+</sup> T cells. These findings further confirm that the increased effector CD8<sup>+</sup> T cells in patients is not exhausted which would have been characterised by low expression of intracellular IFN $\gamma$  and IL-2 (164).

T cell reactivity to platelets has been determined by culturing patients PBMC them directly with pooled platelets from HC in an IFN $\gamma$  ELISpot assay and comparing them to cells from HC. In this assay, each dot represents an activated cell that secretes IFN $\gamma$  and hence the higher the dot counts the higher the activity. PBMC from patients with ITP yielded significantly higher count compared to PBMC from HC when cultured with platelets demonstrating higher alloreactivity to platelets. Patients' PBMC still had higher IFN $\gamma$ -secreting cells compared to those of HC when cultured without platelets. These findings suggest that patients' T cells are functional, capable of secreting proinflammatory cytokines such as IFN $\gamma$  and that they have higher activity demonstrated as higher IFN $\gamma$ -secreting cells which is further driven by platelets.

Upon examining the effect of using TPO-RA on CD8<sup>+</sup> T cell functionality, significantly higher CD8<sup>+</sup>IL-2<sup>+</sup> and CD8<sup>+</sup> IFN $\gamma$ <sup>+</sup> T cells were observed in patients receiving TPO-RA compared to those on no treatment. CD8<sup>+</sup>TNF $\alpha$ <sup>+</sup> and CD8<sup>+</sup>GnB<sup>+</sup> T cells were also higher, however, not statistically significant which may suggest that TPO-RA could drive CD8<sup>+</sup> T cell activation indirectly via increasing platelet production leading to further stimulation of T cells.

Elt is a small molecule that is thought to deliver its function via binding to the transmembrane domain of the TPO-R (165). And due to its small nature, it could have an off-target effect either through binding to other receptors or via its reported *in vitro* and potentially *in vivo* iron-chelating properties (125,166,167). Therefore, T-cell phenotypic changes has been examined in patients receiving Elt and compared them to Romi and HC. Romi-treated patients had significantly higher effector CD8<sup>+</sup> T cells compared to both Elt-treated patients and HC, confirming our previous findings of increased CD8<sup>+</sup> T cells expressing proinflammatory

cytokines. However, Elt seemed to significantly lower the effector CD8<sup>+</sup> T cells in patients compared to Romi, although still higher than HC. On the other hand, Romi-treated patients had the lowest naïve CD8<sup>+</sup> T cells compared to Elt-treated and HC. Elt seemed to have a normalising effect on naïve CD8<sup>+</sup> T cells by increasing them.

To recapitulate the interaction between Elt and CD8<sup>+</sup> T cells *in vivo*, PBMC were stimulated with anti CD3/CD28 to mimic the stimulatory condition of ITP and were cultured with serial concentrations of Elt. CD8<sup>+</sup> T cell functionality was assessed via their intracellular cytokines which was significantly affected by Elt. Elt significantly reduced CD8<sup>+</sup>GnB<sup>+</sup>, CD8<sup>+</sup>TNFα<sup>+</sup> and the polyfunctional CD8<sup>+</sup>IFNγ<sup>+</sup>TNFα<sup>+</sup> T cell populations in a dose-dependent manner, which was not observed when cultured with Romi. Serial doses of Romi could not be studied, similar to Elt, due to lack of availability. However, the dose used in this study (31.25 μg/ml) corresponds to a supratherapeutic level. These findings are in line with a case report of AA associated with HIV infection in which Elt treatment reduced polyfunctional CD4<sup>+</sup>IFNγ<sup>+</sup>TNFα<sup>+</sup> and CD4<sup>+</sup>IL17<sup>+</sup> T cells. This immunomodulatory property of Elt could explain an additional therapeutic mechanism in ITP through which remission is achieved that is, beside increasing platelet production, it suppresses activated T cells. It could also explain the rationale of its addition to the standard immunosuppressive treatment of the CD8<sup>+</sup> T cell-mediated AA (168–170).

Lastly, Treg were characterised using the phenotype CD3<sup>+</sup>CD4<sup>+</sup>CD25<sup>hi</sup>CD127<sup>lo</sup> as described previously (142,171). The phenotype was also confirmed using the Treg-specific transcription factor FoxP3 which was highly enriched within the described phenotype. Treg, as a percentage from the total CD4<sup>+</sup> T cell population, did not differ significantly between patients and HC. However, it is still considered lower in patients as the total CD4<sup>+</sup> T cell percentage was lower in patients compared to HC which is in line to what has been reported previously (87,101,172). Expectedly, Treg frequency correlated with disease activity being significantly higher in AD

patients compared to SD patients. These findings confirm previous reports suggesting that patients recovery, described as an increase in PLC, is associated with a recovery in Treg frequency (99,101).

A previous report has suggested that Treg are functionally impaired in patients with ITP (98). In this study, the functionality of Treg, as assessed by the intracellular expression of IL-2, did not differ significantly between patients and HC. As the suppressive function of Treg is based on their interaction with other immune cells, Treg/effector CD8<sup>+</sup> T cell ratio was calculated in patients and compared to HC. Treg/effector CD8<sup>+</sup> T cell ratio was significantly lower in patients compared to HC, and the reduction was more pronounced in AD compared to SD. As Cao and colleagues describe similar correlations between T<sub>h17</sub> and Treg (87), these findings further demonstrate that the role of Treg in ITP pathophysiology should be considered in relation to other subsets rather than an absolute numerical or functional Treg abnormality.

## 12. Characterising the T cell involvement in the bone marrow pathophysiology of immune thrombocytopaenia (ITP)

### 12.1. Introduction

Early studies on ITP describe it as a disorder of increasing platelet destruction taking place mainly in the spleen (62,130). This justified splenectomy to be a treatment option for patients with ITP, achieving variable response rates (112,173).

Megakaryocyte (MK) development and maturation leading to platelet production has also been implicated in ITP pathophysiology. Houwerzijl and colleagues were the first to report that ITP negatively impacts the structure of MK *in vivo* (79).

As demonstrated in the previous chapter (Chapter 11), ITP is associated with T cell changes suggestive of their active role in the disease pathophysiology. However, it is not clear if such pathology is also present in the BM of patients with ITP.

In this chapter, BM trephines of 21 patients with ITP are examined and compared them to 8 disease-controls. This examination consisted of multi-colour Immunohistofluorescent (IHF) detecting multiple cells namely; CD42<sup>+</sup> MK, CD4<sup>+</sup> and CD8<sup>+</sup> T cells. This examination was done by an automated process, minimising any analytical bias and variability between analysed samples.

MK frequency differed significantly in patients with ITP and it was influenced by disease chronicity and TPO-RA treatment. T cell changes were also described in the BM of patients with ITP.

MK-T cell interaction, defined by their close proximity to each other, was determined. This interaction was significantly prominent in patients with ITP and was influenced by disease duration. MK-T cell clustering, defined as the presence of multiple T cells around a single MK, was also determined.

A strong correlation between MK-T cell interaction and MK-T cell clustering in patients with ITP, which was present in controls.

## 12.2. Results

### 12.2.1 Patients characteristics

Bone marrow (BM) biopsies were taken from 21 ITP patients (Table 12-1) and 8 non-ITP subjects which served as disease-controls. The control subjects had no history of thrombocytopenia and no evidence of BM pathology as reported by the clinical histopathologists. The patient cohort for the BM examination was different from the patients studied in the previous section (Section 11).

Eight of the patients with ITP were male and 13 were female, whereas all the control subjects were males. The median patients' age was 51 years (range 27-88) and the control median age was 70 years (range 39-74). At the time of BM biopsy sampling 6 of the ITP patients were receiving TPO-RA (Elt n=1; and Romi n=5), 3 on prednisolone and the remainder were on no treatment.

Based on the duration of the disease at the time of collection, 8 patients were classified as newly-diagnosed, 3 as persistent and 10 as chronic patients.

All BM trephines were examined independently at the histopathology department at the Hammersmith hospital, reporting findings consistent with a diagnosis of ITP and not associated with any other BM pathology.

Patient ID	Age	Gender	Dx classification	Treatment*	Platelet count (x 10 <sup>9</sup> /L)*
1	24	F	Chronic	No treatment	27
2	48	M	Chronic	Eltrombopag	19
3	55	M	Chronic	No treatment	95
4	18	M	Chronic	No treatment	40
5	44	F	Persistent	No treatment	319
6	49	M	Chronic	No treatment	111
7	51	F	Chronic	Prednisolone	135
8	77	F	Chronic	Romiplostim	30
9	24	F	Newly-Diagnosed	No treatment	3
10	39	F	Newly-Diagnosed	Romiplostim	17
11	44	F	Newly-Diagnosed	Prednisolone	33
12	67	F	Newly-Diagnosed	Romiplostim	12
13	27	M	Chronic	No treatment	32
14	32	M	Persistent	Prednisolone	7
15	58	M	Chronic	Romiplostim	155
16	76	F	Newly-Diagnosed	No treatment	75
17	77	F	Newly-Diagnosed	No treatment	26
18	52	F	Chronic	No treatment	5
19	74	M	Newly-Diagnosed	No treatment	62
20	79	F	Persistent	Romiplostim	42
21	88	F	Newly-Diagnosed	No treatment	9

**Table 12-1. Clinical parameters of the patients with ITP enrolled in this bone marrow study.** The patients' IDs for this part of the study are different from the ones used in the previous section 11.2.1. \*Received treatment and platelet count at the time of sample collection.

### **12.2.2. Automated Identification of the different cells in the BM trephines**

Whole stained BM trephines were captured using three different lasers to detect the differentially-labelled cells, namely CD4<sup>+</sup> and CD8<sup>+</sup> T cells and CD42b<sup>+</sup> mature MK.

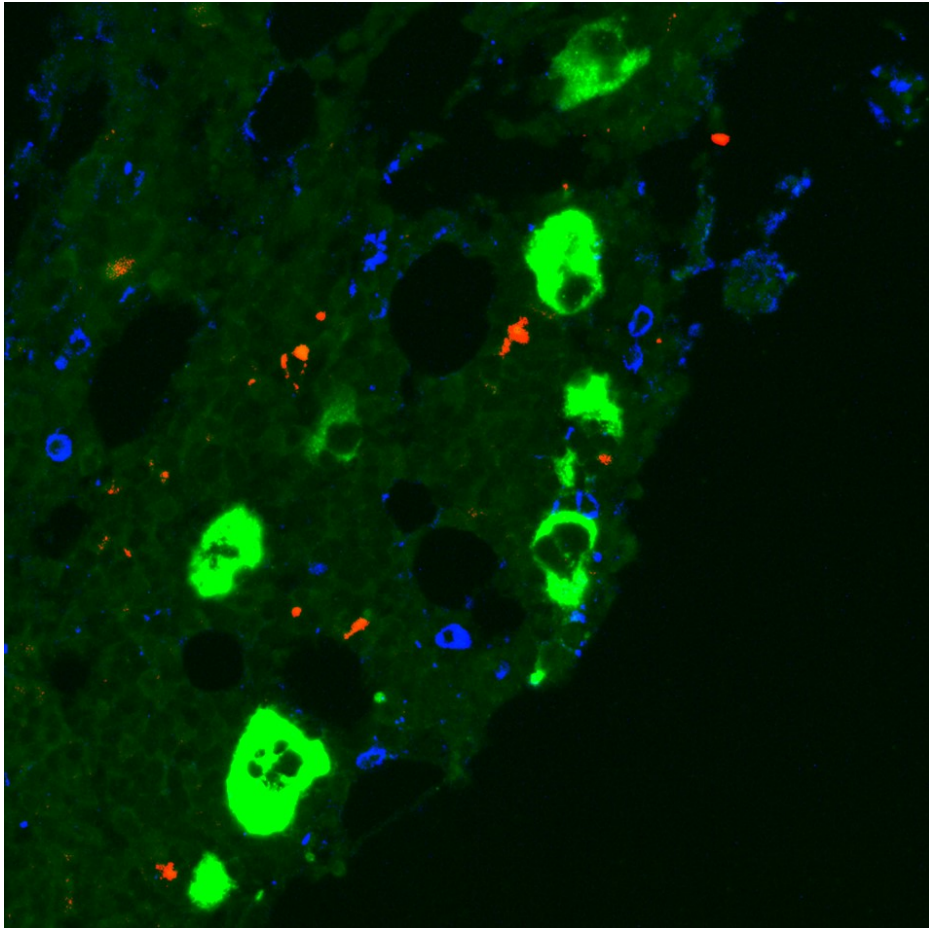
With the assistance of Mr Stephen Rothery from the FILM facility, a macro was developed to examine the whole trephine sections (0.57 – 4.97 mm<sup>2</sup>). This macro was set read each fluorescent channel, representing a separate marker, individually and count these cells based on a pre-set size and signal intensity limits. After that, the macro combined these channels together to determine the frequency of MK-T cell IP as well as clustering in the whole trephine. The fluorescent signal intensity of each marker was set at a fixed threshold and was applied to all trephines. This was done in order to minimise the impact of background staining on the automated counting process and ensure consistency between the trephines.

A size gate/limit was set, based on previously described physical characteristics of T cells and MK (174), to better identify the cells and exclude non-specifically stained sections. A minimum diameter of 5 µm was set to identify CD4<sup>+</sup> and CD8<sup>+</sup> T cells, whereas a minimum diameter of 20 µm was set for MK (Figure 12-1A).

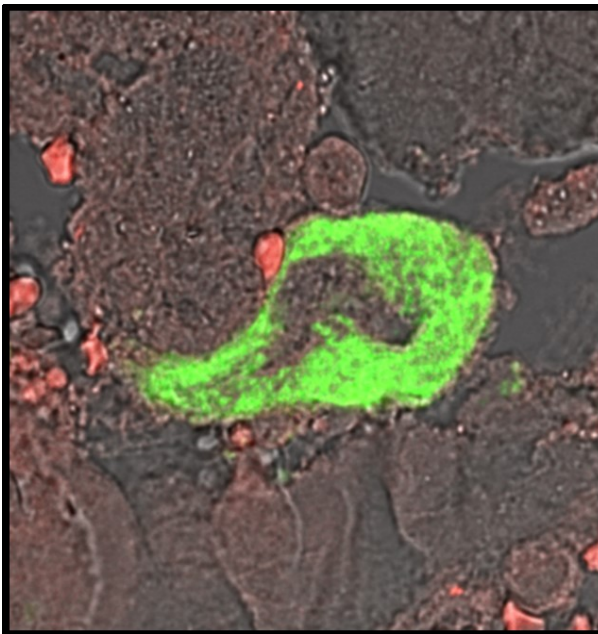
After optimising the signal intensity and the size thresholds, these parameters were provided to the macro to analyse all the captured trephines excluding any analytical biases.

As some sections showed variation in their cellular distribution, cellular density was calculated based on the cell frequency per mm<sup>2</sup> of the trephine. Cellular interaction between MK and T cells was characterised based on their immediate proximity (IP). Any T cell that were within the range of a single pixel, the smallest value that could be set, from the MK membrane was considered to be in IP (Figure 12-1B). MK-T cell clustering was determined when multiple T cells were in IP to a single MK (Figure 12-2).

A.



B.



C.

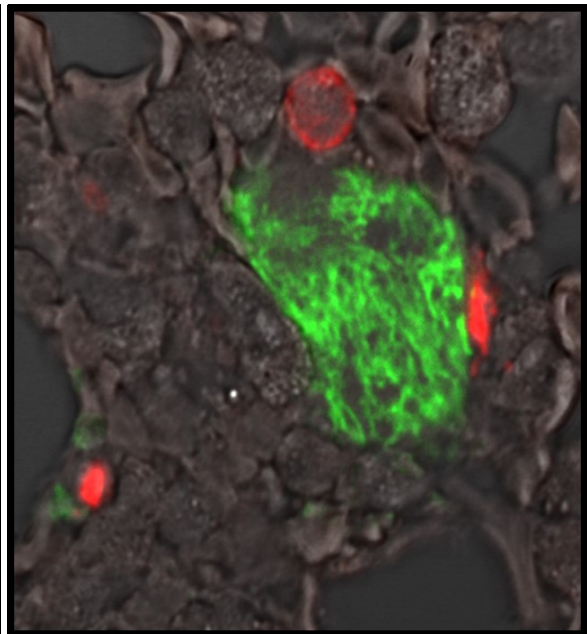
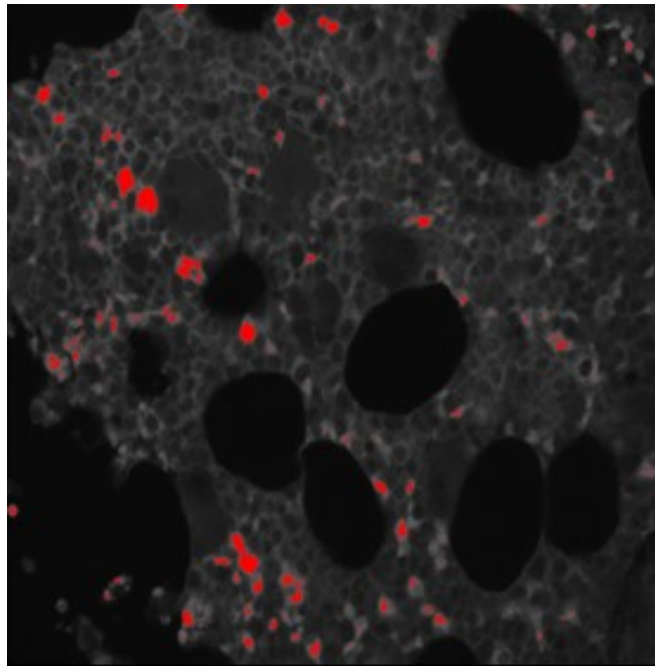
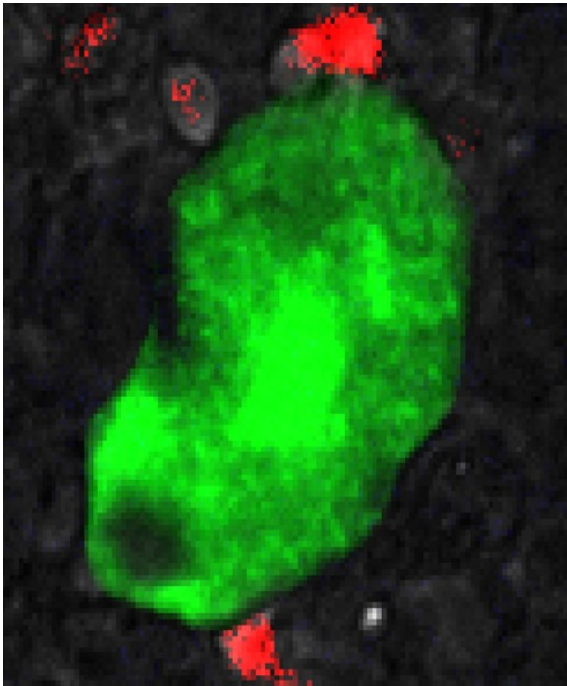


**Figure 12-1. IHF staining of bone marrow trephine.** IHF staining of BM trephines showing (A) CD42b<sup>+</sup> mature MK (green) with CD4<sup>+</sup> T cells (red) and CD8<sup>+</sup> T cells (blue). Images showing (B) CD4<sup>+</sup> T cell interacting with MK, and (C) a CD4<sup>+</sup> cluster around a single MK. Images were captured at (A) 20x magnification and (B-C) 40x magnification.

A.



B.



C.

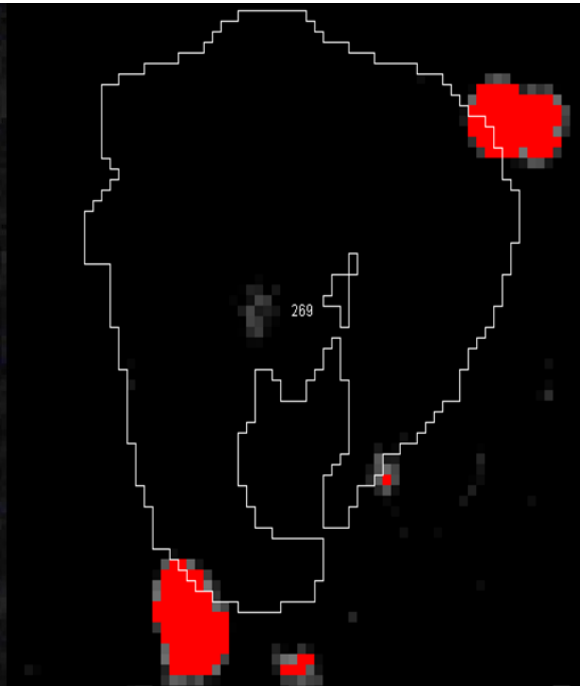


**Figure 12-2. Identifying MK and T cells IPs and clustering.**

Based on the established fluorescent signal intensity and the size limit, the macro could (A) identify the cells of interest in a trephine and highlight them in red. (B) A focused field of a single MK in close proximity with multiple T cells, which the software can differentiate and (C) outline the MK and count the number of clustered T cells.

### **12.2.3. Increased MK frequency in patients with ITP, more prominently in TPO-RA patients**

Differences in MK density, defined as the frequency of MK per  $\text{mm}^2$ , were observed in the BM of patients with ITP compared to controls (Figure 12-3). Patients had significantly higher MK density compared to controls [ $94.03/\text{mm}^2$  vs  $52.33/\text{mm}^2$ ; P value  $< 0.01$ ] (Figure 12-4A). This increase in MK density was more prominent in patients who received TPO-RAs compared to those who did not and to the control group [ $155.7$  vs  $88.69$  vs  $52.33/\text{mm}^2$ ; P value  $< 0.01$ ] (Figure 12-4B). No significant difference was observed in MK densities between acute and chronic patients [P value  $> 0.05$ ].

Although MK diameter was not significantly different between controls and the patients [P value  $> 0.05$ ], MK of patients on TPO-RA had significantly longer diameters compared to controls [ $21.84$  vs  $18.09\mu\text{m}$ ; P value  $< 0.05$ ] (Figure 12-4C). Moreover, chronic patients had significantly longer MK diameter compared to patients in the acute phase of the disease [ $21.59$  vs  $16.83\mu\text{m}$ ; P value  $< 0.05$ ] (Figure 12-4D).

## Controls

## Patients

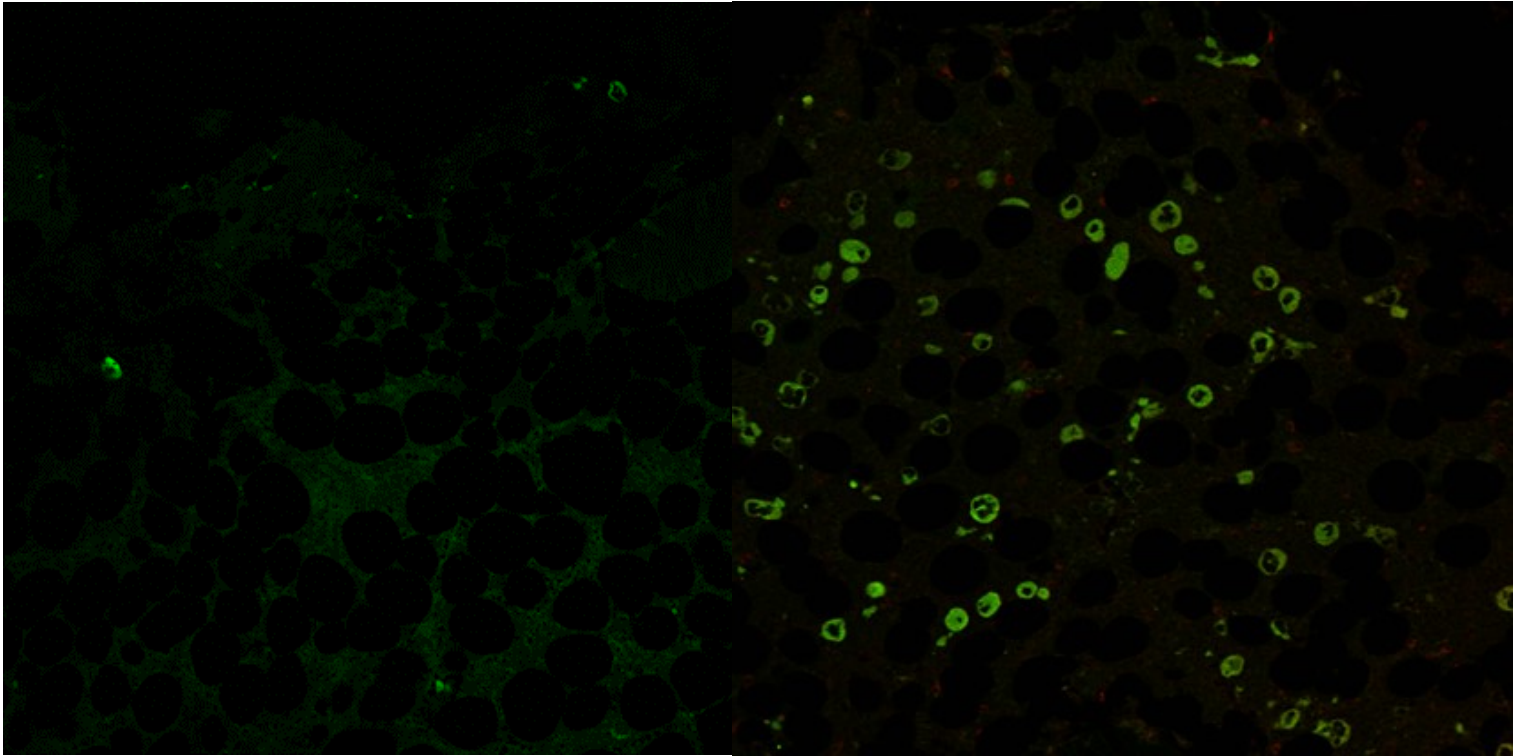


**Figure 12-3. Examples of BM trephine staining in controls and patients with ITP.** Images showing an overview of the BM trephines stained for MK (green) and CD4<sup>+</sup> T cells (red). The contrast difference in MK density between controls and patients can be visually appreciated. Images were captured at 20x magnification using the exact fluorescent settings.

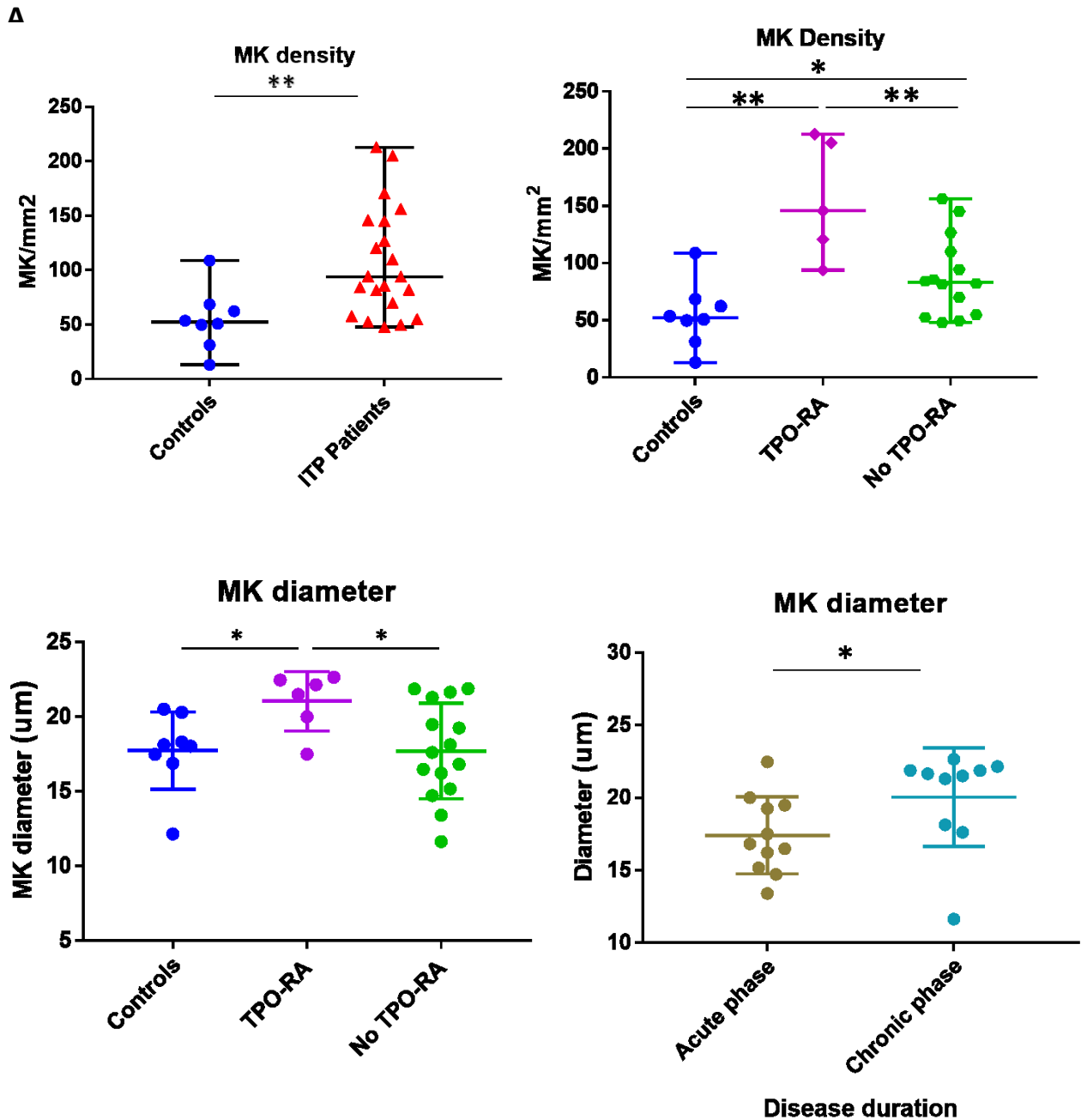


**Figure 12-4. MK densities and diameters in patient cohorts and controls.**

Figures showing (A) the significant difference in MK density between controls (blue) and patients with ITP (red). (B) The figure shows the difference in MK densities between patients receiving TPO-RA (purple) and those not receiving TPO-RAs (green) in comparison to controls. The differences in MK diameter (C) based on treatment; between patients who are on TPO-RAs and those who are not, (D) based on disease duration; between patients in the acute (oil green) and chronic (turquoise blue) phases of the disease.

#### **12.2.4. T cell changes within the bone marrow in patients with ITP**

Unlike peripheral blood findings described in the previous chapter of significantly reduced CD4<sup>+</sup> and increased CD8<sup>+</sup> T cells in patients with ITP (Chapter 11), BM CD4<sup>+</sup> (Figure 12-5A) and CD8<sup>+</sup> T cell densities (Figure 12-5B) were slightly increased in patients when compared with controls [P value > 0.05]. However, CD4/CD8 T cell ratio was significantly lower in patients compared to control [1.7 vs 4.3; P value < 0.01] (Figure 12-5C), similar to the described finding in peripheral blood (Chapter 11). No significant differences were observed in the CD4<sup>+</sup> and CD8<sup>+</sup> T cell densities as well as CD4/CD8 T cell ratio between patients according to their treatment nor disease duration (P value > 0.05).

Interestingly, the diameter of CD4<sup>+</sup> T cells was significantly shorter in patients compared to controls [4.2 vs. 4.67µm; P value < 0.05] (Figure 12-5D). This could indicate apoptotic changes of the BM CD4<sup>+</sup> T cells (175), however, this is something that needs further evaluation. No observed difference in the CD8<sup>+</sup> T cells (Figure 12-5E), and no significant differences were found in the CD4<sup>+</sup> and CD8<sup>+</sup> T cell diameter between patients based on their treatment or disease duration.

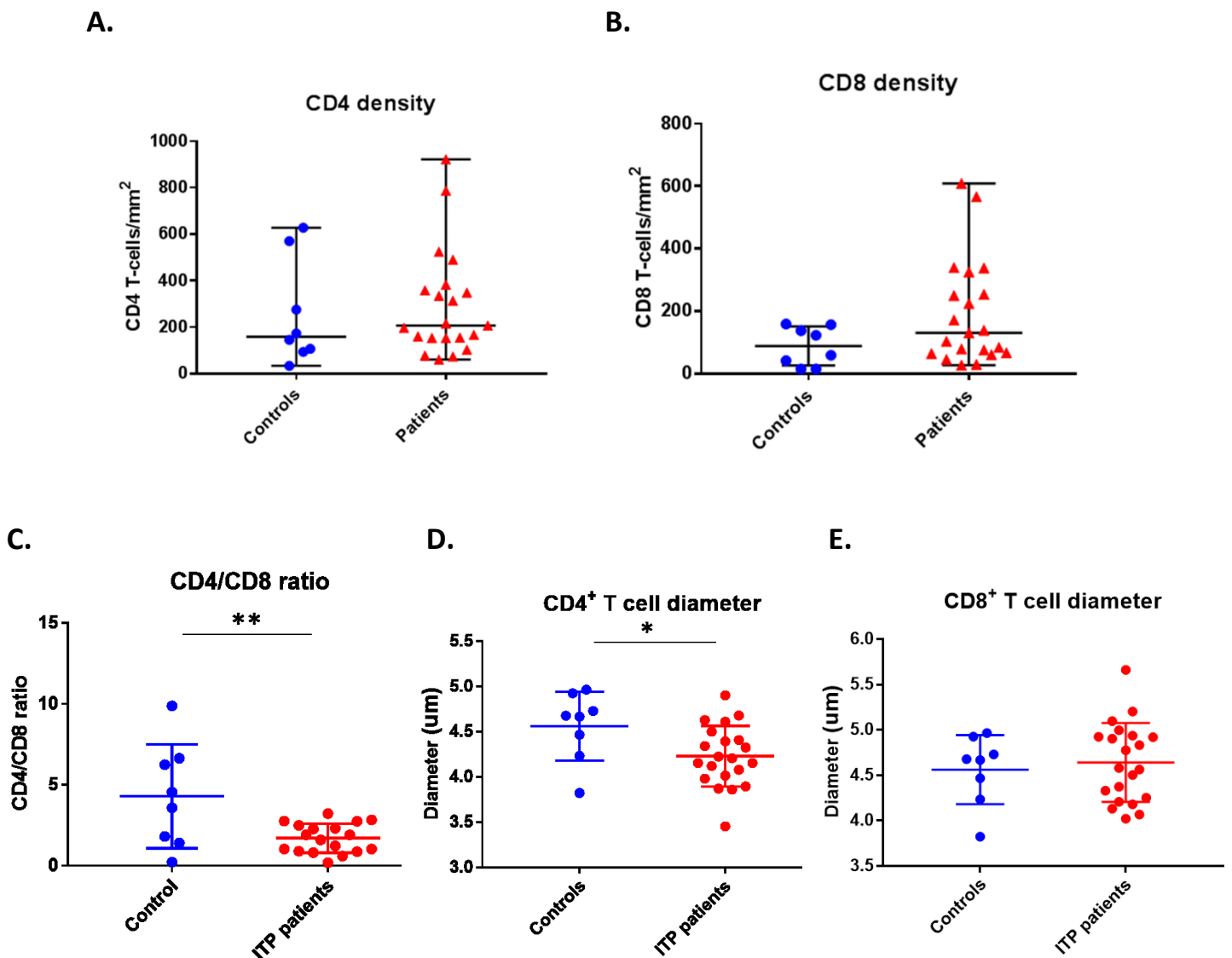


**Figure 12-5. T cell densities and diameters in the BM of controls and patients with ITP.**

Figures showing (A) CD4<sup>+</sup> and (B) CD8<sup>+</sup> T cell density in controls (blue) compared to patients (red). (C) CD4/CD8 ratio was significantly lower in patients, as well as (D) CD4<sup>+</sup> T cell diameter compared to controls. (E) CD8<sup>+</sup> T cell diameter was slightly higher in patients.

### **12.2.5. Increased MK-T cell interaction in the BM of patients with ITP**

The frequency of MK-T cell interaction was determined by the frequency of their immediate proximity (IP).

The frequency of both MK-CD4<sup>+</sup> T cell IP and MK-CD8<sup>+</sup> T cell were significantly higher in patients compared to controls [26 vs 7.5; P value < 0.05] (figure 12-6A) and [9.5 vs 3; P value < 0.05] IP (Figure 12-6B), respectively.

Chronic patients had higher frequency of MK-CD4<sup>+</sup> T cell IP [37 vs 14; P value < 0.05] (figure 12-6C) and MK-CD8 IP [13 vs 3; P value < 0.05] (figure 12-6D) compared to acute patients, suggesting evolution of disease. However, there was no difference in MK-T cell IPs in patients treated with TPO-RA and those who are not on TPO-RA [P value > 0.05].

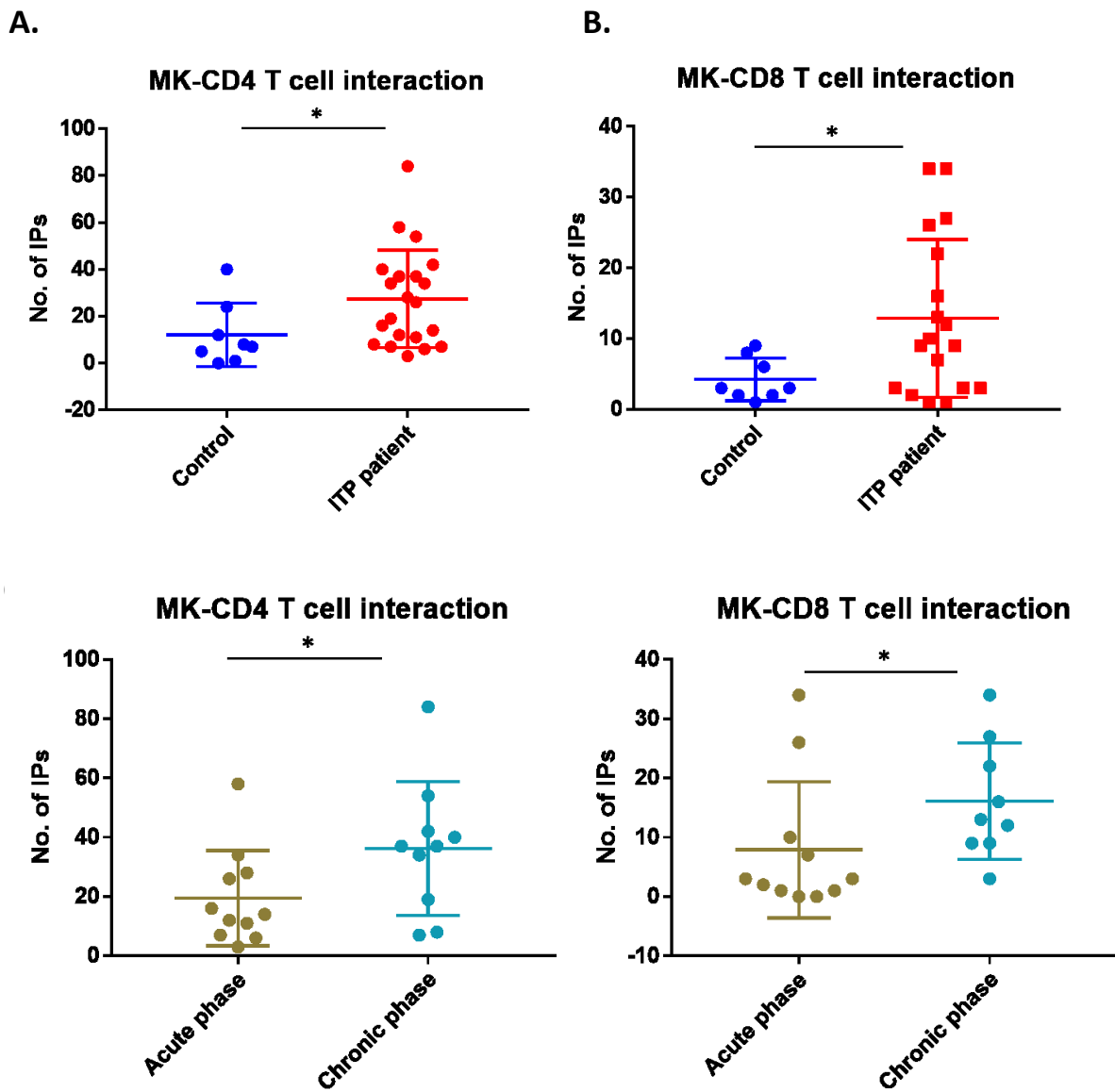


**Figure 12-6. MK - T cell IPs in controls and patients with ITP.**

Figures showing the significantly higher (A) MK-CD4<sup>+</sup> and (B) MK-CD8<sup>+</sup> T cell IPs in patients (red) compared to controls (blue). The increase in (C) MK-CD4<sup>+</sup> and (D) MK-CD8<sup>+</sup> T cell IPs were more prominent in chronic patients (turquoise blue) compared to acute patients (oil green).

### 12.2.6. Increased MK-T cell clustering in the BM of patients with ITP

MK-T cell clustering was defined as more than one T cell in IP to a single MK.

There was a significant increase of MK-CD4<sup>+</sup> T cell clustering in patients compared to controls [7 vs 1; P value < 0.01] (Figure 12-7A). However, there was no significant difference in MK-CD8<sup>+</sup> T cell clustering between patients and controls [P value > 0.05] (Figure 12-7B). Interestingly, 3 patients with ITP had very high numbers of CD8 clustering, suggesting there may be different types of disease.

The chronicity of the disease did not influence the rate of either MK-CD4<sup>+</sup> T cell nor MK-CD8<sup>+</sup> T cell clustering. Hence the differences in MK-T cell clustering were not statistically significant between acute and chronic patients [P value > 0.05] (Figures 12-7C-D).

There was a strong correlation between numbers of IPs and clustering of IPs in both CD4-MK [ $r=0.93$ ; P value < 0.0001] (Figure 12-7E) and CD8-MK [ $r=0.90$ ; P value < 0.0001] (Figure 12-7F) in patients with ITP, but not in controls.

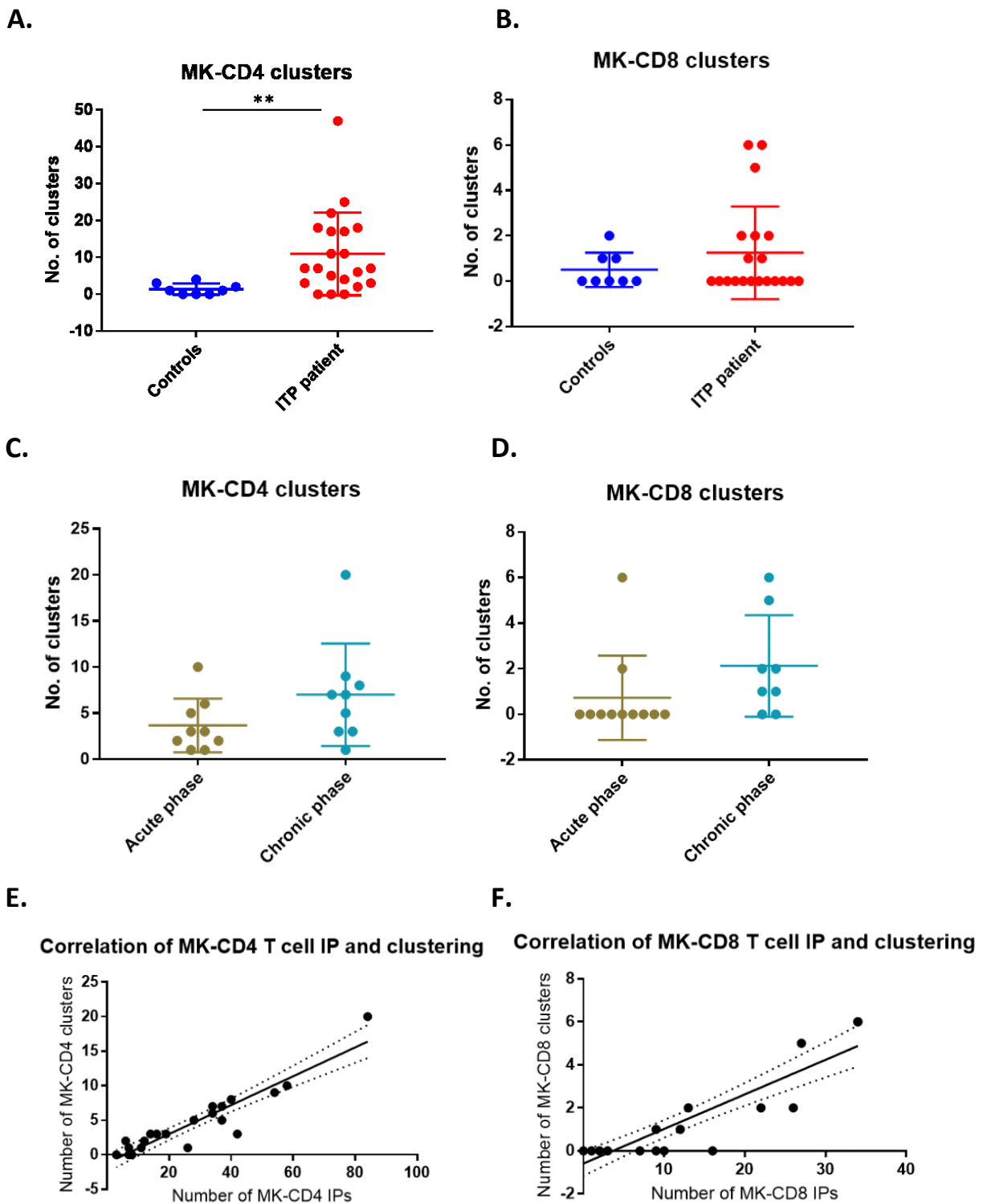


**Figure 12-7. MK - T cell clustering in controls and patients with ITP and its correlation to IP.** Figures showing the significantly higher (A) MK-CD4+ T cell clustering in patients compared to control. (B) MK-CD8+ clustering did not differ significantly, nor the disease duration had an impact on MK-T cell clustering (C-D). The significant correlation between MK and T cell subsets IP and clustering are demonstrated (E-F).

### 12.3. Discussion

ITP is a disease diagnosed by excluding other conditions that could lead to a reduced platelet count. Routine BM examination is not generally indicated in patients with ITP following the international consensus report and the American Society of Haematology guidelines (110,111). This has led to a shift in studies focusing on the peripheral blood pathophysiology rather than its central pathology i.e. BM pathology.

Addressing the BM pathology, previous studies used a single-colour IHC staining of bone marrow trephines to examine BMs of patients with ITP. This is usually followed by counting stained cells manually in a single or multiple power fields of the trephines. Using this approach, human error is unavoidable which would not be corrected appropriately by having multiple human assessors. This approach also may not demonstrate the interactive nature between different cells as it will only stain on type of cells, making evaluating such interaction prone to error.

To address these challenges in this study, multi-colour Immunohistofluorescent staining (IHF) has been used to identify multiple cellular components of the BM. Using this technique allowed us to assess MK and T cell interaction precisely based on their staining positively. Moreover, an automated approach has been used to identify the different cells, quantify them and assess their interaction based on their close proximity to each other. This automated approach was achieved through developing a macro which is a set of commands to perform different analytical functions based on provided parameters on the signal intensity and cell size. This macro eliminated any variabilities in examining the slides between the different users.

The expected response to the peripheral thrombocytopenic nature of ITP is a compensatory increase in platelet production from the BM either via a rise in MK density or their capacity to produce more platelets demonstrated as an increase in their size. The significant increase in

MK density found in the cohort of patients in this study is consistent with this idea. This is in line to what has been previously demonstrated using a similar single-staining IHC technique (79,176). However, other reports suggested that MK density either remained unchanged in patients or even lowered relatively in comparison to controls (177–179). This could be attributed to the difference in the technique and the marker used to identify and count the MK as some of these studies have used CD41 and CD61 which are early megakaryocytic markers and hence the inclusion of early MK might have influenced such findings. The increase in the MK density was, as would be expected, more prominent in patients receiving TPO-RAs, which act on TPO-R on MK as well as MK progenitors, leading to the increased MK density in the BM (117,118).

This study did not address overall MK's morphology nor link it to previously published studies, however, MK's diameter, as a physical feature, was measured in patients and controls. MKs in patients with ITP have been previously reported to be structurally abnormal with apoptotic and para-apoptotic features by electron microscopy (79,80), which could be expected to impact MK diameter. No significant differences in MK diameters were observed between patients and controls in this study. However, an observed longer diameters i.e. larger MK in chronic ITP patients compared to acute ITP, which has not been previously described. These findings suggest that these changes could be either part of the physiological response to chronic thrombocytopaenic state of the disease, or it is part of the pathological progression of MK in patients with ITP representing apoptotic changes. However, a longer follow up post treatment and more detailed examination such as electron microscopy would address if these changes are reversible which could be corrected by treatment.

CD4<sup>+</sup> and CD8<sup>+</sup> T cell densities did not differ significantly between patients and controls in our study, which are in agreement with previous studies reporting no significant differences of CD4<sup>+</sup> and CD8<sup>+</sup> T cell density in the BM of patients with ITP (178,180).

The interaction of MK with different immune cells in ITP has been of interest to many researchers, especially the *in vivo* interaction. MK capacity to produce proplatelets has been shown to be affected by autoantibodies from patients with ITP *in vitro* (82,84). This autoantibody-mediated pathology was also supported by *in vivo* evidence of MK being surrounded by IgG antibodies in the BM of patients with ITP (178). However, the role of T cell in interacting with MK in the BM in ITP remains to be explored *in vivo*.

In our patients' cohort, MK-CD4<sup>+</sup> and MK-CD8<sup>+</sup> T cell interactions were significantly higher in patients compared to controls. Moreover, this observation was more prominent in chronic patients compared to patients with a disease duration of less than a year suggesting evolution of disease over time. Although the increased MK-T cell interaction could be a coincidental finding due to the increased MK density, this seems to be a physiological response as there was no significant difference in MK density between Acute and chronic patients. Furthermore, the correlation between MK-T cell interactions and clustering in patients, but not in controls, further supports the active interaction between MK and T cells rather than just a coincidental colocalisation. The work of Song and colleagues on BM aspirates have shown that there was a significant increase in the IL-17<sup>+</sup> CD3<sup>+</sup>CD8<sup>-</sup> T cells and CD8<sup>+</sup> effector memory populations in patients (180). The proximity between MK and CD4<sup>+</sup> and CD8<sup>+</sup> described here suggest that these may be active interactions rather than just co-localisation within the BM microenvironment. These findings also suggest a novel mechanism in which both major T cell subsets, CD4<sup>+</sup> and CD8<sup>+</sup>, are actively involved in the BM pathology in ITP. This involvement might be an indication of chronicity in which T cells are triggered and actively interact with MK following an initial T cell-independent pathology.

The clustering of CD4<sup>+</sup> T cells around MK was more prominent in patients compared to controls. This was an unexpected finding and suggests there may be education of the immune cells by megakaryocytes. This has not been previously described in human data. Mouse

literature suggests that MKs can interact with T cells at early stages of megakaryocytic development. MK progenitors were observed to be capable of driving Th<sub>1</sub>/Th<sub>17</sub> response (59) via MHC-II. However, MHC Class II expression falls over time and late megakaryocytes would therefore not have the possible machinery to interact with T cells. Human MKs have some differences to mouse MKs. The work presented here shows this needs further evaluation. The rate of T cell clustering was higher in chronic patients, although not statistically significant, compared to acute patients. As this study has not determined the subset of these CD4<sup>+</sup> T cells, such as the proinflammatory Th<sub>17</sub> or Treg, the interactive nature between MK and these CD4<sup>+</sup> T cells could not be determined (60,180).

Although MK-CD8<sup>+</sup> T cell clusters were not increased as a whole compared to controls, a small number of patients did have very high numbers of CD8 clusters. This could reflect the heterogeneity of the disease; where only a proportion of patients might have a CD8<sup>+</sup> T cell-mediated disease or it could be attributed to the functional differences between the interactive nature CD4<sup>+</sup> and CD8<sup>+</sup> T cells. The killing function of CD8<sup>+</sup> T cells does not require long period of time when it is detected in *in vitro* and *in vivo* conditions (181–183) in contrast to CD4<sup>+</sup> T cells. I.e., once a CD8 cell has engaged with the megakaryocyte, it may induce MK death, and hence not be detectable by this method.

Interestingly, MK-T cell interaction, calculated as IPs, and MK-T cell clustering had a significant correlation in patients with ITP but not in controls. As this has not been described before, it would be interesting to see if immunosuppressive therapy could interrupt such correlation.

The challenges in studying the pathophysiology of ITP in BM can be identified as both technical and clinical challenges. Technically, using multi-coloured IHF imaging especially in

paraffin-embedded fixed tissues requires rehydrating the tissue and optimising the antigen retrieval conditions which greatly impact the staining quality.

In order to establish the nature of MK-T cell interaction, ideally different established markers to identify T cell subsets should be used, as demonstrated previously in peripheral blood (Chapter 11). However, the different steps of preparing BM trephines of fixation, paraffin-embedding, deparaffinisation and antigen retrieval significantly affect the integrity of many molecules that could be used to identify T cell subsets.

Due to these technical challenges and despite efforts to standardise such protocols (184), many scientists have resorted to using single-coloured IHC staining of serial slides (185,186).

Clinically, BM examination is not routinely indicated in patients with ITP (110,111). BM examinations may be reserved for old patients, which studies have shown to be of little value (80,179), patients with presence of lymphadenopathy or splenomegaly, or for patients with persistent ITP not responding to first- and second-line therapies (134). Therefore, the BM studied in these patients may reflect only a particular pathology in persistent or treatment-resistant patients, rather than common features shared between patients with ITP.

## ***13. In vitro* assessment of the megakaryocyte-CD8<sup>+</sup> T cell interaction and its regulation**

### **13.1. Introduction**

The findings described in chapter 11 show activity of CD8 cells in the peripheral blood in patients with ITP. The findings from chapter 12, suggest an active role of T cell in the bone marrow pathology in ITP. These findings included strong evidence of interactions between both CD4 and CD8 cells and megakaryocytes. However, given the fixed nature of the trephines, the nature of these interactions and its regulation could not be further explored in this system. Furthermore, little is known of the ability of MKs to interact with the immune system. Early MK progenitors in mice have been described to express functional MHC-II capable of mounting a T<sub>h1</sub>/T<sub>h17</sub> response (59).

In this chapter, an *in vitro* megakaryopoietic assay has been developed to generate MKs from BM-derived CD34<sup>+</sup> HSC. This established *in vitro* culture system is used to generate MK from HSC cells using a set of cytokines driving HSC towards MK differentiation and maturation (47,82,187,188).

The proliferation of HSC and their differentiation into MK were imaged using the imaging system Incucyte, which captured serial images at 2-hour intervals over the course of 6 days. The flow cytometric approach was based on tracking the expression of the early HSC marker and other established MK-lineage specific markers.

Given the interactions described in chapter 12, and the paucity of data exploring T cell interactions with MKs, this system was first used to investigate the change in expression of MHC class I and II as CD34 HSC develop in to MKs. Furthermore, it was used to explore whether immune regulators such as PD-L1 and PD-L2 are also expressed on developing MKs. These are important regulatory processes which inhibit T cell proliferation, which are yet to be explored.

In order to explore how ITP may change the nature of the bone marrow environment, MKs were then cultured with plasma from patients with ITP, the impact of such co-culture was determined by MK cell death as well as the surface expression of PD-L1 on MK.

The functionality of the described receptors on MK in governing the MK-CD8<sup>+</sup> T cell interaction was assessed.

## 13.2. Results

### 13.2.1. Megakaryocyte development and maturation from bone marrow-derived CD34<sup>+</sup> HSC.

Isolated BM-derived CD34<sup>+</sup> haematopoietic stem cells (HSC) from healthy donors were cultured in media supplemented to promote the production of megakaryocyte (MKs). The cells were cultured for 10 days and their abundance was tracked over a period of 6 days using the Incucyte system (Figure 13-1 A-C). Cells were multiplying steadily within the first 72 hours of culture before they started expanding in size and forming colonies (Figure 13-1D). Images of the growing MK in culture were captured and counted automatically every 2 hours across whole wells for a total period of 6 days as described previously (Chapter 10).

The different MK developmental stages were characterised on Day 3 (D3), D7 and D10 using early HSC progenitor markers; CD34 and CD38, early MK progenitor marker; CD41 (GP IIb/) and the mature MK marker; CD42b (GP Ib).

The expression of CD34 was at its highest early in the culture and decreased gradually through the culture until its disappearance by D10 (Figure 13-2A). By D3, almost 20% of the cultured cells expressed CD41. Expression of CD41 continued to increase throughout the culture (Figure 13-2B). CD42b expression appeared as early as D3, although in a very small percentage of the cultured cells (less than 5%). CD42b was at its highest by D10 (Figure 13-2C). Mature MK were identified as CD34<sup>-</sup>CD38<sup>lo</sup>CD41<sup>+</sup>CD42b<sup>+</sup>.

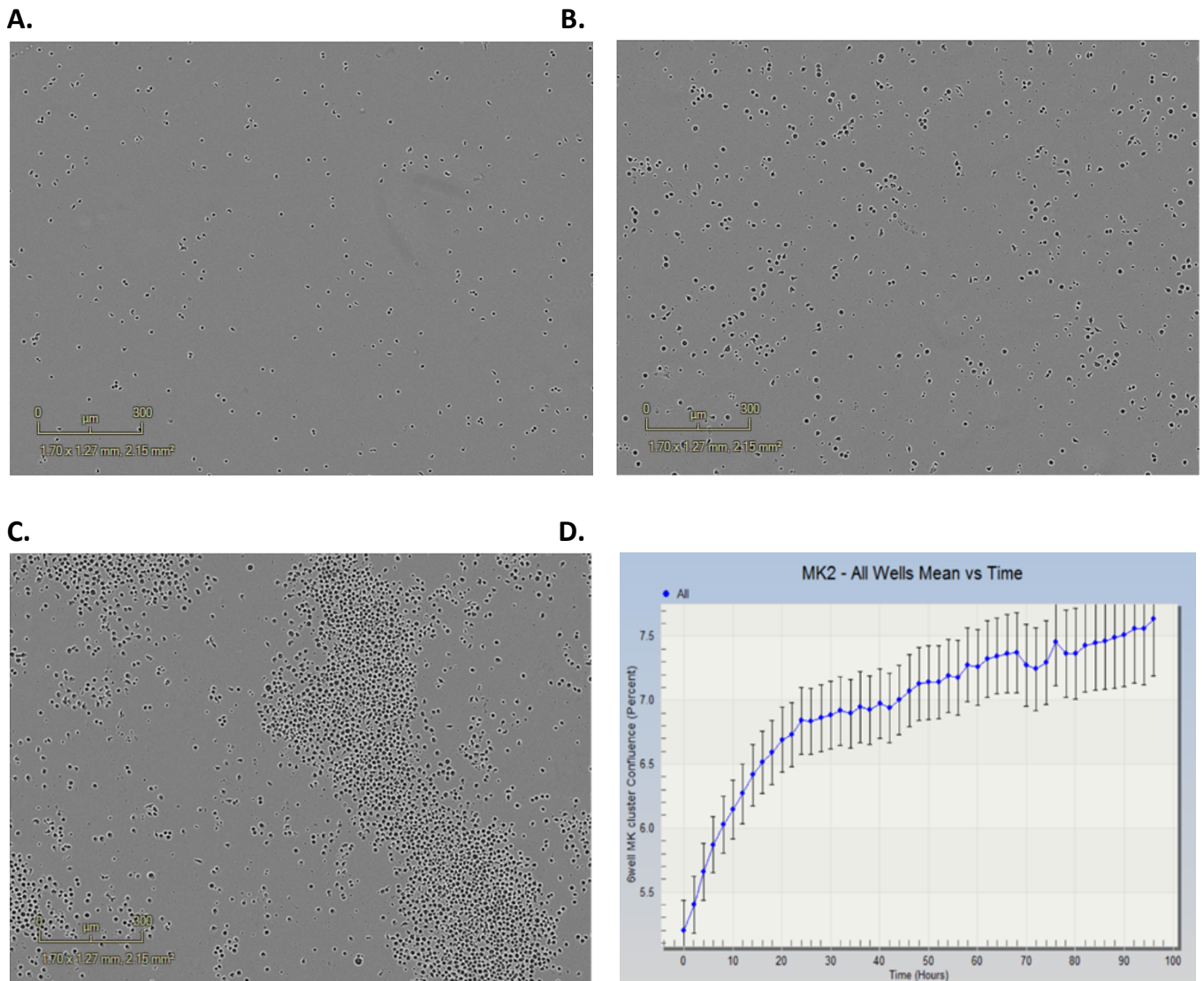


**Figure 13-1. Tracking the development of MK using the real-time imaging system (Incucyte).**

Images showing MK development from CD34<sup>+</sup> HSC at different times points at (A) day 0 (D0), (B) D3 and (C) D6. (D) The graph shows the increase in cellular confluence, the area of the plate covered by cells, over time (n=6). Images were captured at 5x magnification and the 300μm - scale bar for measurements.

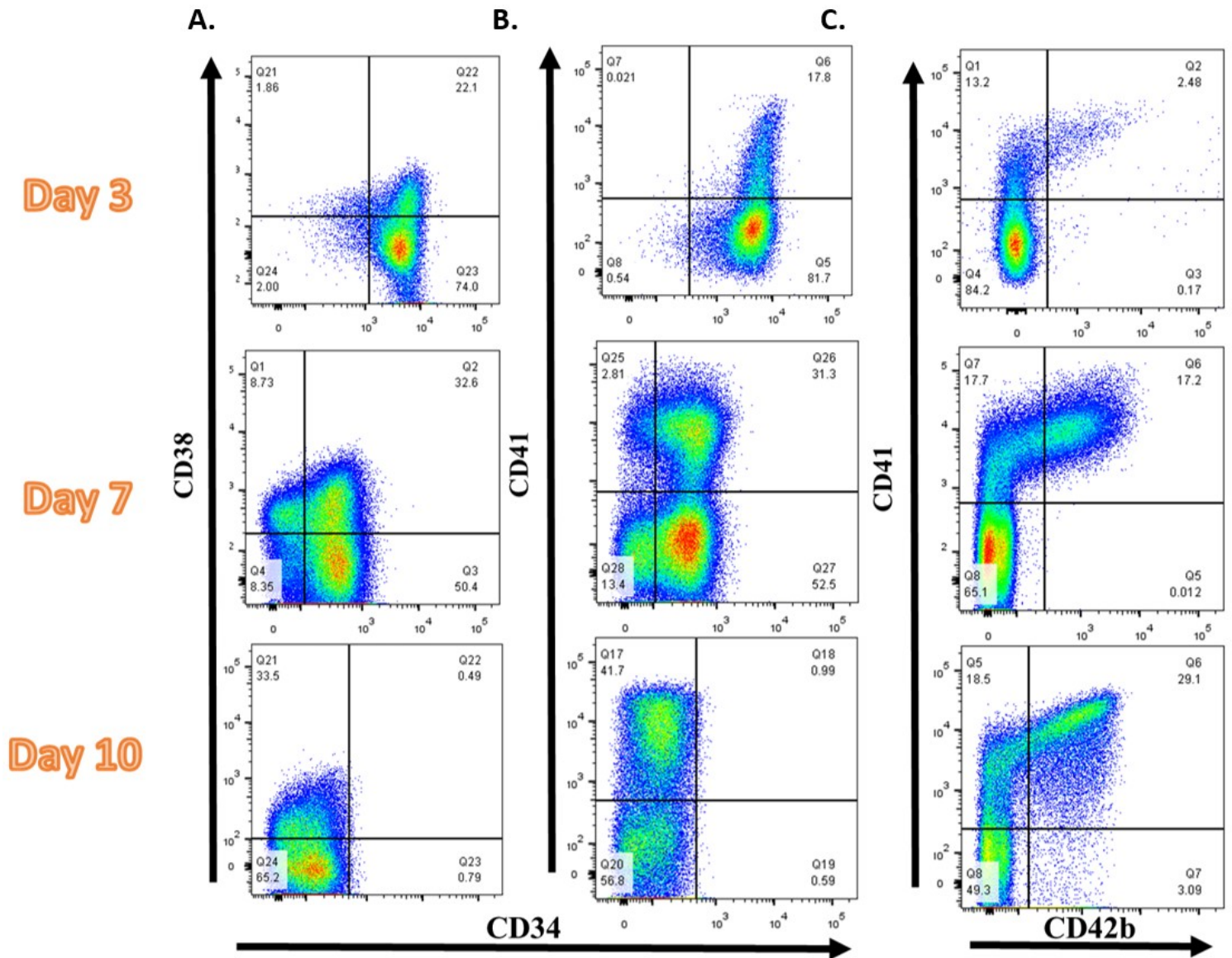


**Figure 13-2. Tracking the development and maturation of MK using flow cytometry.**

Dot plots demonstrating the developing and maturation of MK over time. After gating on the appropriate forward scatter, side scatters and excluding dead cells (A) demonstrates the surface expression of CD34 with CD38 at Day 3, 7 and 10. With development, (B) there was an increase in the expression of CD41 and a reduction in CD34 expression. (C) The dual expression of CD41 and CD42b, representing mature MK, increased through development reaching its highest at D10.

### 13.2.2. MHC-I and MHC-II surface expression on developing MK.

I next examined the surface expression of MHC-I; characterised using anti human HLA-A/B/C and MHC-II; characterised using anti human HLA-DR, on developing MK to determine how they might interact with T cells.

The surface expression of MHC-I remained highly positive throughout developmental stages of MK (Figure 13-3A).

On the other hand, the surface expression of MHC-II on developing MK was at its highest in the early stages of maturation at D3 (Figure 13-3B). As MK continued to mature, there was a reduction in the expression of MHC-II to its lowest levels at D10 (Figure 13-3C). Taken together, mature MKs could be phenotyped as  $CD34^+CD38^{lo}MHC-I^+MHC-II^{lo}CD41^+CD42b^+$ .

Although expression of MHC-II reduces over time, during the intermediate phases, there are dual positive cells which express both CD41 and MHC-II, similar to mice, suggesting that MKs could interact with CD4 cells through this period.

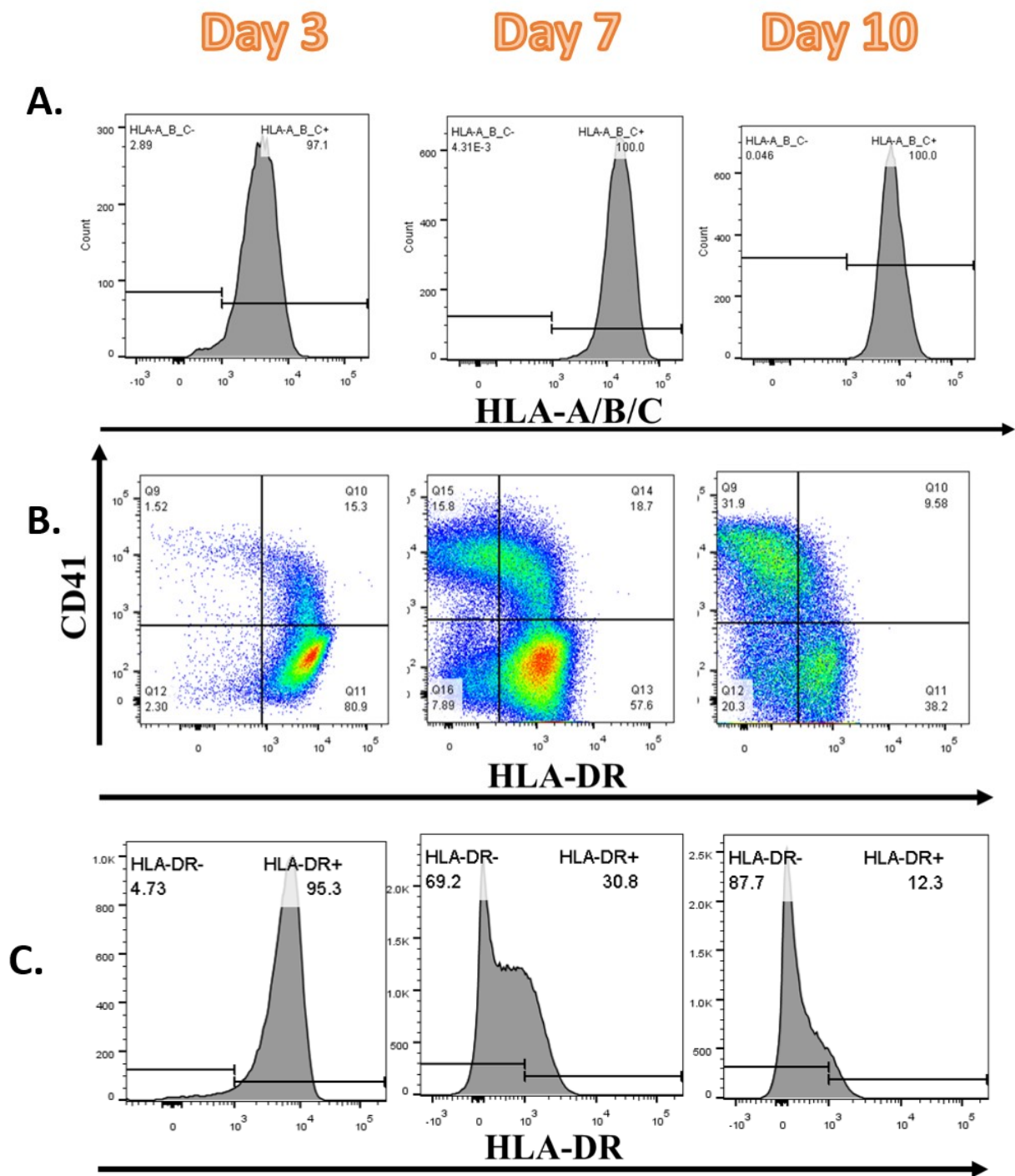


**Figure 13-3. HLA-A/B/C and HLA-DR surface expression on developing MK.**

(A) Histograms showing consistently high surface expression of HLA-A/B/C (MHC-I) at different MK developmental time points at D3, D7 and D10. The surface expression of HLA-DR on developing MK was decreasing over time. This is demonstrated as (B) a shift towards the left when plotted against the expression of CD41 or as (C) histograms demonstrating the expression of HLA-DR on developing MK.

### 13.2.3. PD-L1 and PD-L2 expression in developing MK.

I next determined the surface expression of the immunomodulatory receptors; PD-L1 and PD-L2, that could potentially govern the MK-T cell interaction.

The surface expression of PD-L1 on MK was tracked over time at D3, D7 and D10. PD-L1 expression increased throughout MK maturation reaching its highest at D10 (Figure 13-4A). PD-L1 surface expression on mature MK was confirmed using confocal microscopy demonstrating a differential expression from CD41 and CD42b (Figure 13-4B). To confirm the developmental nature of PD-L1 on MK, median fluorescent intensity (MFI) was compared between the different developmental stages of MK. PD-L1 MFI was significantly higher in mature (CD41<sup>+</sup>CD42b<sup>+</sup>) MK compared to immature (CD41<sup>+</sup>CD42b<sup>-</sup>) MK and early MK progenitor (CD41<sup>-</sup>CD42b<sup>-</sup>) [259.20 vs. 43.32 vs. 5.83; P value < 0.0001], respectively (Figure 13-5A).

Data provided by our collaborator Dr Beth Psaila (Oxford) on PD-L1 expression, quantified as transcripts per kilobase million (TPM), on developing MK using single-cell RNA sequencing confirm a significant increase in PD-L1 expression from immature MK to mature MK [4.3 TPM vs 10 TPM; P value < 0.001] (Figure 13-5B).

Similarly, PD-L2 expression increased throughout MK development. PD-L2 MFI was significantly higher on mature MK when compared to immature and early MK progenitors [674 vs. 429 vs. 248; P value < 0.0001], respectively (Figure 13-5C).

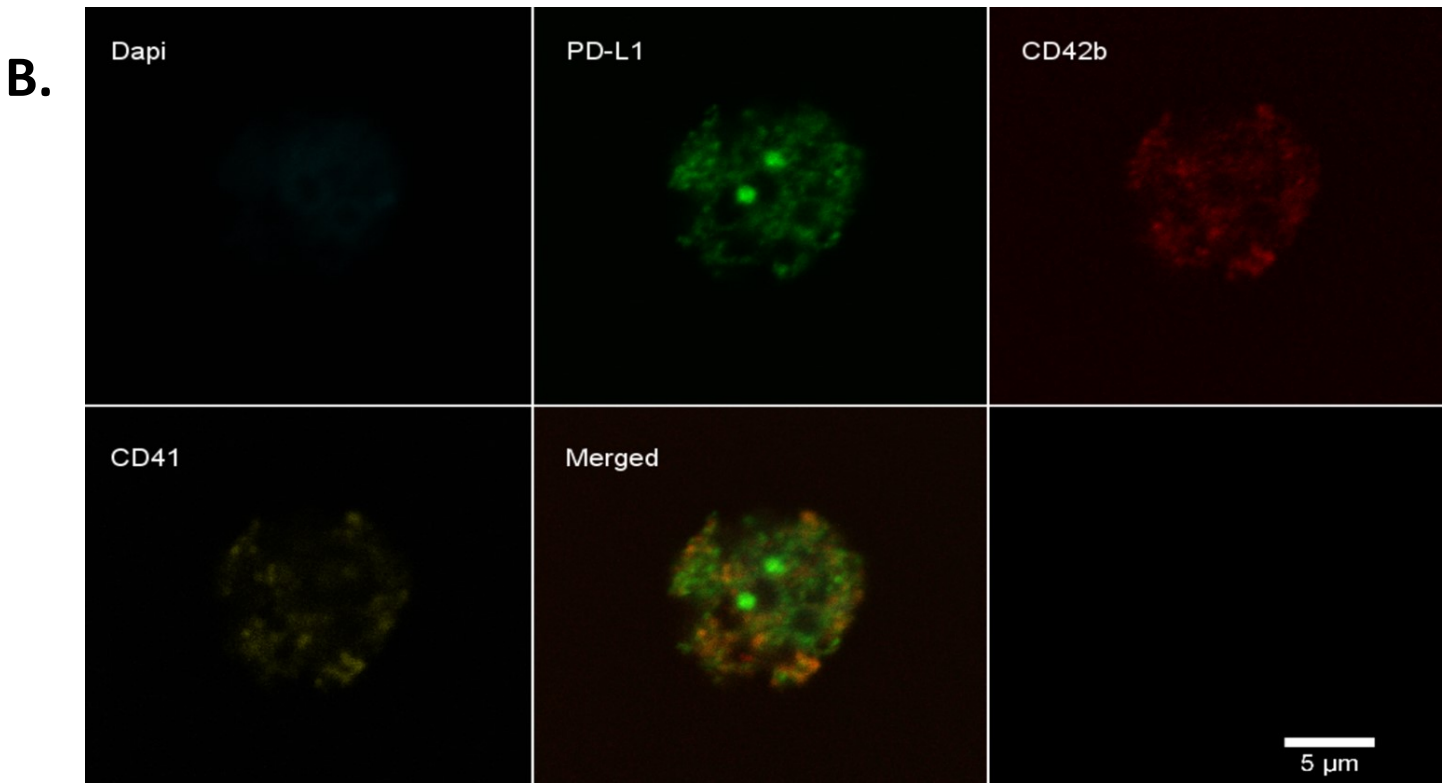
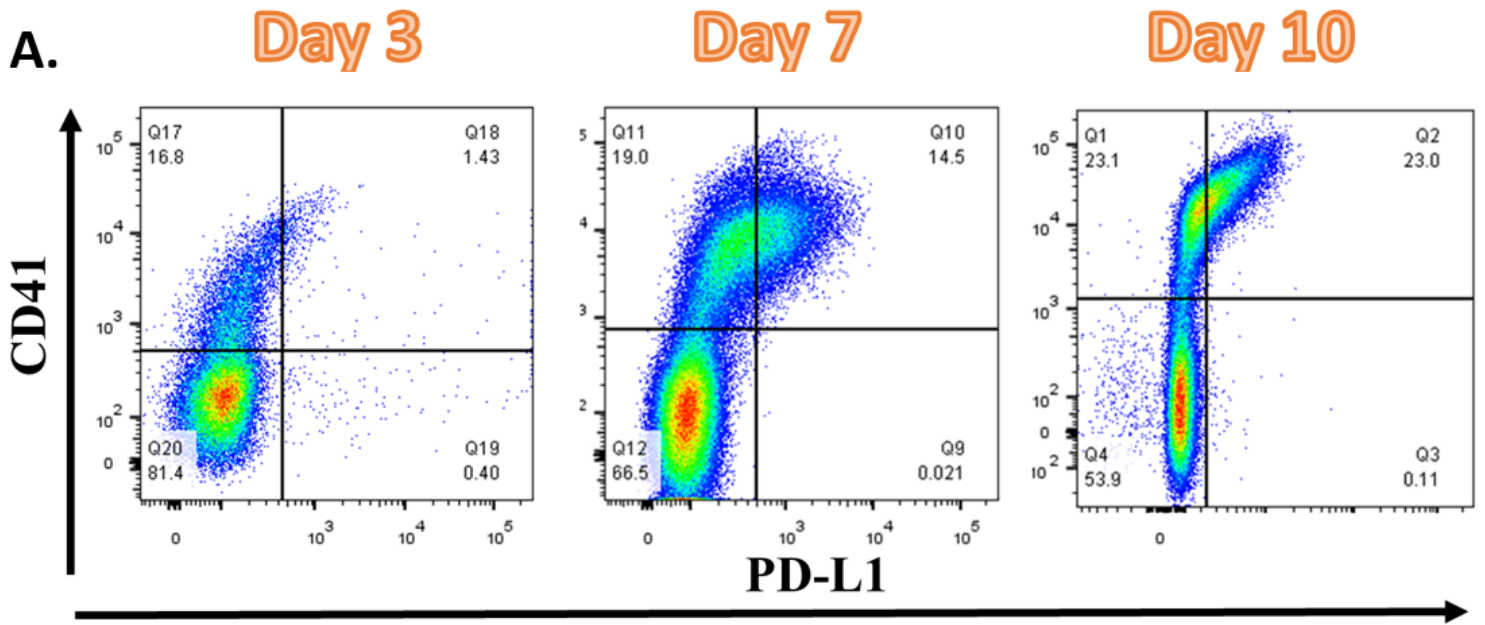
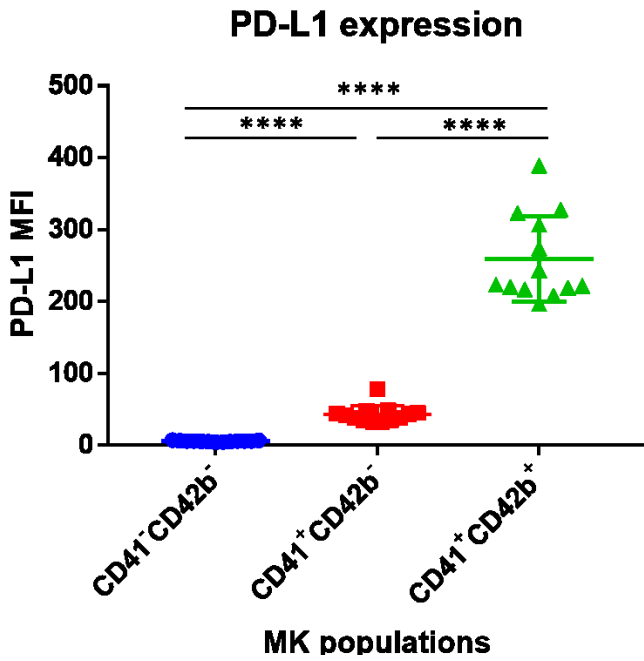


**Figure 13-4. Surface expression of PD-L1 on developing MK.**

(A) Dot plots representing developing MK at different developmental stages; D3, D7 and D10. The dot plots demonstrate the increase in PD-L1 expression on CD41<sup>+</sup> cells. (B) Confocal microscopy of a mature MK showing the differential expression DAPI (Light Blue), PD-L1 (Green), CD42b (Red) and CD41 (Yellow). The image was captured at 20X magnification and a scale bar of 5 $\mu$ m is provided.

A.



B.

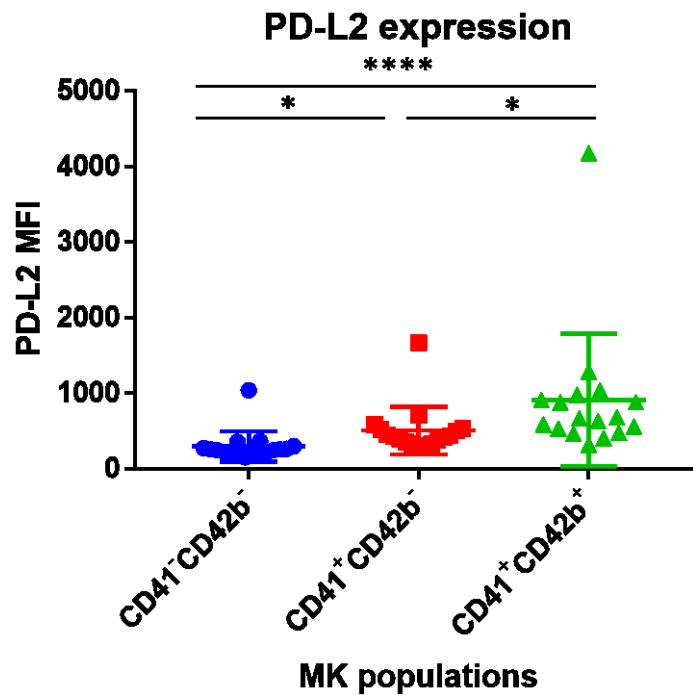
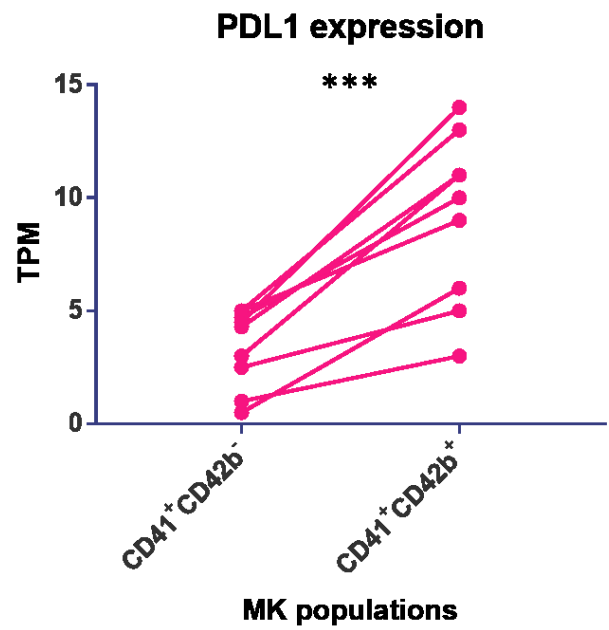


Figure 13-5. PD-L1 and PD-L2 expression on developing MK.

(A) The graph demonstrates the difference of PD-L1 surface expression between early MK progenitor (Blue), Immature (Red) and mature MK (Green). (B) Single-cell RNA sequencing showing the significant difference of PD-L1 expression between immature and mature MK.

(C) PD-L2 surface expression in early MK progenitor, Immature and mature MK.

#### **13.2.4. ITP plasma reduces PD-L1 expression on MK and increases MK death.**

To assess the impact of ITP on mature MK and the expression of PD-L1, mature MK (taken at D7) were cultured overnight with plasma from 5 different patients with ITP. The coculture of MK with plasma from HC or medium served as experimental controls.

Plasma from patients with ITP had the biggest impact on PD-L1 expression on developing MK (Figure 13-6A). PD-L1 MFI was significantly lower when cocultured with plasma from patients (Figure 13-6B) compared to HC plasma [170 vs 364; P value < 0.05] (Figure 13-6C). However, no significant difference observed in PD-L1 expression between MK cultured with medium only and HC plasma [P value > 0.05].

Using L/D discrimination marker, the percentage of dead cells caused by culturing MK with plasma was measured (Figure 13-6D). Culturing MKs in plasma from patients with ITP led to a significant increase in MK cell death compared to HC plasma [9.93% vs 6.79%; P value < 0.05] (Figure 13-6E). There were no significant differences in MK cell death between MK cultured with HC plasma and medium only [P value > 0.05].

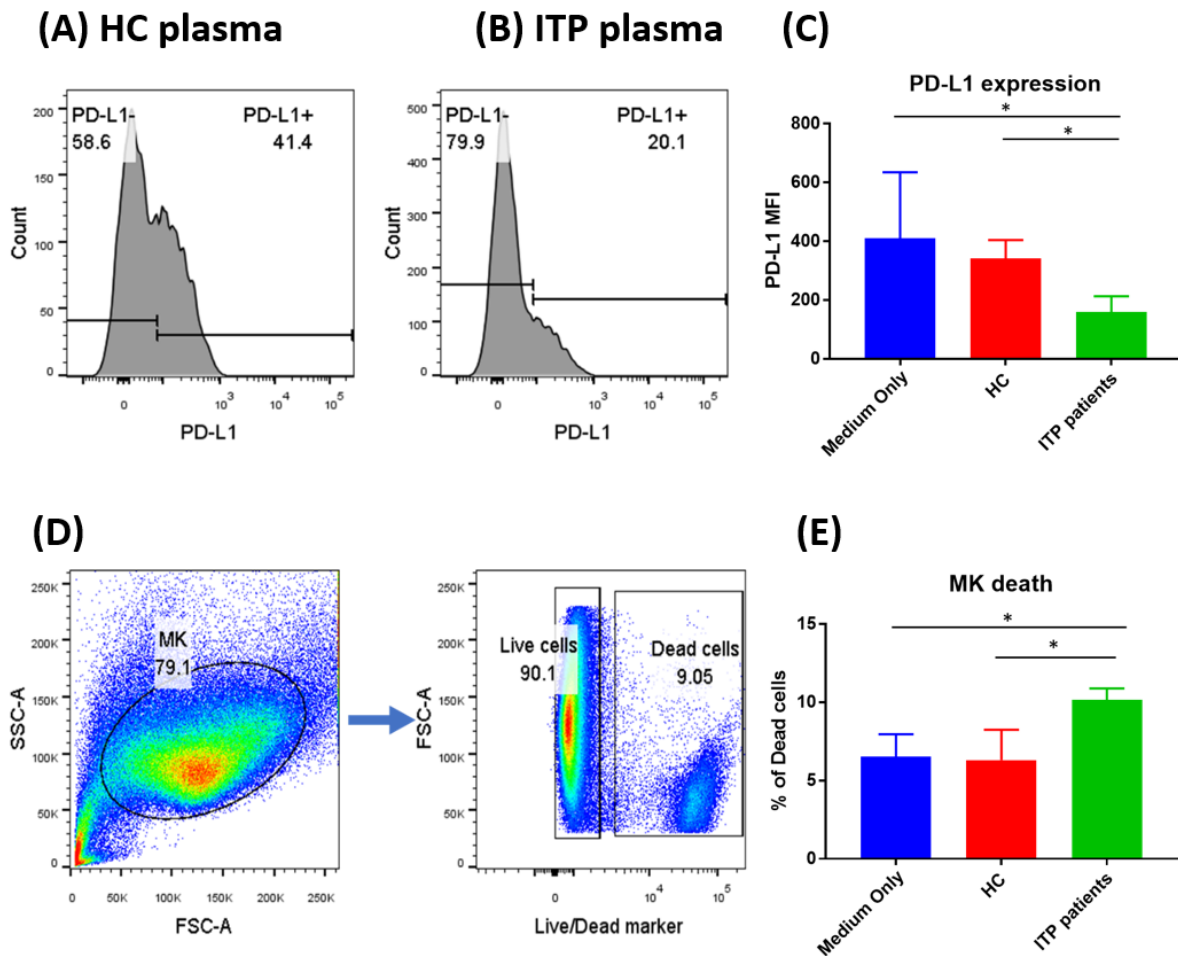


**Figure 13-6. The impact of plasma from patients with ITP on developing MK.**

Histograms demonstrating the expression of PD-L1 on MK cultured with (A) HC plasma and (B) plasma from patients with ITP. (C) The bar chart demonstrates PD-L1 MFI on MK when cultured with medium only (blue), HC plasma (red) and plasma from patients with ITP (green). (D) Dot plots showing the gating strategy to evaluate MK cell death starting from gating on the forward and side scatter followed by the Live/Dead marker staining (B) The bar chart demonstrates the impact of plasma from patients with ITP (green) on MK death compared to plasma from HC (red) and medium only control. Plasma from patients with ITP resulted in the least PD-L1 expression and highest cell death in developing MK.

### **13.2.5. Blocking PD-L1 and PD-L2 on MK promotes the development of the polyfunctional CD8<sup>+</sup> T cells, when cultured with PBMC.**

To underline the mechanism involved in the MK-T cell interactions, blocking antibodies were used to block the different receptors on mature MK before culturing them with PBMC from patients with ITP. These receptors on MK included MHC-I, PD-L1 and PD-L2 (Figure 13-7A). isotype-matched to the blocking antibodies were used as controls in this experiment. This blocking has been confirmed by staining these receptors. Unblocked receptors will be positively stained, whereas blocked receptors will not be stained (Figure 13-7B). After blocking these megakaryocytic receptors, MK were cultured with PBMC from patients with ITP. The outcome of this interaction by determining percentage of polyfunctional CD8<sup>+</sup>IFN $\gamma$ <sup>+</sup>TNF $\alpha$ <sup>+</sup> T cells as described previously (Chapter 11).

Blocking PD-L1 on MK significantly increased the polyfunctional CD8<sup>+</sup> T cells compared to an isotype antibody control or MK cultured in medium only [37.15 %, 19.5% and 18.4%; P value < 0.001] respectively (Figure 13-8). This stimulation of CD8<sup>+</sup> T cells was mainly mediated through MHC-I molecule as blocking MHC-I molecule on MK led to significant reduction of polyfunctional CD8<sup>+</sup> T cells when compared to blocking PD-L1 [13.35% vs. 37.15%; P value < 0.05].

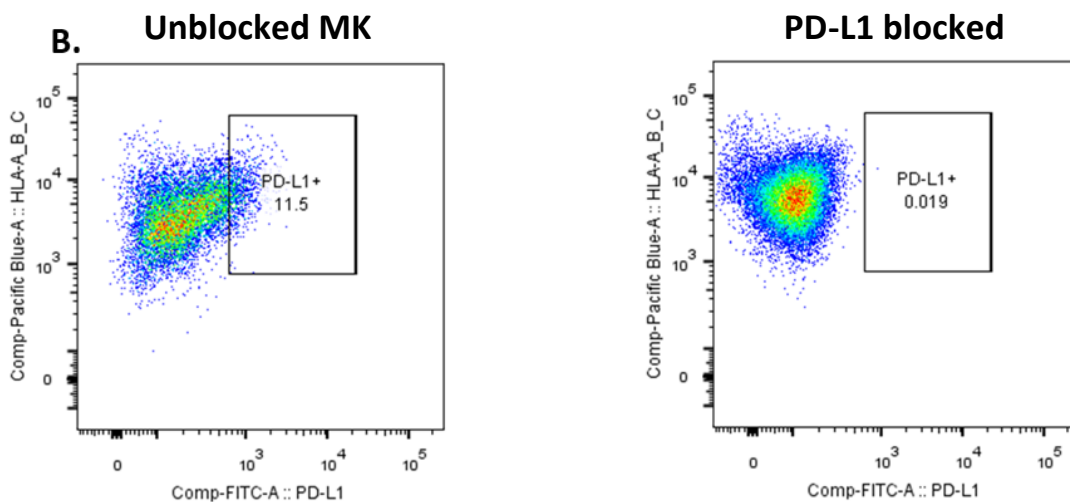
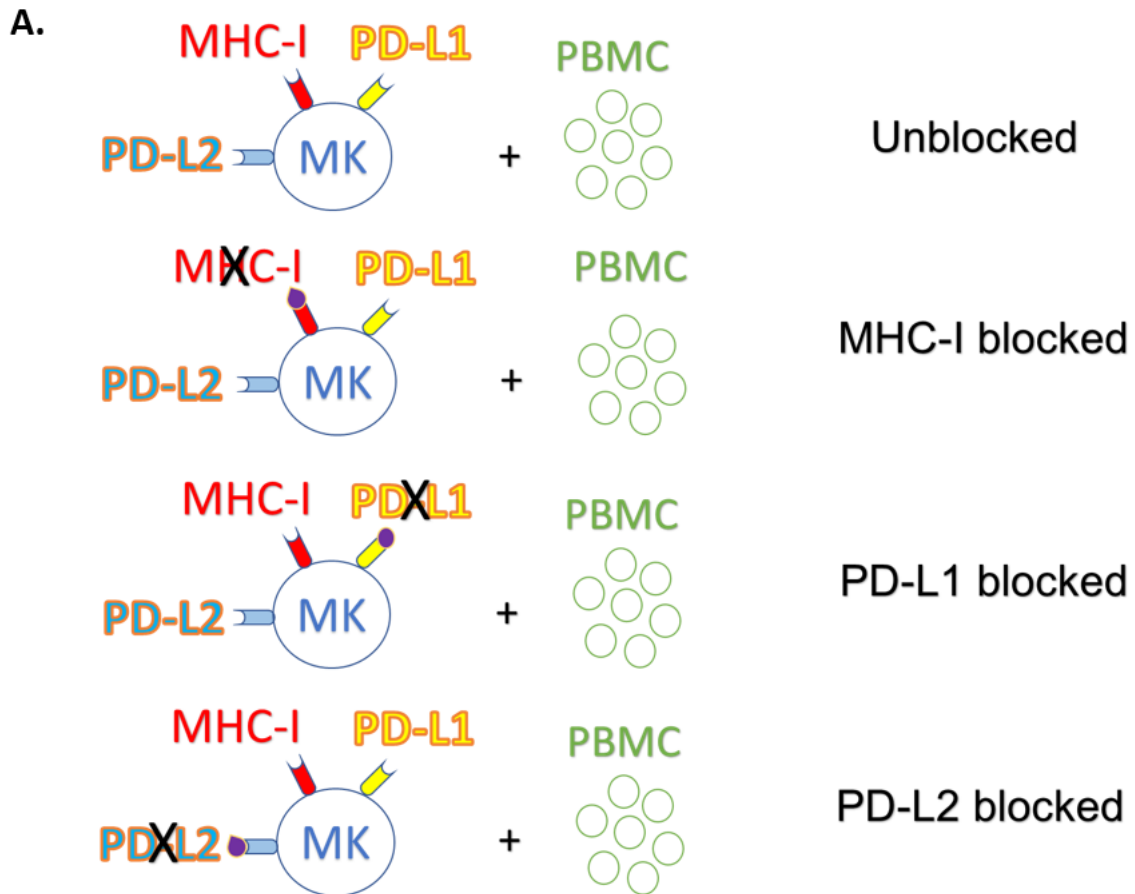


**Figure 13-7. Interrogating MK - T interaction governed by Immune-related molecules.**

(A) Schematic representation of the blocked pathways using blocking antibodies against HLA-A/B/C, PD-L1 and PD-L2 which govern MK-T cell interaction. Drawings demonstrate the blocked surface receptors on MK prior to their culture with PBMC. (B) Dot plots demonstrate an example of confirming the blocking of PD-L1 on MK demonstrated by lack of staining in PD-L1 blocked MKs (right), compared to the positive staining in unblocked MKs (left).

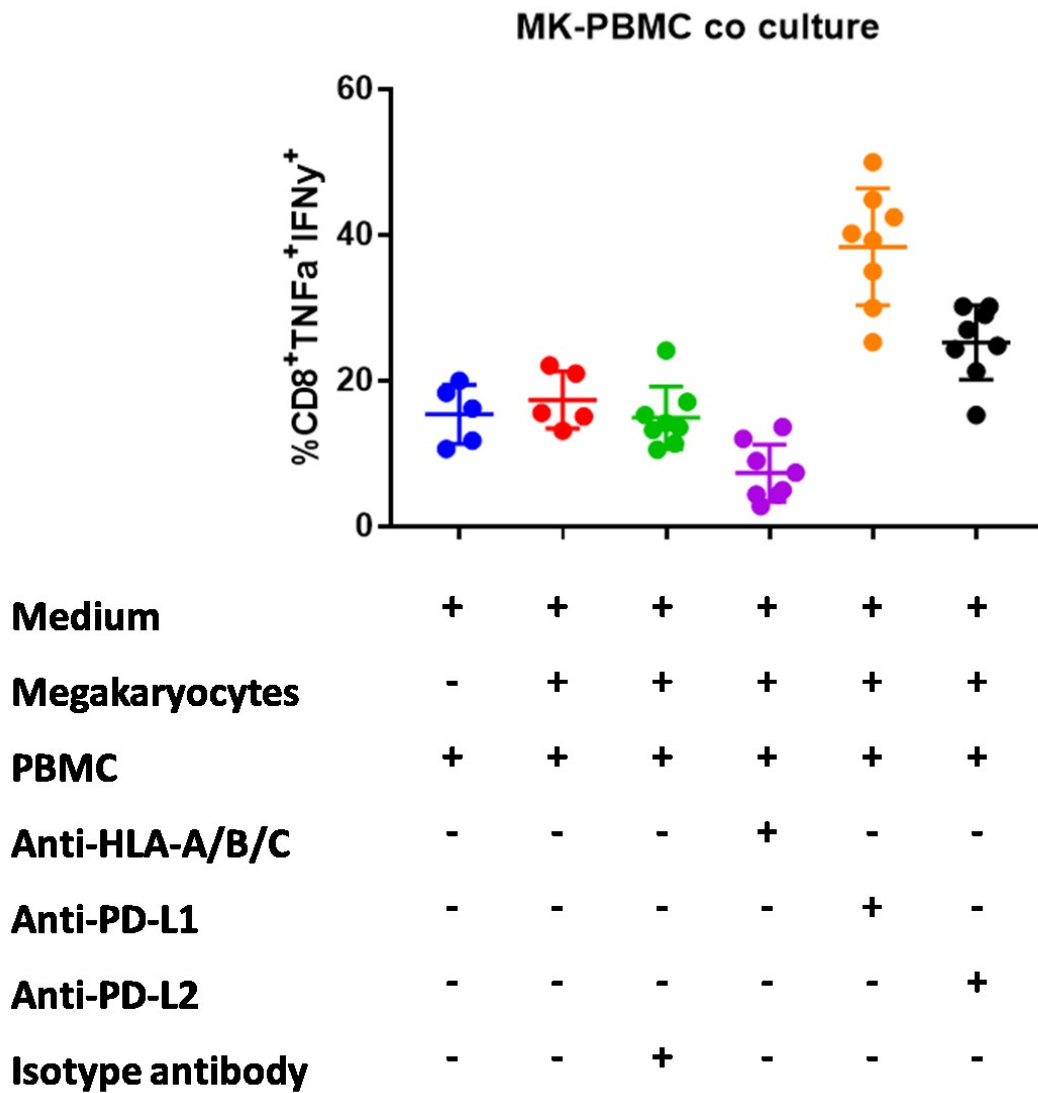


**Figure 13-8. Examination of the molecules governing the MK-T cell interaction.**  
 All experiments were performed in a supplemented media where PBMCs were co-cultured with MK. Different MK surface markers were blocked using blocking antibody prior to their co-culture with PBMCs. Baseline activation of CD8<sup>+</sup> T cells was observed when PBMCs are cultured alone (blue), with MK (red) or isotype control antibody (green). This activation was downregulated by blocking HLA/A/B/C (MHC-I; purple). Blocking PD-L1 on MK led to the highest levels of polyfunctional CD8<sup>+</sup> T cells (orange), and less so with PD-L2 (black) compared to other conditions. + indicates the presence of a blocking antibody.

### 13.3. Discussion.

The pathophysiology of ITP has mostly been considered to be due to platelet destruction in the spleen (130). However, an increasing number of studies have shed light on the platelet-progenitors, MK, and their contribution to the ITP pathophysiology. These studies suggest that megakaryopoiesis and platelet production are impaired in ITP, under the influence of autoantibodies targeting the MK (189–191). The focus of these studies has been centred on MK-related parameters such as survival, apoptosis, ploidy and maturation. However, these are small studies and they lack investigation into the regulatory factors governing possible interaction between MK and immune cells.

To recapitulate the bone marrow pathology in ITP, I developed an *in vitro* megakaryocytic assay to interrogate several aspects of MK development and maturation in ITP. CD34<sup>+</sup> HSC mobilised from peripheral blood of a healthy donor were used to generate MKs. Developing MK can be tracked using established surface markers including loss of the HSC marker CD34, gradual appearance of the early MK progenitor marker CD41 (GP IIb) and mature megakaryocytic marker CD42b (GP Ib) (46,192). These markers followed the reported pattern of MK development of decreasing CD34 and MK maturation of being CD41<sup>+</sup> and CD42b<sup>+</sup> (188,193).

Following on from the BM trephine results described in chapter 12, one of the aims of this study was to interrogate the MK-T cell interaction. In order for MK cells to interact with T cells, they must express specific receptors, MHC class I and II. MHC class I is expressed on all nucleated cells (2), which further confirms our finding of the persistent positive expression of MHC-I at the different developmental stages. The expression of MHC class II has not been fully determined in mature MK in humans. Previous studies have suggested that class II expression is only seen in early MK progenitors (60).

In this study, consistent with existing literature, MHC-II expression began high in stem cells and decreased as MK continued to develop. It was however still expressed at later stages of MK maturation than has previously been described, allowing for potential interactions with T cells even as CD41 begins to be expressed. Although this has not been addressed in this *in vitro* assay, these MHC-II molecules are functional receptors through which MK prime T cells and drive their  $T_{h1}/T_{h17}$  differentiation in disease (59,60).

Currently, only a few studies have addressed the contribution of immune checkpoint molecules PD-1 and PD-L1 to ITP pathophysiology (102–104). These studies have focused on the expression of these molecules in serum and immune cells such as PBMC and DCs showing conflicting results of dysregulated PD-L1 in peripheral blood, potentially due to fluctuations in disease activity. PD-L1 and PD-L2 have clear importance in the pathophysiology of autoimmune conditions. Given the potential for T cell interactions with MKs, this study further addressed the expression pattern of PD-L1 and PD-L2 on MK (something that has not been previously reported) (32,36).

In this *in vitro* megakaryocytic assay, the expression of PD-L1 was tracked from the early MK progenitor stages ( $CD41^-CD42b^-$ ) up to mature MK ( $CD41^+CD42b^+$ ). PD-L1 expression started to appear on immature ( $CD41^+CD42b^-$ ) MK, reaching its highest expression on mature MK ( $CD41^+CD42b^+$ ) suggesting that its high expression could be used as a marker of mature MK. The unpublished work of our collaborator Dr Bethan Psaila at the University of Oxford has confirmed this finding. The single-cell RNA sequencing has demonstrated a significant increase in PD-L1 expression from immature MK to mature MK. The use of confocal microscopy has also confirmed the expression of PD-L1 on mature MK. Mature MK demonstrated differential PD-L1 expression that was not overlapping with to CD41 and CD42b expression. The absence of PD-L1 on HSC has previously been reported and has served as the basis for the patented bioengineered modified HSC that expresses PD-L1 aimed to be used in

transplant of autoimmune disorders such as type I diabetes (194). Similarly, PD-L2 expression was at its highest on mature MK compared to MK progenitor and immature MK.

The capacity of MK to express immunomodulatory molecules such as PD-L1 and PD-L2 has not been reported before. This dual expression of PD-L1 and PD-L2 has only been attributed to professional antigen-presenting cells such as dendritic cells (195). These findings suggest that MK could serve as an immunomodulator of activated immune cells as well as a professional antigen-presenting cell through their MHC-I and MHC-II expression.

In order to examine the influence of ITP on MK and the expression of PD-L1, developing MK were cultured with plasma from patients with ITP or HC. Plasma from patients caused the highest cell death in MK confirming the previous findings of Houwerzijl and colleagues that culturing healthy MK with plasma from ITP patients caused increased cell death (79).

In addition to increasing MK death, plasma from patients significantly reduced the expression of PD-L1 on MK when compared to HC plasma.

The findings described here that plasma from patient with ITP downregulate PD-L1 on MKs lead us to hypothesise that this may be the cause of the increase in polyfunctional CD8<sup>+</sup> T cells observed in patients.

To examine the interactive nature between MK and CD8<sup>+</sup> T cells and how it is regulated, mature MK were culture at D7 with PBMC from patients with ITP. The outcome of this interaction was determined by quantifying the frequency of polyfunctional CD8<sup>+</sup> T cells. To interrogate the mechanism of MK-T cell interactions and determine whether these molecules are functional and contributing to such interactions, blocking antibodies were used to block key receptors including MHC-I, PD-L1 and PD-L2. Culturing MK derived from HC HSC with patients' PBMC led to a baseline CD8<sup>+</sup> T cell activation that was significantly reduced upon blocking MHC-I. This activation could be attributed to the MHC-I mismatch, which has been

reported to be a key player in BM transplant failure (196). Blocking PD-L1 on MK led to the highest percentages of polyfunctional CD8<sup>+</sup> T cells, which was significantly higher than blocking PD-L2, or MK blocking with isotype-control antibodies. These findings suggest that MK directly interacts with CD8<sup>+</sup> T cells leading to its activation and promoting the production of the polyfunctional CD8<sup>+</sup> T cells. This interaction is mediated via MHC-I, modulated mainly by PD-L1, and PD-L2 also contributes to such immunoregulation.

The use of plasma from patients with ITP to mimic the *in vivo* condition evaluating its impact on cells i.e. impact on the PD-L1 expression on MK in this study, has been used previously (79,191,197). However, further work is needed to specify which element of the plasma is responsible for the demonstrated effect to take this work further. This is to determine whether a cytokine or an antibody mediated such effect.

In this study, PD-L1 expression was described on MK developed from CD34<sup>+</sup> from HC. It would be interesting to examine PD-L1 expression on MK derived from patients HSC and also from MK taken directly from bone marrow aspirates.

Here, the polyfunctionality of CD8<sup>+</sup> was used as an indication of an active interaction between MK and CD8<sup>+</sup> T cells. This approach is more indicative than the surface activation marker CD69 used by Zufferey and colleagues to demonstrate the murine MK capacity to present antigens to CD8<sup>+</sup> T cells (61). MK were cultured directly with PBMC from patients with ITP, with the assumption of the presence of autoreactive CD8<sup>+</sup> T cells in patients PBMC would react directly to the normal peptide presented on the MK MHC-I molecule. However, it would be necessary to repeat such experiment with MK and PBMC from the same person to see whether there would be a similar CD8<sup>+</sup> T cell activation. Future work should also determine whether the effector T cells are able to directly kill MKs.

## 14. Discussion

Consistent with early work from Olsson *et al* (94), this work further confirms the involvement of CD8<sup>+</sup> T cell in the pathophysiology of ITP. In peripheral blood, there was an expansion in the CD8<sup>+</sup> T cell compartment leading to a significant reduction in CD4/CD8 T cell ratio, as previously reported (144–146). This expansion was mostly evident in the significantly increased antigen-experienced terminally-differentiated effector CD8<sup>+</sup> T cells in patients with ITP. The increased effector CD8<sup>+</sup> T cells has been described as a key feature of other autoimmune conditions such as AA (160) and myelodysplasia (150). Furthermore, this effector population was a result of a dynamic interaction rather than a bystander effect as it was shown to be significantly higher in patients with low platelet count which could serve as an indication of disease activity/severity. As there was no corresponding increase in regulatory T cells in these patients, the resulting immune imbalance in the form of reduced Treg/effector CD8<sup>+</sup> T cell ratio could serve as a better indication of disease activity than the debatable Treg frequency or functionality in ITP (87,98,99,101,172).

This is the first study to address CD8<sup>+</sup> T cell polyfunctionality in ITP and demonstrates an active role of CD8<sup>+</sup> T cells in contributing to the previously reported proinflammatory milieu of ITP (86,155,156). The increase in these cytokines is in line with previously reported increased gene expression of IL-2, IFN $\gamma$  and GnB-related genes in CD3<sup>+</sup> T cells in patients with ITP (94,159) It further confirms that these effector CD8<sup>+</sup> T cells are not exhausted, as exhausted cells would express lower intracellular IFN $\gamma$  and IL-2 (136).

The reactivity of these cells, shown in the IFN $\gamma$  ELISpot assay, suggests this activity is driven by platelets. This approach to assess function is safer and more reproducible than the radiological method used by Olsson *et al.* (94)

The upregulated effector CD8<sup>+</sup> T cells displayed downregulated exhaustion markers PD-1 and Tim-3 (151,152). This downregulation prevents the immune system from eliminating these activated cells, which confirms previous reports of low PD-1 and Tim-3 in patients with ITP. This further confirms the immune-dysregulatory nature of the effector CD8<sup>+</sup> T cells and could be attributed to the low gene expression of the anti-apoptotic BCL2 in patients with ITP (91,153,154).

The novel immunomodulatory impact of Elt on CD8<sup>+</sup> T cells described here is of particular interest in autoimmune diseases of the bone marrow. Elt is a mainstay of treatment in both ITP and AA, and in both diseases long term remissions are being described (133,198). In this study, Elt-treated patients had significantly lower effector CD8<sup>+</sup> T cells compared to Romi-treated subjects. Furthermore, Elt significantly reduced CD8<sup>+</sup> T cell functionality *in vitro*, in a dose-dependent manner which was not seen with supratherapeutic dose of Romi. These findings highlight a possible additional therapeutic benefit of Elt, besides correcting the platelet count, in ITP and refractory AA (168–170).

Our group has previously reported the iron chelating effect of eltrombopag on myocyte and liver cell lines (125). Iron is required by all cells for the essential DNA synthesis, however, rapidly proliferating cells i.e. neoplastic cells uptake iron at much higher rate compared to normal (199) . Consistent with this, iron chelators have previously been shown to reduce proliferation of T cells and inhibit their activation (200,201). This mechanism of immune modulation – reduction in highly proliferative cells and impairing their activation through iron chelation - would be consistent with the impact of high doses of Elt on the metabolically active CD8<sup>+</sup> cells described here *ex vivo*. This needs further functional confirmation.

To address whether these CD8<sup>+</sup> T cells are also active in the bone marrow *in vivo*, IHF staining has been used on bone marrows from patients with active disease, a technique widely used to

determine cellular interaction in organs such as brain and lungs (202,203). This is the first study to describe the increased MK-T cell interaction and clustering described here in patients with ITP compared to controls. These novel findings demonstrate an active role of T cells in the BM pathology in ITP, which appears to occur in addition to the reported *in vivo* involvement of autoantibodies (178,204). This further demonstrates the complexity of ITP pathophysiology that it is not only taking place in peripheral blood, but also in the BM.

Given the unexpected interactions with both CD4 and CD8 cells we further characterised whether MKs have the ability to interact with T cells at all stages of maturation. Consistent with expected biology, MHC-I was expressed on all stages of MK maturation, confirming that it is expressed on all nucleated cells (2). MHC-II expression began high in HSC and decreased as MK continued to develop, similar to what has been described previously in mouse MK development. Unexpectedly however, MHC class II remained present on some mature CD41<sup>+</sup>CD42b<sup>+</sup> MK. This helps to explain the CD4 cell interactions described in the trephine biopsies (59).

To further determine the interactions of MK cells with T cells, and given the importance of PD-L1 and PD-L2 contribution in autoimmune disorders such as SLE and graft-versus-host disease (GVHD) (32,36), we assessed the expression of these checkpoint inhibitors on MKs which is something that has not been previously reported. While PD-L1 was not expressed on HSCs, it increased throughout MK development reaching its highest on mature MK. Single-cell RNA sequencing confirmed this increase in PD-L1 expression from immature MK to mature MK. Similarly, PD-L2 expression was at its highest on mature MK compared to their progenitors.

The expression of MHC-I, MHC-II, PD-L1 and PD-L2 have only been attributed to professional antigen-presenting cells such as dendritic cells (195). These findings suggest a

novel role for human MK serving as a professional antigen-presenting cell, presenting peptides via their MHC-I and MHC-II, as well as controlling T cell activation through PD-L1 and PD-L2 receptors. The ability of MKs to change their nature and surface expression also shows it to be a plastic system which could be changed with infection or inflammation.

I therefore explored the MK development *in vivo* in two manipulatable systems. First, I explored the impact of plasma from patients with ITP on MK development. In addition to the previously reported increased MK death (79), patients plasma significantly reduced the expression of PD-L1 on maturing MK. Second, I explored the impact of MKs on T cells. Upon culturing MK with PBMC from patients, blocking MHC-I led a significant reduction of polyfunctional CD8<sup>+</sup> T cells, while blocking PD-L1 on MK resulted in an increase in polyfunctional CD8<sup>+</sup> T cells. This preliminary data suggests that human MK-CD8<sup>+</sup> T cell interaction is mediated via MHC-I, and that PD-L1 could be the main regulator of this interaction (Figure 14-1).

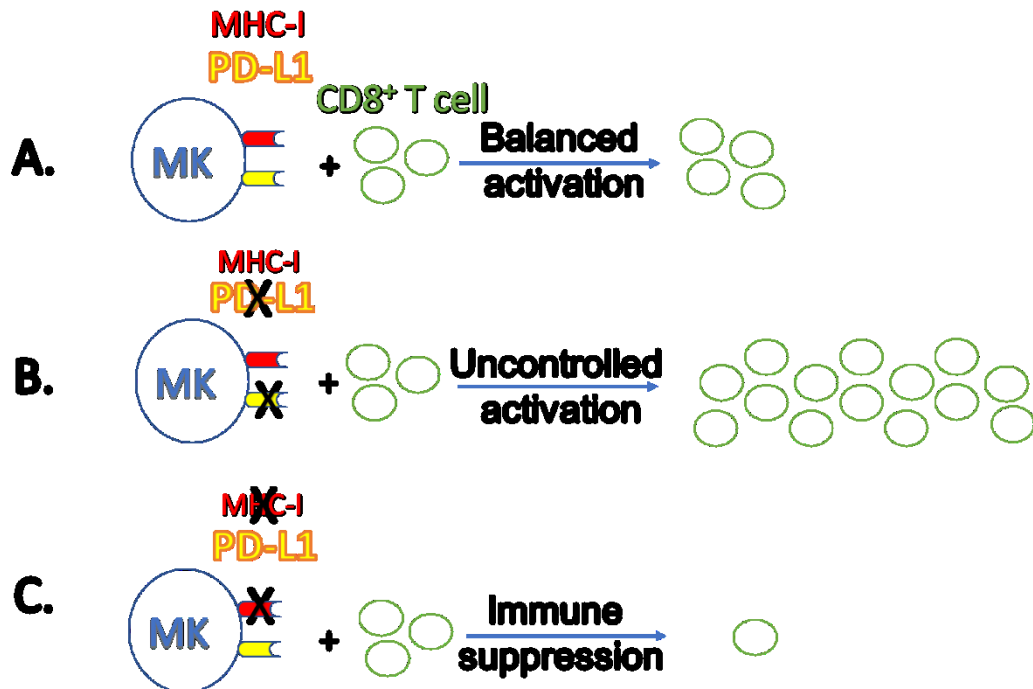


**Figure 14-1. Proposed mechanism of MK-CD8<sup>+</sup> T cell interaction.**

The figure demonstrates how MK could interact with CD8<sup>+</sup> T cell leading to balanced CD8<sup>+</sup> T cell activation due to their interaction via MHC-I and PD-L1. (B) The absence of PD-L1 leads to a continuous unbalanced CD8<sup>+</sup> T cell activation, whereas (C) the absence of MHC-I causes a suppression via the dominant expression of PD-L1.

These findings highlight two areas for further exploration. First that MKs are modulated by their culture conditions, with changes in their ability to interact with immune cells depending on their environment, and second that they have the ability to interact with and modulate the adaptive immune system. This highlights the emerging knowledge of the role of MK cells as well as platelets in host defense and immunity (54). How this system is hijacked in autoimmunity in conditions such as ITP is not yet clear, but shows the importance of better understanding this system.

### **14.1. Limitations of this study**

1. This study has provided a comprehensive analysis of the CD8<sup>+</sup> T cell compartment in the periphery of patients with ITP. In contrast (and due to time restrictions) Treg functionality was addressed only by intracellular expression of IL-2. Treg suppression assay would have been more reflective of functionality.
2. For ELISpot analysis, PBMC have been initially used. Ideally, isolated CD8<sup>+</sup> T cells should have been used to underline the CD8<sup>+</sup> T cell-specificity to platelets, as the source of IFN $\gamma$  could be from CD4<sup>+</sup> T cells or B cells. Whole platelets have been used in this proof-of-principle experiment to demonstrate the specificity of T cells. Alternatively, a platelet-derived antigen should have been used such as platelets GP IIb/IIIa presented on a multimer to elucidate CD8<sup>+</sup> T cell response.
3. A major shortcoming of the *in vivo* BM study was the use of disease-control rather than healthy controls BM. Obtaining healthy donor BM is very challenging due to the invasive nature of the procedure and the associated risks. In view of this, the controls used in this study were from subjects with other conditions in remission and without reported BM abnormalities. Ideally, the studied parameters should have been compared

between patients with ITP and HC to allow for better interpretation of the findings. However, it is most likely that the immune system in these disease controls would be more active than controls, hence differences would be further highlighted if healthy controls had been used.

4. Using plasma from patients with ITP to mimic the *in vivo* condition in an *in vitro* system has been previously used (79,191,197). However, the resulted effects could be due to multiple factors, that are yet to be determined.
5. Here, MK were cultured directly with PBMC from patients with ITP, with the assumption of the presence of autoreactive CD8<sup>+</sup> T cells in patients PBMC. However, it would be necessary to repeat such experiment with MK, derived from a patient's HSC, and CD8<sup>+</sup> T cells from the same patient to determine self-reactivity to MK.

## 14.2. Future work

The work presented here describes the presence of platelet-activated CD8<sup>+</sup> T cells in the peripheral blood as well as interactions between CD4<sup>+</sup> and CD8<sup>+</sup> T cells and MKs in the bone marrow of patients with ITP. Further work is needed to determine whether these cells are directly targeting platelets or MKs. For example, whether CD8 cells directly lyse platelets or activate their thrombotic cascade is yet to be determined. Also, the effect of CD8<sup>+</sup> T cells on MK, and whether they could directly kill MK is to be determined.

With respect to treatment effects, an interesting effect of Elt has been described on activated CD8<sup>+</sup> T cells. This needs to be confirmed by analysing CD8<sup>+</sup> T cells before and after treatment with Elt and Romi. Additionally, Elt effect can also be tested *in vitro* using a cytotoxicity assay to demonstrate a potentially reduced CD8<sup>+</sup>-mediated function. Also, an established cell line

system will be used to interrogate the mechanisms behind these results i.e. to assess the iron chelating effect on T cell activity (166).

The *in vivo* MK-T cell interaction could be further assessed using advanced microscopy such as electron microscopy, to assess interaction at the level of the synapses.

The *in vitro* megakaryocytic assay was used to describe PD-L1 expression on MK developed from CD34<sup>+</sup> from HC. It would be interesting to examine PD-L1 expression on MK derived from patients HSC and also from MKs isolated directly from the bone marrow aspirate of patients with ITP. Additionally, further work is needed to specify which element of the plasma is responsible for the demonstrated effect on MK. This is to determine which cytokine or antibody mediated such effect.

### **14.3. Conclusion**

ITP is an autoimmune disorder characterised by a proinflammatory milieu. This study demonstrates the involvement of CD8<sup>+</sup> T cells in the disease pathology. This involvement is characterised by a skew towards an effector phenotype defined by the high expression of intracellular IL-2, IFN $\gamma$ , TNF $\alpha$ , GrB and Perforin. These autoreactive CD8<sup>+</sup> T cells display immune dysregulation in the form of low expression of exhaustion markers; PD-1 and Tim-3, and are activated by platelets.

Elt, in addition to the thrombopoietic effect it shares with Romi, appears to have an additional immunomodulatory effect. It affects CD8<sup>+</sup> T cells by normalising T cell subsets as well as reducing their polyfunctionality in a dose-dependent manner.

T cells are also involved in the BM pathology of ITP. This involvement includes an increased MK-T cell interaction and clustering. This interaction, when recapitulated *in vitro*, was an

active interaction mediated via MHC-I. The newly described PD-L1 expression on MK may be the main regulator of MK-T cell interaction, which is downregulated in ITP.

## 15. References

1. Salgame P, Abrams J, Clayberger C, Goldstein H, Convit J, Modlin R, et al. Differing lymphokine profiles of functional subsets of human CD4 and CD8 T cell clones. *Science* (80). 1991 Oct 11;254(5029):279–82.
2. Murphy K, Weaver C. Principles of Adaptive Immunity. In: Janeway's Immunobiology. 9th ed. Garland Science; 2017. p. 11–25.
3. Alberts B, Johnson A, Lewis J. Helper T Cells and Lymphocyte Activation. In: *Molecular Biology of the Cell*. 4th Edition. New York: Garland Science; 2002.
4. Berger A. Th1 and Th2 responses: what are they? *BMJ*. 2000 Aug 12;321(7258):424–424.
5. Montoya-Ortiz G. Immunosenescence, aging, and systemic lupus erythematosus. *Autoimmune Dis*. 2013 Jan;2013:267078.
6. Li D, Cai W, Gu R, Zhang Y, Zhang H, Tang K, et al. Th17 cell plays a role in the pathogenesis of Hashimoto's thyroiditis in patients. *Clin Immunol* 2013 Dec;149(3):411–20.
7. Lee HS, Park H-W, Song W-J, Jeon EY, Bang B, Shim E, et al. TNF- $\alpha$  enhance Th2 and Th17 immune responses regulating by IL23 during sensitization in asthma model. *Cytokine*. 2016 Mar;79:23–30.
8. Zinkernagel RF, Doherty PC. Immunological surveillance against altered self components by sensitised T lymphocytes in lymphocytes choriomeningitis. *Nature*. 1974;251(5475):547–8.
9. Callan MF, Steven N, Krausa P, Wilson JD, Moss PA, Gillespie GM, et al. Large clonal expansions of CD8+ T cells in acute infectious mononucleosis. *Nat Med*. 1996;2(8):906–11.
10. Altman JD, Moss PAH, Goulder PJR, Barouch DH, McHeyzer-Williams MG, Bell JL, et al. Phenotypic Analysis of Antigen-Specific T Lymphocytes. *Science* (80). 1996 Oct 4;274(5284):94–6.
11. Kuzushima K. Tetramer-assisted identification and characterization of epitopes recognized by HLA A\*2402-restricted Epstein-Barr virus-specific CD8+ T cells. *Blood*. 2003 Feb 15;101(4):1460–8.
12. Ogg GS, Jin X, Bonhoeffer S, Dunbar PR, Nowak MA, Monard S, et al. Quantitation of HIV-1-specific cytotoxic T lymphocytes and plasma load of viral RNA. *Science* (80). 1998;279(5359):2103–6.
13. Murali-Krishna K, Altman JD, Suresh M, Sourdive DJD, Zajac AJ, Miller JD, et al. Counting antigen-specific CD8 T cells: A reevaluation of bystander activation during viral infection. *Immunity*. 1998;8(2):177–87.
14. John B, Harris TH, Tait ED, Wilson EH, Gregg B, Ng LG, et al. Dynamic imaging of CD8+ T cells and dendritic cells during infection with *Toxoplasma gondii*. *PLoS Pathog*. 2009;5(7).
15. Sunshine GH, Mitchell TJ. Antigen Presentation by Spleen Dendritic Cells. *J Invest Dermatol*. 1985 Jul;85(1):S110–4.
16. Lieberman J. The ABCs of granule-mediated cytotoxicity: New weapons in the arsenal. *Nat Rev Immunol*. 2003;3(5):361–70.

17. Bromley SK, Burack WR, Johnson KG, Somersalo K, Sims TN, Sumen C, et al. The immunological synapse. *Annu Rev Immunol*. 2001 Apr;19(1):375–96.
18. Zhang N, Bevan MJ. CD8+ T Cells: Foot Soldiers of the Immune System. *Immunity*. 2011;35(2):161–8.
19. Xing Y, Hogquist KA. T-Cell Tolerance: Central and Peripheral. *Cold Spring Harb Perspect Biol*. 2012 Jun 1;4(6):a006957–a006957.
20. Abbas AK, Benoist C, Bluestone JA, Campbell DJ, Ghosh S, Hori S, et al. Regulatory T cells: Recommendations to simplify the nomenclature. Vol. 14, *Nature Immunology*. 2013. p. 307–8.
21. Mahmud SA, Manlove LS, Farrar MA. Interleukin-2 and STAT5 in regulatory T cell development and function. *JAK-STAT*. 2013;2(1):e23154.
22. Wu Y, Borde M, Heissmeyer V, Feuerer M, Lapan AD, Stroud JC, et al. FOXP3 Controls Regulatory T Cell Function through Cooperation with NFAT. *Cell*. 2006 Jul;126(2):375–87.
23. Hossain DMS, Panda AK, Manna A, Mohanty S, Bhattacharjee P, Bhattacharyya S, et al. FoxP3 Acts as a Cotranscription Factor with STAT3 in Tumor-Induced Regulatory T Cells. *Immunity*. 2013 Dec;39(6):1057–69.
24. Komatsu N, Hori S. Full restoration of peripheral Foxp3+ regulatory T cell pool by radioresistant host cells in scurfy bone marrow chimeras. *Proc Natl Acad Sci*. 2007 May 22;104(21):8959–64.
25. Chatila TA, Blaeser F, Ho N, Lederman HM, Voulgaropoulos C, Helms C, et al. JM2, encoding a fork head–related protein, is mutated in X-linked autoimmunity–allergic dysregulation syndrome. *J Clin Invest*. 2000 Dec 15;106(12):R75–81.
26. Pellerin L, Jenks JA, Bégin P, Bacchetta R, Nadeau KC. Regulatory T cells and their roles in immune dysregulation and allergy. Vol. 58, *Immunologic Research*. 2014. p. 358–68.
27. Glocker E-O, Kotlarz D, Boztug K, Gertz EM, Schäffer AA, Noyan F, et al. Inflammatory Bowel Disease and Mutations Affecting the Interleukin-10 Receptor. *N Engl J Med*. 2009 Nov 19;361(21):2033–45.
28. Grinberg-Bleyer Y, Baeyens A, You S, Elhage R, Fourcade G, Gregoire S, et al. IL-2 reverses established type 1 diabetes in NOD mice by a local effect on pancreatic regulatory T cells. *J Exp Med*. 2010 Aug 30;207(9):1871–8.
29. Glisic-Milosavljevic S, Waukau J, Jailwala P, Jana S, Khoo H-J, Albertz H, et al. At-Risk and Recent-Onset Type 1 Diabetic Subjects Have Increased Apoptosis in the CD4+CD25+high T-Cell Fraction. *Sollid L, editor. PLoS One*. 2007 Jan 3;2(1):e146.
30. Nishimura H, Nose M, Hiai H, Minato N, Honjo T. Development of lupus-like autoimmune diseases by disruption of the PD-1 gene encoding an ITIM motif-carrying immunoreceptor. *Immunity*. 1999 Aug;11(2):141–51.
31. Liang SC, Latchman YE, Buhlmann JE, Tomczak MF, Horwitz BH, Freeman GJ, et al. Regulation of PD-1, PD-L1, and PD-L2 expression during normal and autoimmune responses. *Eur J Immunol*. 2003 Oct [cited 2014 Aug 23];33(10):2706–16.
32. Saha A, Aoyama K, Taylor PA, Koehn BH, Veenstra RG, Panoskaltsis-Mortari A, et al. Host

- programmed death ligand 1 is dominant over programmed death ligand 2 expression in regulating graft-versus-host disease lethality. *Blood*. 2013 Oct 24;122(17):3062–73.
33. Muenst S, Soysal SD, Gao F, Obermann EC, Oertli D, Gillanders WE. The presence of programmed death 1 (PD-1)-positive tumor-infiltrating lymphocytes is associated with poor prognosis in human breast cancer. *Breast Cancer Res Treat*. 2013 Jun 12;139(3):667–76.
  34. Matsuzaki J, Gnjatic S, Mhawech-Fauceglia P, Beck A, Miller A, Tsuji T, et al. Tumor-infiltrating NY-ESO-1-specific CD8 + T cells are negatively regulated by LAG-3 and PD-1 in human ovarian cancer. *Proc Natl Acad Sci*. 2010 Apr 27;107(17):7875–80.
  35. Freeman GJ, Long AJ, Iwai Y, Bourque K, Chernova T, Nishimura H, et al. Engagement of the Pd-1 Immunoinhibitory Receptor by a Novel B7 Family Member Leads to Negative Regulation of Lymphocyte Activation. *J Exp Med*. 2000 Oct 2;192(7):1027–34.
  36. Mozaffarian N, Wiedeman a. E, Stevens a. M. Active systemic lupus erythematosus is associated with failure of antigen-presenting cells to express programmed death ligand-1. *Rheumatology*. 2008 Apr 4;47(9):1335–41.
  37. Long MW, Williams N, Ebbe S. Immature megakaryocytes in the mouse: physical characteristics, cell cycle status, and in vitro responsiveness to thrombopoietic stimulatory factor. *Blood*. 1982;59(3):569–75.
  38. Gordon MY, Bearpark AD, Clarke D, Dowding CR. Haemopoietic stem cell subpopulations in mouse and man: discrimination by differential adherence and marrow repopulating ability. *Bone Marrow Transplant*. 1990;5 Suppl 1:6–8.
  39. Ichikawa M, Asai T, Saito T, Seo S, Yamazaki I, Yamagata T, et al. AML-1 is required for megakaryocytic maturation and lymphocytic differentiation, but not for maintenance of hematopoietic stem cells in adult hematopoiesis. *Nat Med*. 2004;10(3):299–304.
  40. Bartley TD, Bogenberger J, Hunt P, Li YS, Lu HS, Martin F, et al. Identification and cloning of a megakaryocyte growth and development factor that is a ligand for the cytokine receptor Mpl. *Cell*. 1994;77(7):1117–24.
  41. Choi ES, Nichol JL, Hokom MM, Hornkohl AC, Hunt P. Platelets generated in vitro from proplatelet-displaying human megakaryocytes are functional. *Blood*. 1995;85(2):402–13.
  42. Seo A, Ben-Harosh M, Sirin M, Stein J, Dgany O, Kaplelushnik J, et al. Bone marrow failure unresponsive to bone marrow transplant is caused by mutations in thrombopoietin. *Blood*. 2017 Aug 17;130(7):875–80.
  43. Bluteau D, Lordier L, Di Stefano A, Chang Y, Raslova H, Debili N, et al. Regulation of megakaryocyte maturation and platelet formation. Vol. 7, *Journal of Thrombosis and Haemostasis*. 2009. p. 227–34.
  44. Zimmet J, Ravid K. Polyploidy: Occurrence in nature, mechanisms, and significance for the megakaryocyte-platelet system. Vol. 28, *Experimental Hematology*. 2000. p. 3–16.
  45. Geddis AE. Megakaryopoiesis. *Semin Hematol*. 2010 Jul;47(3):212–9.
  46. Miyawaki K, Iwasaki H, Jiromaru T, Kusumoto H, Yurino A, Sugio T, et al. Identification of unipotent megakaryocyte progenitors in human hematopoiesis. *Blood*. 2017;129(25):blood-2016-09-741611.

47. Tomer A. Human marrow megakaryocyte differentiation: Multiparameter correlative analysis identifies von Willebrand factor as a sensitive and distinctive marker for early (2N and 4N) megakaryocytes. *Blood*. 2004;104(9):2722–7.
48. Italiano JE, Lecine P, Shivdasani RA, Hartwig JH. Blood platelets are assembled principally at the ends of proplatelet processes produced by differentiated megakaryocytes. *J Cell Biol*. 1999;147(6):1299–312.
49. Junt T, Schulze H, Chen Z, Massberg S, Goerge T, Wagner DD, et al. Dynamic Visualization Within of Thrombopoiesis. *Science*. 2007;317(5845):1767–70.
50. Lecine P, Italiano JE, Kim SW, Villeval JL, Shivdasani RA. Hematopoietic-specific beta 1 tubulin participates in a pathway of platelet biogenesis dependent on the transcription factor NF-E2. *Blood*. 2000;96(4):1366–73.
51. Kunishima S, Kobayashi R, Itoh TJ, Hamaguchi M, Saito H. Mutation of the beta1-tubulin gene associated with congenital macrothrombocytopenia affecting microtubule assembly. Vol. 113, *Blood*. 2009. p. 458–61.
52. Larson MK, Watson SP. Regulation of proplatelet formation and platelet release by integrin alpha IIb beta3. *Blood*. 2006;108(5):1509–14.
53. Andonegui G, Kerfoot SM, McNagny K, Ebbert KVJ, Patel KD, Kubes P. Platelets express functional Toll-like receptor-4. *Blood*. 2005 Oct 1;106(7):2417–23.
54. Semple JW, Italiano JE, Freedman J. Platelets and the immune continuum. *Nat Rev Immunol*. 2011 Apr 1;11(4):264–74.
55. Iannacone M, Sitia G, Isogawa M, Marchese P, Castro MG, Lowenstein PR, et al. Platelets mediate cytotoxic T lymphocyte-induced liver damage. *Nat Med*. 2005 Nov 30;11(11):1167–9.
56. Aslam R, Speck ER, Kim M, Crow AR, Bang KWA, Nestel FP, et al. Platelet Toll-like receptor expression modulates lipopolysaccharide-induced thrombocytopenia and tumor necrosis factor-alpha production in vivo. *Blood*. 2006;107:637–41.
57. Zhang G, Han J, Welch EJ, Ye RD, Voyno-Yasenetskaya TA, Malik AB, et al. Lipopolysaccharide Stimulates Platelet Secretion and Potentiates Platelet Aggregation via TLR4/MyD88 and the cGMP-Dependent Protein Kinase Pathway. *J Immunol*. 2009 Jun 15;182(12):7997–8004.
58. Dinkla S, van Cranenbroek B, van der Heijden WA, He X, Wallbrecher R, Dumitriu IE, et al. Platelet microparticles inhibit IL-17 production by regulatory T cells through P-selectin. *Blood*. 2016 Apr 21;127(16):1976–86.
59. Kang H-K, Chiang M-Y, Ecklund D, Zhang L, Ramsey-Goldman R, Datta SK. Megakaryocyte Progenitors Are the Main APCs Inducing Th17 Response to Lupus Autoantigens and Foreign Antigens. *J Immunol*. 2012 Jun 15;188(12):5970–80.
60. Finkielstein A, Schlinker AC, Zhang L, Miller WM, Datta SK. Human megakaryocyte progenitors derived from hematopoietic stem cells of normal individuals are MHC class II-expressing professional APC that enhance Th17 and Th1/Th17 responses. *Immunol Lett*. 2015 Jan;163(1):84–95.
61. Zufferey A, Speck ER, Machlus KR, Aslam R, Guo L, McVey MJ, et al. Mature murine megakaryocytes present antigen-MHC class I molecules to T cells and transfer them to

- platelets. *Blood Adv.* 2017;1(20):1773–85.
62. Harrington WJ, Minnich V, Hollingsworth JW, Moore C V. Demonstration of a thrombocytopenic factor in the blood of patients with thrombocytopenic purpura. 1951. *J Lab Clin Med.* 1951;38(1):1–10.
  63. Rodeghiero F, Stasi R, Gernsheimer T, Michel M, Provan D, Arnold DM, et al. Standardization of terminology, definitions and outcome criteria in immune thrombocytopenic purpura of adults and children: Report from an international working group. Vol. 113, *Blood.* 2009. p. 2386–93.
  64. Marieke Schoonen W, Kucera G, Coalson J, Li L, Rutstein M, Mowat F, et al. Epidemiology of immune thrombocytopenic purpura in the general practice research database. *Br J Haematol.* 2009;145(2):235–44.
  65. Kurata Y, Fujimura K, Kuwana M, Tomiyama Y, Murata M. Epidemiology of primary immune thrombocytopenia in children and adults in Japan: A population-based study and literature review. *Int J Hematol.* 2011;93(3):329–35.
  66. Moulis G, Palmaro A, Montastruc J-L, Godeau B, Lapeyre-Mestre M, Sailler L. Epidemiology of incident immune thrombocytopenia: a nationwide population-based study in France. *Blood.* 2014 Oct 10;3308–15.
  67. Lusher JM, Iyer R. Idiopathic thrombocytopenic purpura in children. *Semin Thromb Hemost.* 1977;3(3):175–99.
  68. Kashiwagi H, Tomiyama Y. Pathophysiology and management of primary immune thrombocytopenia. *Int J Hematol.* 2013 Jul;98(1):24–33.
  69. Shulman NR, Marder VJ, Weinrach RS. Similarities Between Known Antiplatelet Antibodies and The Factor Responsible For Thrombocytopenia In Idiopathic Purpura. Physiologic, Serologic and Isotopic Studies. *Ann N Y Acad Sci.* 1965;124(2):499–542.
  70. McMillan R. Autoantibodies and autoantigens in chronic immune thrombocytopenic purpura. *Semin Hematol.* 2000;37(3):239–48.
  71. McMillan R, Wang L, Tani P. Prospective evaluation of the immunobead assay for the diagnosis of adult chronic immune thrombocytopenic purpura (ITP). *J Thromb Haemost.* 2003;1(3):485–91.
  72. Cines DB, Blanchette VS. Immune thrombocytopenic purpura. *N Engl J Med.* 2002;346(13):995–1008.
  73. Gernsheimer T, Stratton J, Ballem PJ, Slichter SJ. Mechanisms of response to treatment in autoimmune thrombocytopenic purpura. *N Engl J Med.* 1989;320(15):974–80.
  74. Handin RI, Stossel TP. Effect of corticosteroid therapy on the phagocytosis of antibody-coated platelets by human leukocytes. *Blood.* 1978;51(5):771–9.
  75. Mizutani H, Furubayashi T, Imai Y, Kashiwagi H, Honda S, Take H, et al. Mechanisms of corticosteroid action in immune thrombocytopenic purpura (ITP): experimental studies using ITP-prone mice, (NZW x BXSB) F1. *Blood.* 1992;79(4):942–7.
  76. Lazarus AH, Crow AR. Mechanism of action of IVIG and anti-D in ITP. *Transfus Apher Sci.* 2003;28(3):249–55.

77. Chen X, Chen S, Li C, Zhu Y, Peng B. Skewed T-cell subsets and enhanced macrophages phagocytosis in the spleen of patients with immune thrombocytopenia failing glucocorticoids. *Int J Hematol.* 2011;94(3):248–54.
78. Lepage A, Leboeuf M, Cazenave JP, de la Salle C, Lanza F, Uzan G. The alpha(IIb)beta(3) integrin and GPIb-V-IX complex identify distinct stages in the maturation of CD34(+) cord blood cells to megakaryocytes. *Blood.* 2000;96(13):4169–77.
79. Houwerzijl EJ, Blom NR, Van Der Want JLL, Esselink MT, Koornstra JJ, Smit JW, et al. Ultrastructural study shows morphologic features of apoptosis and para-apoptosis in megakaryocytes from patients with idiopathic thrombocytopenic purpura. *Blood.* 2004;103(2):500–6.
80. Mahabir VK, Ross C, Popovic S, Sur ML, Bourgeois J, Lim W, et al. A blinded study of bone marrow examinations in patients with primary immune thrombocytopenia. *Eur J Haematol.* 2013 Feb;90(2):121–6.
81. Chang M, Nakagawa PA, Williams SA, Schwartz MR, Imfeld KL, Buzby JS, et al. Immune thrombocytopenic purpura (ITP) plasma and purified ITP monoclonal autoantibodies inhibit megakaryocytopoiesis in vitro. *Blood.* 2003;102:887–95.
82. McMillan R, Wang L, Tomer A, Nichol J, Pistillo J. Suppression of in vitro megakaryocyte production by antiplatelet autoantibodies from adult patients with chronic ITP. *Blood.* 2004 Feb 15;103(4):1364–9.
83. Takahashi R, Sekine N, Nakatake T. Influence of monoclonal antiplatelet glycoprotein antibodies on in vitro human megakaryocyte colony formation and proplatelet formation. *Blood.* 1999;93:1951–8.
84. Iraqi M, Perdomo J, Yan F, Choi PY-I, Chong BH. Immune thrombocytopenia: antiplatelet autoantibodies inhibit proplatelet formation by megakaryocytes and impair platelet production in vitro. *Haematologica.* 2015 Feb 14
85. Schweizer C, Reu FJ, Ho AD, Hensel M. Low rate of long-lasting remissions after successful treatment of immune thrombocytopenic purpura with rituximab. *Ann Hematol.* 2007;86(10):711–7.
86. Semple JW, Milev Y, Cosgrave D, Mody M, Hornstein A, Blanchette V, et al. Differences in serum cytokine levels in acute and chronic autoimmune thrombocytopenic purpura: relationship to platelet phenotype and antiplatelet T-cell reactivity. *Blood.* 1996;87(10):4245–54.
87. Cao J, Li X-Q, Chen C, Zeng L-Y, Cheng H, Li Z-Y, et al. Imbalance of th17/treg cells ratio in peripheral blood of patients with immune thrombocytopenia. *Zhongguo Shi Yan Xue Ye Xue Za Zhi.* 2011;19(3):730–3.
88. Shan NN, Ji X Bin, Wang X, Li Y, Liu X, Zhu XJ, et al. In vitro recovery of Th1/Th2 balance in PBMCs from patients with immune thrombocytopenia through the actions of IL-18BPα/Fc. *Thromb Res.* 2011;128(6).
89. Cao J, Chen C, Li L, Zeng LY, Li ZY, Yan ZL, et al. Effects of high-dose dexamethasone on regulating interleukin-22 production and correcting Th1 and Th22 polarization in immune thrombocytopenia. *J Clin Immunol.* 2012;32(3):523–9.
90. Ye X, Zhang L, Wang H, Chen Y, Zhang W, Zhu R. The Role of IL-23 / Th17 Pathway in Patients

- with Primary Immune Thrombocytopenia. *PLoS One*. 2015;1–13.
91. Bal G, Futschik ME, Hartl D, Ringel F, Kamhieh-Milz J, Sterzer V, et al. Identification of novel biomarkers in chronic immune thrombocytopenia (ITP) by microarray-based serum protein profiling. *Br J Haematol*. 2016 Feb;172(4):602–15.
  92. Olsson B, Andersson P, Jacobsson S, Carlsson L, Wadenvik H. Disturbed apoptosis of T-cells in patients with active idiopathic thrombocytopenic purpura. *Thromb Haemost*. 2004 Nov 8;139–44.
  93. Shimomura T, Fujimura K, Takafuta T, Fujii T, Katsutani S, Noda M, et al. Oligoclonal accumulation of T cells in peripheral blood from patients with idiopathic thrombocytopenic purpura. *Br J Haematol*. 1996;95(4):732–7.
  94. Olsson B, Andersson P-O, Jernås M, Jacobsson S, Carlsson B, Carlsson LMS, et al. T-cell-mediated cytotoxicity toward platelets in chronic idiopathic thrombocytopenic purpura. *Nat Med*. 2003 Sep;9(9):1123–4.
  95. Olsson B, Jernås M, Wadenvik H. Increased plasma levels of granzymes in adult patients with chronic immune thrombocytopenia. *Thromb Haemost*. 2012 Nov 29;107(06):1182–4.
  96. Ma L, Simpson EK, Li J, Zhu G, Chen P, Semple JW, et al. CD8+ T cells are predominantly protective in a murine model of ITP and is required for effective steroid therapy. *Blood*. 2013;122.
  97. Li S, Wang L, Zhao C, Li L, Peng J, Hou M. CD8+ T cells suppress autologous megakaryocyte apoptosis in idiopathic thrombocytopenic purpura. *Br J Haematol*. 2007;139(4):605–11.
  98. Yu J, Heck S, Patel V, Levan J, Yu Y, Bussel JB, et al. Defective circulating CD25 regulatory T cells in patients with chronic immune thrombocytopenic purpura. *Blood*. 2008;112(4):1325–8.
  99. Ji L, Zhan Y, Hua F, Li F, Zou S, Wang W, et al. The ratio of Treg/Th17 cells correlates with the disease activity of primary immune thrombocytopenia. *PLoS One*. 2012 Jan;7(12):e50909.
  100. Bao W, Bussel JB, Heck S, He W, Karpoff M, Boulad N, et al. Improved regulatory T-cell activity in patients with chronic immune thrombocytopenia treated with thrombopoietic agents. *Blood*. 2010 Nov 25;116(22):4639–45.
  101. Stasi R, Cooper N, Del Poeta G, Stipa E, Laura Evangelista M, Abruzzese E, et al. Analysis of regulatory T-cell changes in patients with idiopathic thrombocytopenic purpura receiving B cell-depleting therapy with rituximab. *Blood*. 2008 May 13;112(4):1147–50.
  102. Birtas Atesoglu E, Tarkun P, Demirsoy ET, Geduk A, Mehtap O, Batman A, et al. Soluble Programmed Death 1 (PD-1) Is Decreased in Patients With Immune Thrombocytopenia (ITP). *Clin Appl Thromb*. 2016 Apr 14;22(3):248–51.
  103. Zhong J, Chen S, Xu L, Lai J, Liao Z, Zhang T, et al. Lower expression of PD-1 and PD-L1 in peripheral blood from patients with chronic ITP. *Hematology*. 2016;21(9):552–7.
  104. Wang Y, Pang N, Wang X, Liu Y, Wang X, Wang L, et al. Percentages of PD-1 + CD4 + T cells and PD-L1 + DCs are increased and sPD-1 level is elevated in patients with immune thrombocytopenia. *Hum Vaccin Immunother*. 2018 Apr 3;14(4):832–8.
  105. George JN, Arnold DM. Immune thrombocytopenia (ITP) in adults: Clinical manifestations and

- diagnosis. UpToDate. 2018
106. Neunert C, Noroozi N, Norman G, Buchanan GR, Goy J, Nazi I, et al. Severe bleeding events in adults and children with primary immune thrombocytopenia: a systematic review. *J Thromb Haemost.* 2015;13(3):457-464.
  107. Arnold DM. Platelet count or bleeding as the outcome in ITP trials? *Am J Hematol.* 2012 Oct;87(10):945–6.
  108. Hill Q A., Newland AC. Fatigue in immune thrombocytopenia. *Br J Haematol.* 2015;170(2):141-9..
  109. Cooper N, Kruse A, Kruse C, Watson S, Morgan M, Bussel JB, et al. Results from the ITP World IMPACT Survey (I-WISH): Patients with Immune Thrombocytopenia (ITP) Experience Impaired Quality of Life (QoL) Regarding Daily Activities, Social Interactions, Emotional Well-Being and Working Lives. *Blood.* 2018;132(Suppl 1):4804.
  110. Provan D, Stasi R, Newland AC, Blanchette VS, Bolton-Maggs P, Bussel JB, et al. International consensus report on the investigation and management of primary immune thrombocytopenia. *Blood.* 2010 Jan 14;115(2):168–86.
  111. Neunert C, Lim W, Crowther M, Cohen A, Solberg Jr L. The American Society of Hematology 2011 evidence-based practice guideline for immune thrombocytopenia. *Blood.* 2011;117(16):4190–207.
  112. Kojouri K, Vesely SK, Terrell DR, George JN. Splenectomy for adult patients with idiopathic thrombocytopenic purpura: A systematic review to assess long-term platelet count responses, prediction of response, and surgical complications. *Blood.* 2004.
  113. Rodeghiero F, Ruggeri M. Short- and long-term risks of splenectomy for benign haematological disorders: should we revisit the indications? *Br J Haematol.* 2012 Jul;158(1):16–29.
  114. Arnold DM, Heddle NM, Carruthers J, Cook DJ, Crowther MA, Meyer RM, et al. A pilot randomized trial of adjuvant rituximab or placebo for nonsplenectomized patients with immune thrombocytopenia. *Blood.* 2012 Feb 9;119(6):1356–62.
  115. Ghanima W, Khelif A, Waage A, Michel M, Tjønnfjord GE, Romdhan N Ben, et al. Rituximab as second-line treatment for adult immune thrombocytopenia (the RITP trial): a multicentre, randomised, double-blind, placebo-controlled trial. *Lancet.* 2015 Apr;385(9978):1653–61.
  116. Nomura S. Advances in diagnosis and treatments for immune thrombocytopenia. Vol. 9, *Clinical Medicine Insights: Blood Disorders.* 2016. p. 15–22.
  117. Kuter DJ. New thrombopoietic growth factors. Vol. 109, *Blood.* 2007. p. 4607–16.
  118. Broudy VC, Lin NL. AMG531 stimulates megakaryopoiesis in vitro by binding to Mpl. *Cytokine.* 2004;25(2):52–60.
  119. Alexander WS, Metcalf D, Dunn a R. Point mutations within a dimer interface homology domain of c-Mpl induce constitutive receptor activity and tumorigenicity. *EMBO J.* 1995;14(22):5569–78.
  120. Erickson-Miller CL, Delorme E, Tian S-S, Hopson CB, Landis AJ, Valoret EI, et al. Preclinical Activity of Eltrombopag (SB-497115), an Oral, Nonpeptide Thrombopoietin Receptor Agonist.

- Stem Cells. 2009;27(2):424–30.
121. Will B, Kawahara M, Luciano JP, Bruns I, Parekh S, Erickson-Miller CL, et al. Effect of the nonpeptide thrombopoietin receptor agonist Eltrombopag on bone marrow cells from patients with acute myeloid leukemia and myelodysplastic syndrome. *Blood*. 2009;114(18):3899–908.
  122. González-López TJ, Pascual C, Álvarez-Román MT, Fernández-Fuertes F, Sánchez-González B, Caparrós I, et al. Successful discontinuation of eltrombopag after complete remission in patients with primary immune thrombocytopenia. *Am J Hematol*. 2015 Mar;90(3):E40–3.
  123. Álvarez Román MT, Fernández Bello I, Arias-Salgado EG, De Paz R, Jiménez Yuste V, Martín Salces M, et al. Effect of thrombopoietin-receptor agonists on a proliferation-inducing ligand (APRIL) plasma levels in patients with immune thrombocytopenia. *Vol. 78, British Journal of Clinical Pharmacology*. 2014. p. 674–6.
  124. Bart-Smith EE, Kordasti S, Kulasekararaj AG, Richardson D, Mufti GJ, Marsh JCW. Successful treatment of aplastic anaemia associated with HIV infection with eltrombopag: Implications for a possible immunomodulatory role. *AIDS*. 2014;28(18):2786–8.
  125. Koumoutsea E V, Cooper N, Psaila B, Sola-Visner M, Porter JB. Eltrombopag mobilizes intracellular iron stores at concentrations lower than those required with other clinically available iron chelators. *Blood*. 2014;124(21).
  126. Maecker HT, Trotter J. Flow cytometry controls, instrument setup, and the determination of positivity. *Cytom Part A*. 2006;69(9):1037–42.
  127. Hulspas R, O’Gorman MRG, Wood BL, Gratama JW, Robert Sutherland D. Considerations for the control of background fluorescence in clinical flow cytometry. *Cytom Part B - Clin Cytom*. 2009;76(6):355–64.
  128. Schindelin J, Arganda-Carreras I, Frise E, Kaynig V, Longair M, Pietzsch T, et al. Fiji: an open-source platform for biological-image analysis. *Nat Methods*. 2012;9(7):676–82.
  129. Choi ES, Nichol JL, Hokom MM, Hornkohl C, Hunt P. Platelets generated in vitro from proplatelet-displaying human megakaryocytes are functional. *Blood*. 1995;85(2):402–13.
  130. Aster RH, Keene WR. Sites of Platelet Destruction in Idiopathic Thrombocytopenic Purpura. *Br J Haematol*. 1969;16(1):61–74.
  131. Wybran J, Fudenberg HH. Cellular Immunity to platelets in idiopathic thrombocytopenic purpura. *Blood*. 1972;40(6):856–61.
  132. Newland A, Godeau B, Priego V, Viallard J-F, López Fernández MF, Orejudos A, et al. Remission and platelet responses with romiplostim in primary immune thrombocytopenia: final results from a phase 2 study. *Br J Haematol*. 2015 Nov;172(2):262–73.
  133. Jose Gonzalez-Lopez T, Pascual C, Teresa Alvarez-Roman M, Fernandez-Fuertes F, Sanchez-Gonzalez B, Caparrós I, et al. Successful discontinuation of eltrombopag after complete remission in patients with primary immune thrombocytopenia. *Am J Hematol*. 2015;90(3):E40–3.
  134. Cooper N. State of the art – how I manage immune thrombocytopenia. *Br J Haematol*. 2017;177(1):39–54.

135. Boyd SD, Liu Y, Wang C, Martin V, Dunn-Walters DK. Human lymphocyte repertoires in ageing. *Curr Opin Immunol*. 2013 Aug;25(4):511–5.
136. Wherry EJ. T cell exhaustion. *Nat Immunol*. 2011;12(6):492–9.
137. Precopio ML, Betts MR, Parrino J, Price DA, Gostick E, Ambrozak DR, et al. Immunization with vaccinia virus induces polyfunctional and phenotypically distinctive CD8 + T cell responses. *J Exp Med*. 2007 Jun;204(6):1405–16.
138. Rodeghiero F, Stasi R, Gernsheimer T, Michel M, Provan D, Arnold DM, et al. Standardization of terminology, definitions and outcome criteria in immune thrombocytopenic purpura of adults and children: report from an international working group. *Blood*. 2009 Mar 12;113(11):2386–93.
139. Appay V, Van Lier RAW, Sallusto F, Roederer M. Phenotype and function of human T lymphocyte subsets: Consensus and issues. *Cytom Part A*. 2008;73(11):975–83.
140. Maecker HT, McCoy JP, Nussenblatt R. Standardizing immunophenotyping for the Human Immunology Project. *Nat Rev Immunol*. 2012 Feb 17;12:191-200.
141. Perfetto SP, Chattopadhyay PK, Lamoreaux L, Nguyen R, Ambrozak D, Koup RA, et al. Amine reactive dyes: An effective tool to discriminate live and dead cells in polychromatic flow cytometry. *J Immunol Methods*. 2006 Jun;313(1–2):199–208.
142. Moncunill G, Han H, Dobaño C, McElrath MJ, De Rosa SC. OMIP-024: Pan-leukocyte immunophenotypic characterization of PBMC subsets in human samples. *Cytom Part A*. 2014 Dec;85(12):995–8.
143. Kuwana M, Kaburaki J, Ikeda Y. Autoreactive T cells to platelet GPIIb-IIIa in immune thrombocytopenic purpura: Role in production of anti-platelet autoantibody. *J Clin Invest*. 1998;102(7):1393–402.
144. Hu Y, Ma D, Shan N, Zhu Y, Liu X, Zhang L, et al. Increased Number of Tc17 and Correlation with Th17 Cells in Patients with Immune Thrombocytopenia. Zimmer J, editor. *PLoS One*. 2011 Oct 24;6(10):e26522.
145. Flint SM, Gibson A, Lucas G, Nandigam R, Taylor L, Provan D, et al. A distinct plasmablast and naive B-cell phenotype in primary immune thrombocytopenia. *Haematologica*. 2016 Jun 1;101(6):698–706.
146. El-Rashedi FH, El-Hawy MA, Helwa MA, Abd-Allah SS. Study of CD4 + , CD8 + , and natural killer cells (CD16 + , CD56 + ) in children with immune thrombocytopenic purpura. *Hematol Oncol Stem Cell Ther*. 2017 Mar;10(1):8–14.
147. Howard RR, Fasano CS, Frey L, Miller CH. Reference intervals of CD3, CD4, CD8, CD4/CD8, and absolute CD4 values in asian and non-asian populations. *Cytometry*. 1996 Sep 15;26(3):231–2.
148. Wikby A, Månsson IA, Johansson B, Strindhall J, Nilsson SE. The immune risk profile is associated with age and gender: findings from three Swedish population studies of individuals 20–100 years of age. *Biogerontology*. 2008 Oct 28;9(5):299–308.
149. McBride JA, Striker R. Imbalance in the game of T cells: What can the CD4/CD8 T-cell ratio tell us about HIV and health? Coyne CB, editor. *PLOS Pathog*. 2017 Nov 2;13(11):e1006624.

150. Kook H, Zeng W, Guibin C, Kirby M, Young NS, Maciejewski JP. Increased cytotoxic T cells with effector phenotype in aplastic anemia and myelodysplasia. *Exp Hematol.* 2001;29(11):1270–7.
151. Zhou Q, Munger ME, Veenstra RG, Weigel BJ, Hirashima M, Munn DH, et al. Coexpression of Tim-3 and PD-1 identifies a CD8+ T-cell exhaustion phenotype in mice with disseminated acute myelogenous leukemia. *Blood.* 2011 Apr 28;117(17):4501–10.
152. Severson JJ, Serracino HS, Mateescu V, Raeburn CD, McIntyre RC, Sams SB, et al. PD-1+Tim-3+ CD8+ T Lymphocytes Display Varied Degrees of Functional Exhaustion in Patients with Regionally Metastatic Differentiated Thyroid Cancer. *Cancer Immunol Res.* 2015 Jun 1;3(6):620–30.
153. Zahran AM, Youssef MAM, Elsayh KI, Embaby MM, Ibrahim AIM. Clinical Significance of T-Cell Immunoglobulin Mucin 3 Expression on Peripheral Blood Mononuclear Cells in Pediatric Acute Immune Thrombocytopenia. *Clin Appl Thromb.* 2018 Sep 4;24(6):936–43.
154. Zhong J, Chen S, Xu L, Lai J, Liao Z, Zhang T, et al. Lower expression of PD-1 and PD-L1 in peripheral blood from patients with chronic ITP. *Hematology.* 2016 Oct 20;21(9):552–7.
155. Yoshimura C, Nomura S, Nagahama M, Ozaki Y, Kagawa H, Fukuhara S. Plasma-soluble Fas (APO-1, CD95) and soluble Fas ligand in immune thrombocytopenic purpura. *Eur J Haematol.* 2000 Apr;64(4):219–24.
156. Rocha AMC, Souza C, Rocha GA, de Melo FF, Clementino NCD, Marino MCA, et al. The levels of IL-17A and of the cytokines involved in Th17 cell commitment are increased in patients with chronic immune thrombocytopenia. *Haematologica.* 2011 Oct;96(10):1560–4.
157. Ma D, Zhu X, Zhao P, Zhao C, Li X, Zhu Y, et al. Profile of Th17 cytokines (IL-17, TGF-beta, IL-6) and Th1 cytokine (IFN-gamma) in patients with immune thrombocytopenic purpura. *Ann Hematol.* 2008 Nov;87(11):899–904.
158. Ma L, Liang Y, Fang M, Guan Y, Si Y, Jiang F, et al. The cytokines (IFN- $\gamma$ , IL-2, IL-4, IL-10, IL-17) and Treg cytokine (TGF- $\beta$ 1) levels in adults with immune thrombocytopenia. *Pharmazie.* 2014;69(9):694–7.
159. Zhang F, Chu X, Wang L, Zhu Y, Li L, Ma D, et al. Cell-mediated lysis of autologous platelets in chronic idiopathic thrombocytopenic purpura. *Eur J Haematol.* 2006;76(5):427–31.
160. Dufour C, Corcione A, Svahn J, Haupt R, Battilana N, Pistoia V. Interferon gamma and tumour necrosis factor alpha are overexpressed in bone marrow T lymphocytes from paediatric patients with aplastic anaemia. Vol. 115, *British journal of haematology.* 2001. p. 1023–31.
161. Precopio ML, Betts MR, Parrino J, Price DA, Gostick E, Ambrozak DR, et al. Immunization with vaccinia virus induces polyfunctional and phenotypically distinctive CD8 + T cell responses. *J Exp Med.* 2007 Jun 11;204(6):1405–16.
162. Akinsiku OT, Bansal A, Sabbaj S, Heath SL, Goepfert PA. Interleukin-2 production by polyfunctional HIV-1-specific CD8 T cells is associated with enhanced viral suppression. *J Acquir Immune Defic Syndr.* 2011 Oct 1;58(2):132–40.
163. Kagina BMN, Abel B, Scriba TJ, Hughes EJ, Keyser A, Soares A, et al. Specific T Cell Frequency and Cytokine Expression Profile Do Not Correlate with Protection against Tuberculosis after Bacillus Calmette-Guérin Vaccination of Newborns. *Am J Respir Crit Care Med.* 2010 Oct 15;182(8):1073–9.

164. McKinney EF, Smith KG. T cell exhaustion and immune-mediated disease—the potential for therapeutic exhaustion. *Curr Opin Immunol*. 2016 Dec;43:74–80.
165. Nakamura T, Miyakawa Y, Miyamura A, Yamane A, Suzuki H, Ito M, et al. A novel nonpeptidyl human c-Mpl activator stimulates human megakaryopoiesis and thrombopoiesis. *Blood*. 2006;
166. E.V. K, P. K, J.B. P, N. C, B. P, M. S-V. Eltrombopag (ELT) reverses iron mediated suppression of insulin secretion in pancreatic cells by chelating iron and decreasing ROS. *Blood*. 2016;128(22):1278.
167. Zhao Z, Sun Q, Sokoll LJ, Streiff M, Cheng Z, Grasmeyer S, et al. Eltrombopag mobilizes iron in patients with aplastic anemia. *Blood*. 2018 May 24;131(21):2399–402.
168. Risitano AM, Kook H, Zeng W, Chen G, Young NS, Maciejewski JP. Oligoclonal and polyclonal CD4 and CD8 lymphocytes in aplastic anemia and paroxysmal nocturnal hemoglobinuria measured by  $\text{V}\beta$  CDR3 spectratyping and flow cytometry. *Blood*. 2002;
169. Sloand E, Kim S, Maciejewski JP, Tisdale J, Follmann D, Young NS. Intracellular interferon-gamma in circulating and marrow T cells detected by flow cytometry and the response to immunosuppressive therapy in patients with aplastic anemia. *Blood*. 2002;
170. Townsley DM, Scheinberg P, Winkler T, Desmond R, Dumitriu B, Rios O, et al. Eltrombopag Added to Standard Immunosuppression for Aplastic Anemia. *N Engl J Med*. 2017 Apr 20;376(16):1540–50.
171. Mahnke YD, Beddall MH, Roederer M. OMIP-015: Human regulatory and activated T-cells without intracellular staining. *Cytom Part A*. 2013 Feb;83A(2):179–81.
172. Sakakura M, Wada H, Tawara I, Nobori T, Sugiyama T, Sagawa N, et al. Reduced Cd4+Cd25+ T cells in patients with idiopathic thrombocytopenic purpura. *Thromb Res*. 2007;120(2):187–93.
173. Aleem A. Durability and factors associated with long term response after splenectomy for primary immune thrombocytopenia (ITP) and outcome of relapsed or refractory patients. *Platelets*. 2011;22(1):1–7.
174. Levine R, KC H, Lamberg J. The significance of megakaryocyte size. *Blood*. 1982;60(5):1122–31.
175. Böhmer RM, Bandala-Sanchez E, Harrison LC. Forward light scatter is a simple measure of T-cell activation and proliferation but is not universally suited for doublet discrimination. *Cytom Part A*. 2011 Aug;79A(8):646–52.
176. Onubogu I, Cooper N, Naresh K, Crawley J, Trivedi P. Alternative Methods Of Thrombocytopenia: Patients With ITP Have Increased Megakaryocyte/T Cell Interactions In The Bone Marrow and Higher Serum TRAIL Levels. *Blood*. 2013;122(21):3531.
177. Satoh T, Miyazaki K, Shimada N, Nagane K, Inukai T, Nakajima H, et al. Detection of Anti-Thrombopoietin Antibodies in Patients with Immune Thrombocytopenia. *Blood*. 2014;124(21):4187.
178. Toltl LJ, Ross C, Kelton JG, Arnold DM. Bone Marrow Specimens From Patients with Immune Thrombocytopenia (ITP) Demonstrate Increased Megakaryocyte-Bound IgG and Increased T-Helper Cells. *Blood*. 2011;118(21):2233.

179. Gunduz E, Kivanc BK, Arik D, İsiksoy S, Bal C, Akay OM. Bone marrow examination in patients with immune thrombocytopenia: is there anything different in older patients? *Eur J Haematol.* 2014;93(2):157–60.
180. Song Y, Wang YT, Huang XJ, Kong Y. Abnormalities of the bone marrow immune microenvironment in patients with immune thrombocytopenia. *Ann Hematol.* 2016;95(6):959–65.
181. Fu X, Tao L, Rivera A, Williamson S, Song X-T, Ahmed N, et al. A Simple and Sensitive Method for Measuring Tumor-Specific T Cell Cytotoxicity. Unutmaz D, editor. *PLoS One.* 2010 Jul 29;5(7):e11867.
182. Mulherkar R, Karabudak A, Ginwala R, Huang X, Rowan A, Philip R, et al. In vivo and in vitro immunogenicity of novel MHC class I presented epitopes to confer protective immunity against chronic HTLV-1 infection. *Vaccine.* 2018 Aug;36(33):5046–57.
183. Ogura H, Preston-Hurlburt P, Perdigoto AL, Amodio M, Krishnaswamy S, Clark P, et al. Identification and Analysis of Islet Antigen-Specific CD8 + T Cells with T Cell Libraries. *J Immunol.* 2018 Aug 6;201(4):ji1800267.
184. Lee S-H, Erber WN, Porwit A, Tomonaga M, Peterson LC. ICSH guidelines for the standardization of bone marrow specimens and reports. *Int J Lab Hematol.* 2008 Oct;30(5):349–64.
185. Taube JM, Klein A, Brahmer JR, Xu H, Pan X, Kim JH, et al. Association of PD-1, PD-1 Ligands, and Other Features of the Tumor Immune Microenvironment with Response to Anti-PD-1 Therapy. *Clin Cancer Res.* 2014 Oct 1;20(19):5064–74.
186. Pinato DJ, Kythreotou A, Mauri FA, Suardi E, Allara E, Shiner RJ, et al. Functional immune characterization of HIV-associated non-small-cell lung cancer. *Ann Oncol.* 2018 Jun 1;29(6):1486–8.
187. Barsam SJ, Psaila B, Forestier M, Page LK, Sloane P a., Geyer JT, et al. Platelet production and platelet destruction: Assessing mechanisms of treatment effect in immune thrombocytopenia. *Blood.* 2011;117(21):5723–32.
188. Psaila B, Barkas N, Iskander D, Roy A, Anderson S, Ashley N, et al. Single-cell profiling of human megakaryocyte-erythroid progenitors identifies distinct megakaryocyte and erythroid differentiation pathways. *Genome Biol.* 2016;
189. Houwerzijl EJ. Ultrastructural study shows morphologic features of apoptosis and para-apoptosis in megakaryocytes from patients with idiopathic thrombocytopenic purpura. *Blood.* 2004 Jan 15;103(2):500–6.
190. McMillan R, Wang L, Tomer A, Nichol J, Pistillo J. Suppression of in vitro megakaryocyte production by antiplatelet autoantibodies from adult patients with chronic ITP. *Blood.* 2004;103:1364–9.
191. White MJ, Kile BT. Apoptotic Processes in Megakaryocytes and Platelets. *Semin Hematol.* 2010;47(3):227–34.
192. Tomer a, Harker L a. Measurements of in vivo megakaryocytopoiesis: studies in nonhuman primates and patients. *Stem Cells.* 1996;14 Suppl 1:18–30.
193. Liu Z, Bussel JB, Lakkaraja M, Ferrer-marin F, Ghevaert C, Feldman HA, et al. Suppression of in

- vitro megakaryopoiesis by maternal sera containing anti-HPA-1a antibodies. *Blood*. 2015;126(10):1234–7.
194. Paolo F. PD-L1 Expressing Hematopoietic Stem Cells and Uses. Vol. 1. United States; US patent 20180214487A1, 2018.
  195. Liang SC, Latchman YE, Buhlmann JE, Tomczak MF, Horwitz BH, Freeman GJ, et al. Regulation of PD-1, PD-L1, and PD-L2 expression during normal and autoimmune responses. Vol. 33, *European journal of immunology*. 2003. p. 2706–16.
  196. Petersdorf EW, Longton GM, Anasetti C, Mickelson EM, McKinney SK, Smith AG, et al. Association of HLA-C disparity with graft failure after marrow transplantation from unrelated donors. *Blood*. 1997 Mar 1;89(5):1818–23.
  197. Lev PR, Grodzielski M, Goette NP, Glembotsky AC, Espasandin YR, Pierdominici MS, et al. Impaired proplatelet formation in immune thrombocytopenia: a novel mechanism contributing to decreased platelet count. *Br J Haematol*. 2014 Jun;165(6):854–64.
  198. Desmond R, Townsley DM, Dumitriu B, Olnes MJ, Scheinberg P, Bevans M, et al. Eltrombopag restores trilineage hematopoiesis in refractory severe aplastic anemia that can be sustained on discontinuation of drug. *Blood*. 2014 Mar 20;123(12):1818–25.
  199. Richardson DR, Baker E. The uptake of iron and transferrin by the human malignant melanoma cell. *Biochim Biophys Acta - Mol Cell Res*. 1990 Jun;1053(1):1–12.
  200. Lederman HM, Cohen A, Lee J, Freedman M, Gelfand E. Deferoxamine: a reversible S-phase inhibitor of human lymphocyte proliferation. *Blood*. 1984;64(3):748–53.
  201. Kemp JD, Thorson JA, Gomez F, Smith KM, Cowdery JS, Ballas ZK. Inhibition of lymphocyte activation with anti-transferrin receptor Mabs: A comparison of three reagents and further studies of their range of effects and mechanism of action. *Cell Immunol*. 1989 Aug;122(1):218–30.
  202. Steinbach K, Vincenti I, Kreutzfeldt M, Page N, Muschaweckh A, Wagner I, et al. Brain-resident memory T cells represent an autonomous cytotoxic barrier to viral infection. *J Exp Med*. 2016 Jul 25;213(8):1571–87.
  203. Joshi NS, Akama-Garren EH, Lu Y, Lee D-Y, Chang GP, Li A, et al. Regulatory T Cells in Tumor-Associated Tertiary Lymphoid Structures Suppress Anti-tumor T Cell Responses. *Immunity*. 2015 Sep;43(3):579–90.
  204. Arnold DM, Nazi I, Toltl LJ, Ross C, Ivetic N, Smith JW, et al. Antibody binding to megakaryocytes in vivo in patients with immune thrombocytopenia. *Eur J Haematol*. 2015 Feb;(15):1–6.